
**Czech Technical University In Prague**

**Faculty of Mechanical Engineering**

**Department of Automotive Engineering**

# Power Transmission Torsional Analysis for A Tilting Test Stand

**By Mehmet Ekmekci**

**In Partial Fulfillment of the Requirement for the Degree of Master of Automotive Engineering**

January 2017

Prague, Czech Republic


**Czech Technical University In Prague**

**Faculty of Mechanical Engineering**

**Department of Automotive Engineering**

# Power Transmission Torsional Analysis for A Tilting Test Stand

**By Mehmet Ekmekci**

**In Partial Fulfillment of the Requirement for the Degree of Master of Automotive Engineering**

January 2017

Prague, Czech Republic

# Certificate

This is to certify that this thesis work entitled “Power Transmission Torsional Analysis for a Tilting Test Stand” submitted by Mr. Mehmet Ekmekci is a genuine thesis work carried under my supervision and guidance and fulfilling the nature and standard required for partial fulfillment of the degree of “Master of Automotive Engineering”. This work embodied in this thesis has not been submitted for a degree elsewhere.

Ing. Jiří Vávra, Ph.D.

# Acknowledgement

I'd like to thank my thesis supervisor Mr. Vavra for his great understanding and patience. The process of writing a thesis and obtaining a degree is the final bridge between school and real life, where we won't always have people so understanding and helpful. I'm greatly in debt for such patience, and for use of is time.

I'd like to thank David Svetlik in particular, who was my colleague and project partner during the duration of the thesis work. It's not always easy to deal with a person who constantly asks questions, at times even on weekends and late nights, but his patience, and great understanding has gone a long way for me to learn much more than I was capable of, and become a better engineer in general.

I can't forget to thank my friends and all of my classmates, who again, have been my partners through this journey. Every question, every small talk that we had about what we have learned in the university, has helped me to understand things better.

Last but not least, I owe a massive gratitude to my family. Everything I do as a grown man is not only to make myself happy, but you as well.

I'd like to dedicate my thesis work to my uncle, Vedat Genc, who arranged me my first and most interesting automotive internship, and whom I believe still watches out there somewhere.

# Abstract

An engine tilting test stand is still in the design process at VTP Roztoky. During this design process, a model has been suggested that starts with the engine, and ends with a dynamometer. Throughout this thesis, first an analytical, and then a dynamic model has been built in the necessary software to examine and evaluate mass properties of rotating parts of a flexible power transmission between a combustion engine and a dynamometer. The natural resonant frequencies of the system have been assessed, and the behavior of the system during the resonant frequencies have been evaluated. Using the dynamic model, the dynamic torques between the relevant parts have been examined, and in some cases converted to other variables to monitor the safety, and possibly failure, of the relevant parts in question. Transient behavior for engine start and engine stop has also been assessed, and monitored for possible critical conditions, and finally, design suggestions have been made to get the system to create alternative options for the parts in question, and possible make the system more efficient and safe.

The analytical model and the dynamic model show the same natural frequencies, which justifies that the system model was properly built in the software GT-Suite. The dynamic variables have been evaluated and it has been found out that both the dual mass flywheel and the hydro motor are safe to use, as long as the resonant frequencies are passed in a short period of time without letting the resonant peak torques build up. The critical dynamic torque value for the dual mass flywheel 480 Nm, and the critical pressure value for the hydro elements 360 bars are both not exceeded. In both cases the simulation results show that the values do not even exceed 200.

The frequency analysis shows that the critical areas are between 0-100 RPM and 800-900 RPM, where the resonant frequencies cross with the engine RPM and create high torque and rotational speed amplitudes. Finally, the future steps regarding the project are discussed, where a suggestion has been made to improve the analytical model by adding extra masses and torsional stiffness, while it is stated that its possible and needed to build a full engine model in 1-D to be able to properly evaluate the transient engine starting and stopping conditions.

# Table of Contents

# List of Figures

# List of Tables

# Abbreviations

| | |
|---|---|
| **DMF** | Dual Mass Flywheel |
| **RPM** | Rotation per minute |
| **Hz** | Hertz |
| **rad** | Radians |

# 1. Introduction

## 1.1. General

An engine tilting test stand is in the process of being designed at VTP Roztoky, Přílepská 1920252 63 Roztoky, for a third party automotive company. This tilting stand will be a 2 axis device, with a maximum rotating range of 45 degrees for each axis, and a maximum carrying capacity of 200 kilograms. The tilting stand is being designed for a specific type of engine, with a maximum torque of 170 Nm at 4000 RPM, and a maximum power of 88 kW at 6000 RPM, while having a torque value of 140 Nm at this rotational speed.

The objective of this design and build is to carry tests for oil separation and lift off by simulating the slope of the vehicle, for both rolling and pitching conditions. The tilting stand can also be used for hill climbing, or downhill conditions without moving the engine itself a single step. The important idea behind the design of the tilting device is to save important costs. Mounting an engine prototype to a chassis to evaluate the lift off and oil tests, and then running actual road tests take an immense amount of time and money to complete, while having an engine stand can easily simulate incredibly close results without any of the drawbacks.

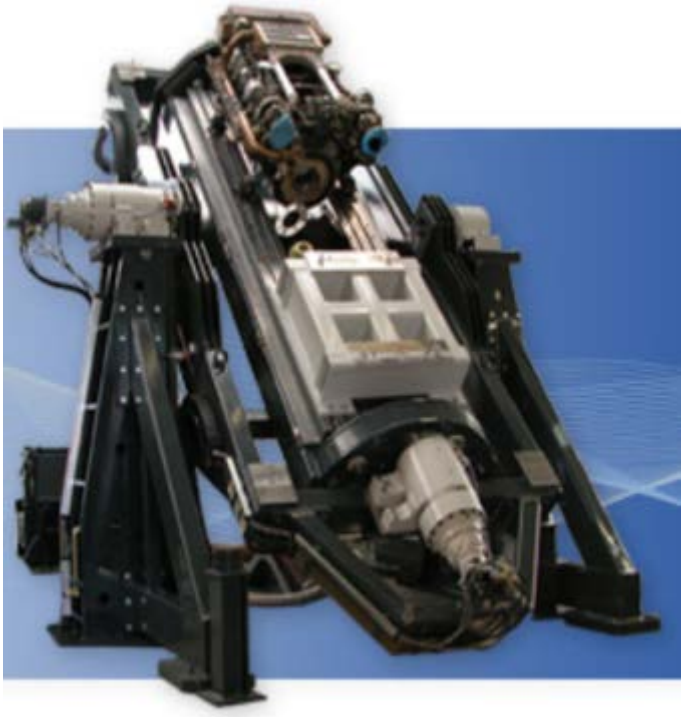

Figure 1.1 – An example of an engine tilting stand, *CFM-Schiller, Engine Tilting Test Rig, 2016*

Throughout this research, 2 multibody models will be built and analyzed to evaluate the dynamic variables that are used in the system that starts with the engine itself, and ends with the dynamometer. First model will be analytical, to evaluate the resonant frequencies of the system being built, while the dynamic model will be used both for the resonant frequency evaluation and evaluation of the dynamic variables. Finally, using the dynamic model, transient engine behavior and the system response will be assessed and possible design modifications will be discussed.

### 1.2. Basic Scheme and Explanation of the system

Mounting just the engine itself to the tilting stand, although sounds very comforting, unfortunately is not possible. To be able to perfectly simulate the conditions needed, the engine will be mounted on the engine tilting stand with a number of parts. These parts will act as a torsional transmission system, both to start the engine in motoring conditions, and to perfectly load the engine, dissipating the energy while the engine runs. The system will start with the engine, going through a dual mass flywheel, which then connects to a planetary gear set for gear reduction, hydro generator, hydro motor which then connects to the dynamometer with Roba DS couplings. A basic scheme of the system can be seen in figure 1.2.

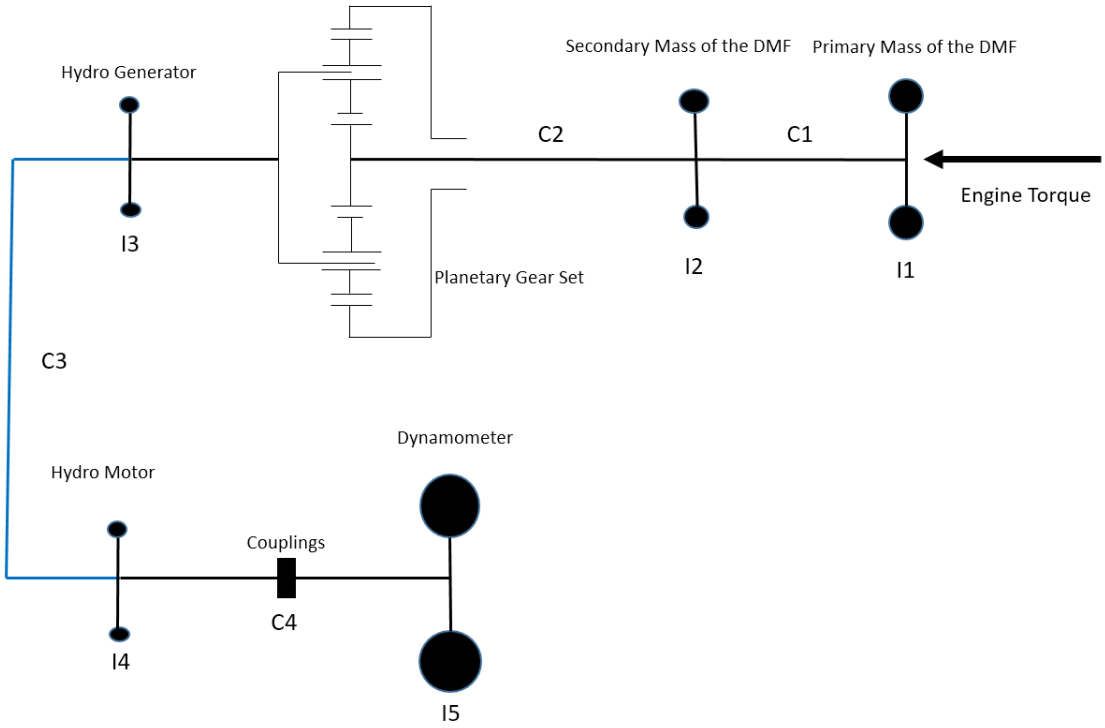


Figure 1.2 – Basic Scheme of the System

On the platform, the dynamometer will be docked to the edge of the system, while engine and parts connected to the engine that can rotate, will be a part of the actual tilting device with the engine itself. The view of the platform without the engine and its parts can be seen on figure 1.3, and the whole system overview can be seen on figure 1.4. Please keep in mind that the system itself is still under design process, and parts of it, or their arrangements can be changed throughout the process. The objective of the thesis is not to create different design parameters, but to evaluate the system within existing conditions to point out the critical conditions. While the engine itself, the hydro generator and the hydro motor, and the dynamometer will stay as a part of the system throughout the design process, the dual mass flywheel and the gear reduction system can be replaced by other more suitable parts.

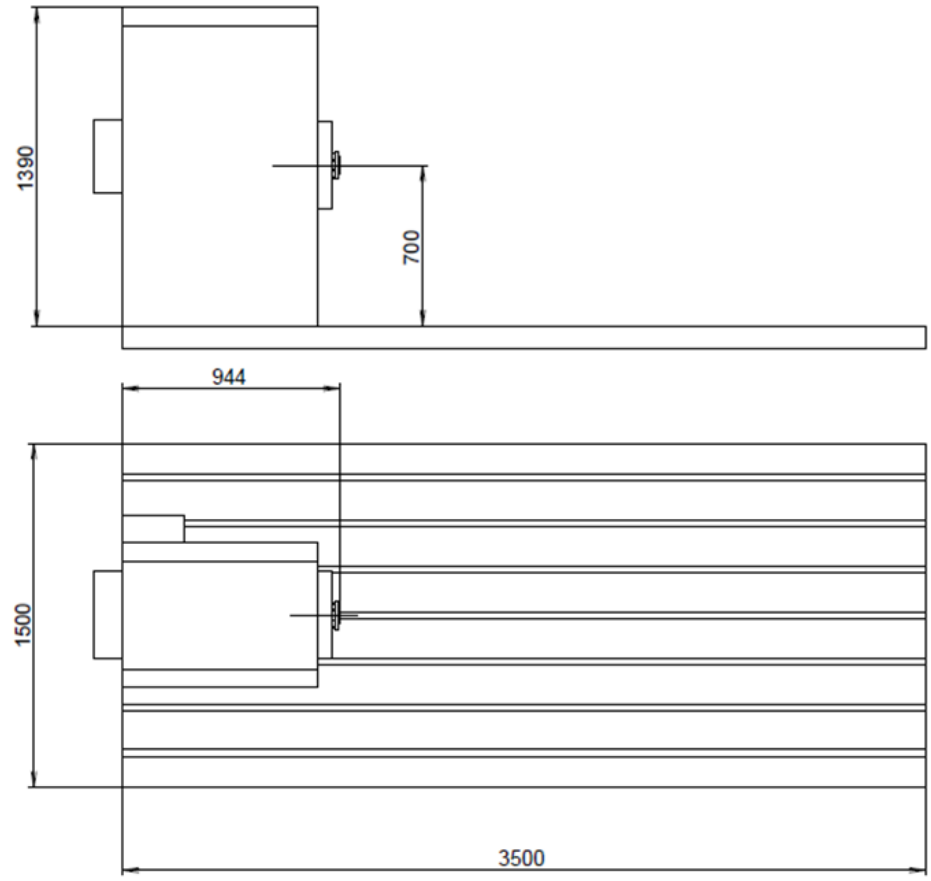


Figure 1.3 – A view of the platform that the engine tilting stand will be built on, *David Svetlik, 2016*

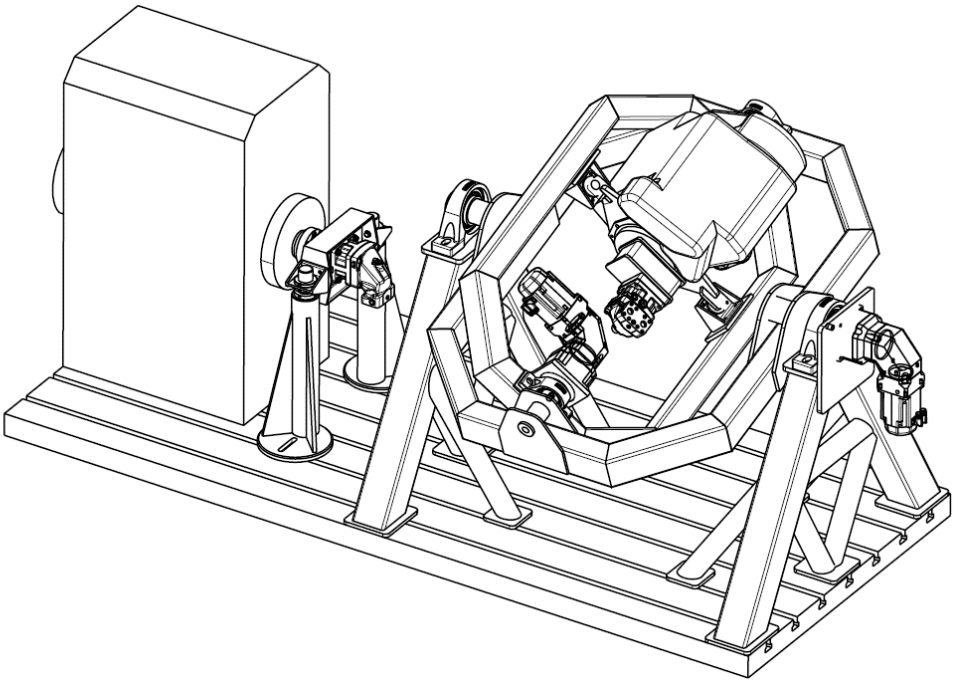

Figure 1.4 – An Overview of the System Design, *David Svetlik, 2016*

### 1.3. Explanation of Method

As it can be seen on figure 1.2, the elements of the system have been categorized by their inertias, and the torsional stiffness in between. Both for the analytical model, and the dynamic model, a total of 5 inertias, and 4 torsional stiffness will be used.

The basic method for the build of the models is to assume that the extra inertias in the system will be reduced to be used as a part of the main inertias. An example of this can be given for the planetary gear set inertia. The inertia of the gear set will be reduced and used as a part of I2, which is normally the inertia for the secondary mass of the dual mass flywheel. This is done in order to create a serially linked system without any breaking connection, therefore the natural frequencies of the system can be found without neglecting any of the inertias.

While the inertias will be reduced to get to the resonant frequencies, the torsional stiffness of the system connections will be calculated separately for each of the 2 parts being connected. Both inertias and torsional stiffness will be thoroughly explained in the next section for each of the parts and connections. The main focus of the research is on the resonant frequencies, and dynamic variables of the parts in the system under full load, therefore the inertias of the shafts will be neglected.

# 2. Evaluation of the Parts of the System

## 2.1. Dual Mass Flywheel

### 2.1.1. Introduction to Dual Mass Flywheels

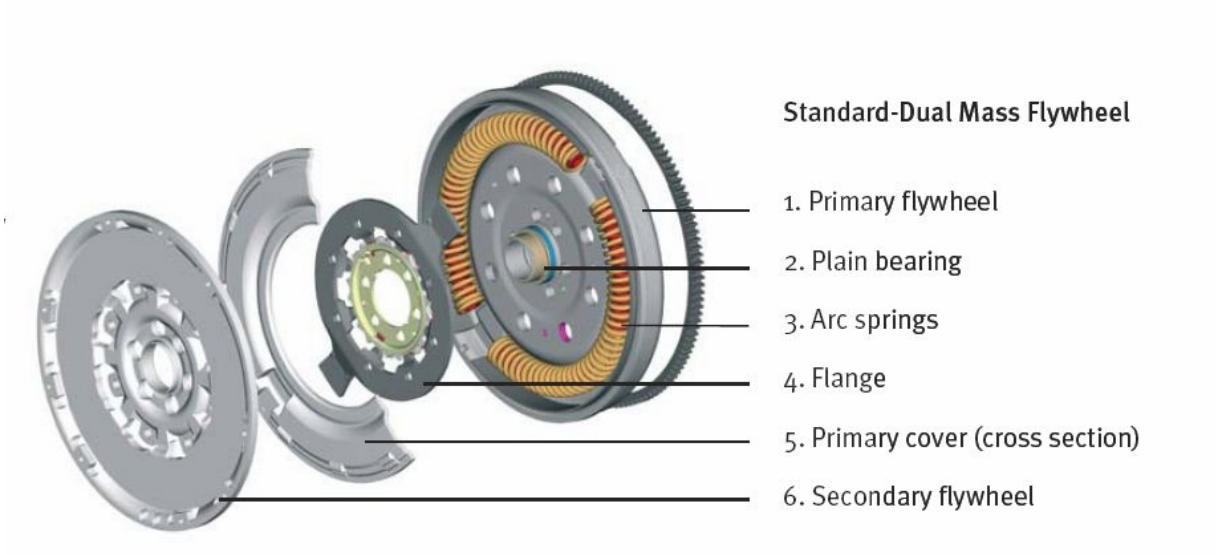


Figure 2.1. – Parts of a Standard Dual Mass Flywheel, *A1 Clutches, 2016*

Conventionally, a flywheel in a vehicle is used for storing the energy, thus work, created within the premises of an internal combustion engine, and then translating it into the desired purpose. The flywheels were not only a part of the modernized vehicles, but also essential parts for other types of machinery such as external combustion engine steamed locomotives, industrial machines, or commercial vehicles like tractors, and typical farming machines.

The first and most important idea behind a flywheel is hidden within the context of its definition. A proper flywheel should transfer the energy created within the engine as close to perfect as possible, and for this reducing the energy losses to minimum is the essential goal. But with the introducing of multiple-cylinder internal combustion engines, throughout the history of vehicular usage, the users have demanded more and more comfort while they are operating with these complex machines. The comfort is one aspect of determining the best use of different types of vehicles, but it's not the only one. While reducing torsional vibration peaks, or preventing resonances for the rotating parts, safety becomes of mere importance, and usually reducing noise and vibrations comes as a result of this important task.

Therefore, the first dual mass flywheel was introduced into the market on 1985 as a solution to escalation of torque and power, therefore the sudden changes in the rotational speed of rotating parts, especially for the low angular speeds. The idea behind the dual mass flywheel is to use 2 rotating masses instead of one, and then by using 2 set of arc springs between these rotating flywheel masses, damping the vibrational escalations between the engine and the transmission. While the first dual mass flywheels didn't use the arc springs, but instead big springs far outside that showed wearing problems, introduction of the arc spring damper changed the whole point of view towards dual mass flywheels, and let the market automatically shift towards using them.

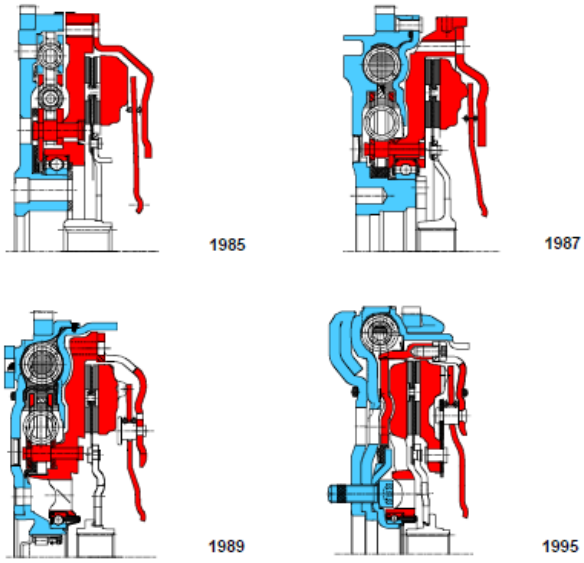


Figure 2.2 – A brief historical change of the dual mass flywheels, Luk Kolloquium, 1998

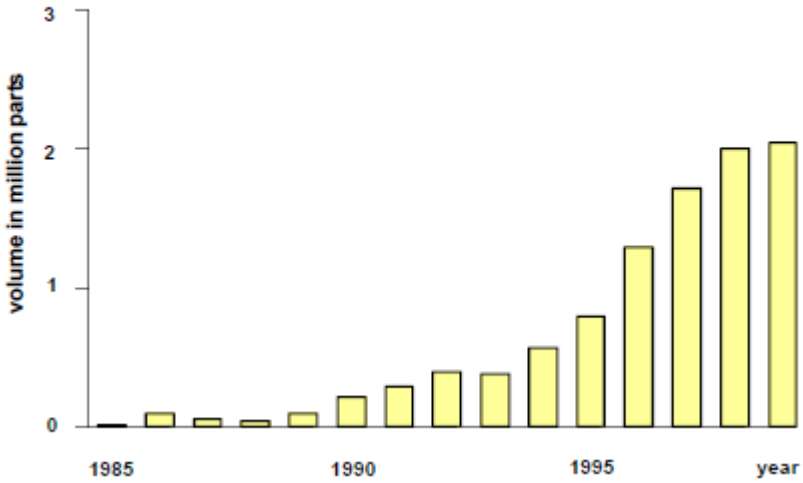


Figure 2.3 – Development of DMF production for German cars, Luk Kolloquium, 1998

While the usage of the dual mass flywheel is increasing with each vehicle produced, one should focus on both the advantages and disadvantages of using the dual mass flywheels. In the following sections we will discuss first the advantages and then disadvantages of the usage of a dual mass flywheel in both modernized vehicles, and our system.

### 2.1.2. Advantages of Dual Mass Flywheels

- **Isolation from Torsional Vibrations**

As it was briefly explained before, a big advantage of a dual-mass flywheel is that it isolates the torsional vibrations coming from the engine, using the angular phase difference between its primary and secondary mass. Although in some instances this can be taken as a complete isolation from torsional vibrations, in practice with the wide range of rpm of an engine, user differences, and the variety environmental variables, the dual-mass flywheel does an effective job in isolating the torsional vibrations, although not impeccable. But to see the difference between conventional torsion damper clutch discs and dual-mass flywheels, the figure below shows the angle accelerations at the transmission input.

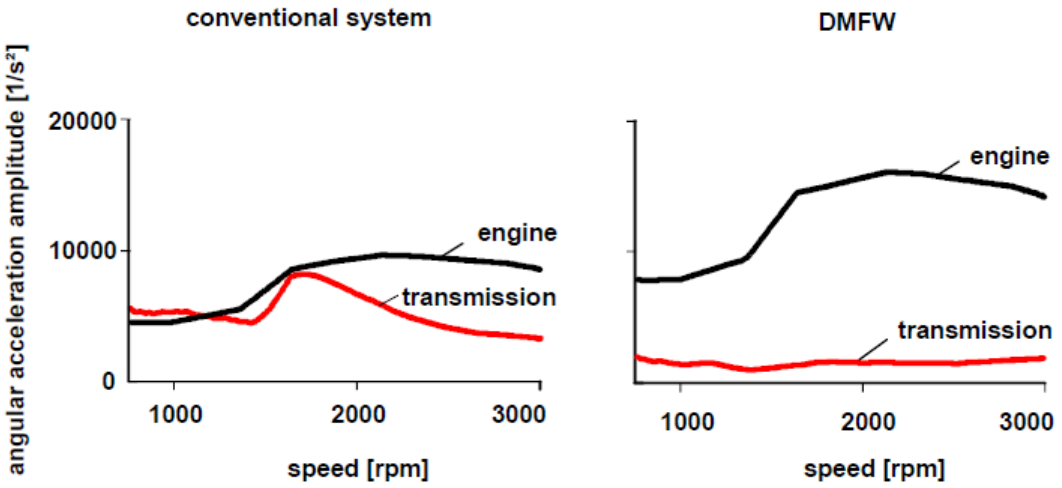


Figure 2.4 – Change of Angular Acceleration on a conventional system and a dual-mass flywheel, *Luk Kolloquium, 1998*

As it can be seen, with a conventional system, at lower speeds there is no significant torsional vibration isolation. This creates a risk of resonance especially at lower speeds, but it should be noted that the resonances can be prevented by using additional proper damping at lower speeds.

The important aspect here is that the dual-mass flywheel almost completely isolates the engine irregularity. It is also safe to say that the resonance will no longer generally occur at low speeds, and in fact in the whole driving range, and gear rattles are eliminated based on the uniform operating characteristic of the secondary mass and therefore no rattles are received in the transmission input shaft.

One drawback of the dual-mass flywheel can be pointed while looking at the second part of figure 2.4, the engine irregularities rise with the use of a dual-mass flywheel due to the reduced mass the primary flywheel has. However, good vibration isolation especially at low speeds can lead to lower consumption, especially with engines that have flat torque characteristics. The risen engine irregularities can be eliminated by tuning the accessory drive.

Elimination of droning can also be listed as an advantage in this section.

- **Transmission Relief**

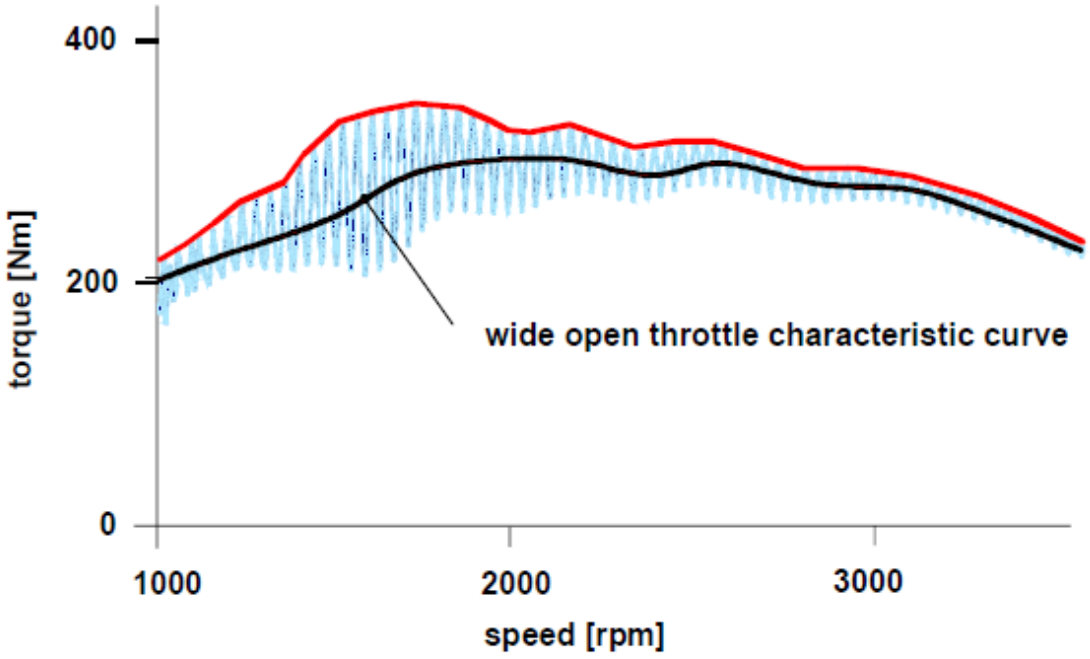


Figure 2.5 – Increase of effective torque due to elimination of engine irregularity, *Luk Kolloquium, 1998*

The risen engine irregularities can be neglected based on the findings of the effective torque's increase. The irregularities are eliminated by appropriate tuning of the drivetrain or accessory drive, therefore the drivetrain, hence the transmission, is relieved of stress and the effective torque increases.

When we look at the wide open throttle characteristics of the engines, and how they are changed under different circumstances, it can also be seen that with the relieved stress, the dual-mass flywheel has a slight advantage over conventional flywheels. With the use of a conventional system, the engine irregularities hence the additional torques create an almost %10 extra load depending on the speed characteristics. This extra load is eliminated with a dual-mass flywheel, when the engine irregularities and the oscillations in torsional vibrations are eliminated, or at least damped to acceptable levels, as figure 2.6 shows, especially with diesel engines.

| | gasoline | diesel |
|---|---|---|
| conventional | 100 % | 100 % |
| DMFW | 105 % | 110 % |

Figure 2.6 – Increase of the transmission load capacity with the use of dual-mass flywheels, *Luk Kolloquium, 1998*

- **Crankshaft Relief**

In a conventional flywheel system, the high massed flywheel is directly connected to the crankshaft. Therefore, the high inertia property of the flywheel creates high reaction forces on the crankshaft. The dual-mass flywheel meanwhile acts more advantageously while the secondary mass is only loosely connected to the first mass through the torsion damper and the roller bearings. This allows the secondary wheel to create almost no physical reactions on the crankshaft.

Another reason of the crankshaft relief is the low mass property of the primary mass. The primary mass of the dual-mass flywheel is lighter than a conventional flywheel, and has an elastic construction like a flex plate of a torque converter.

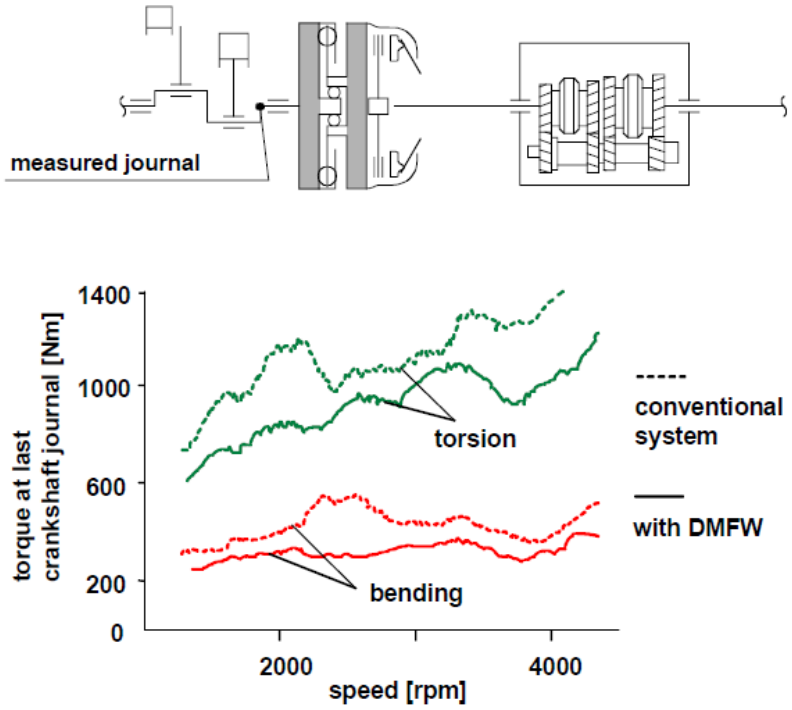


Figure 2.7 – Reduction of torsion and bending vibrations on the crankshaft when a DMF is used, *Luk Kolloquium, 1998*

As it can be seen on figure 2.7 the bending and torsion vibrations drop significantly with the use of a dual-mass flywheel. Also the irregularities in the bending vibrations are reduced, therefore a steady bending vibration profile is achieved.

- **Engine Start**

The typical resonance behavior of the engine during startup has always been problematic. It is known that with higher engine excitations, the resonance amplitudes are higher with the diesel engines. Therefore, it is safe to say that the dual-mass flywheel use is a good fit for diesel engines.

Each time the engine starts, the flywheel in use must pass the resonance frequency. This situation also applies to the dual-mass flywheel, no matter what the mass properties of both primary and secondary masses are. The development and the use of the dual-mass flywheel is a constant struggle against these resonance frequencies and engine startups, although the use of any kind of damping is in favor of the part. This can be basic friction, load friction, or in our case

with the use of an arc spring in the dual-mass flywheel, arc spring damping. But even these damping characteristics have a limit, and both for the safety of the drivetrain and the part itself, they should be immensely considered.

When the engine start is in question, the starting torque is an essential part. The starting torque, which can be defined as the torque engine receives through the starter, defines the acceleration the engine can speed up through, hence with better acceleration the resonance area can be passed faster. With an excessive amount of time to pass through the resonance area, critical failure in the drivetrain components can occur. The situation that the low acceleration of the engine during startup can be named as “suspended start”, and must be avoided for the sake of dual-mass flywheel, therefore the whole drivetrain.

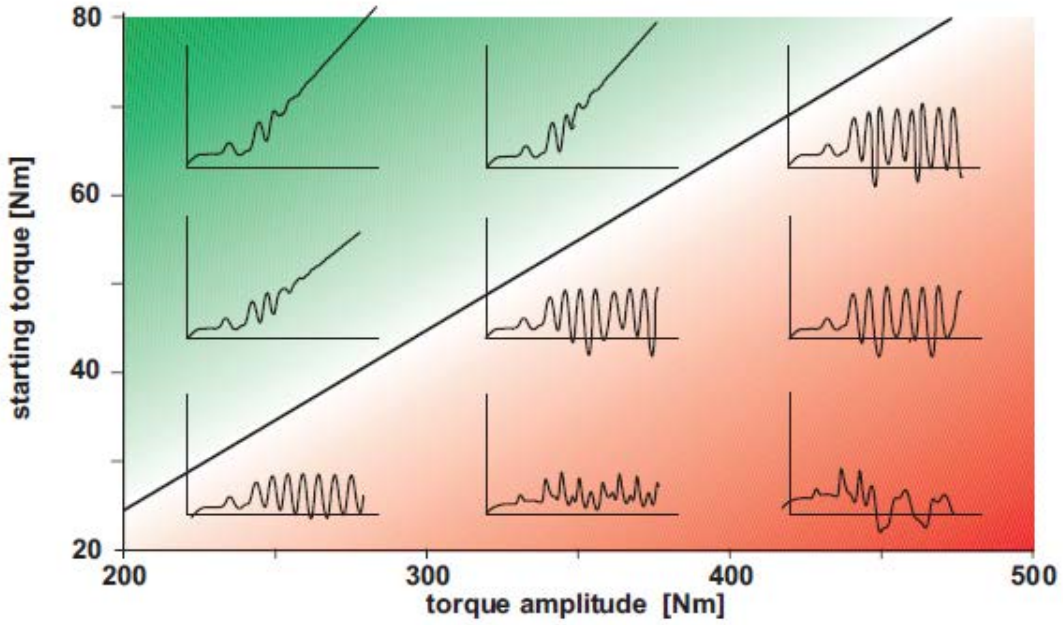


Figure 2.8a. – Influence of the torque amplitude and the starting torque on engine behavior, in correspondence of engine speed(vertical) and time (horizontal), *Luk Kolloquium, 1998*

Figure 2.8a shows how the engine performs well with higher starting torque values. But it shouldn’t be neglected that even with higher starting torques, the torque amplitudes must be considered, and be kept at a minimum. The torque amplitudes can be reduced through means of damping, or simply by design/optimization choices. Figure 2.8b shows the safe and critical zones during engine start up with the consideration of resonance frequencies.

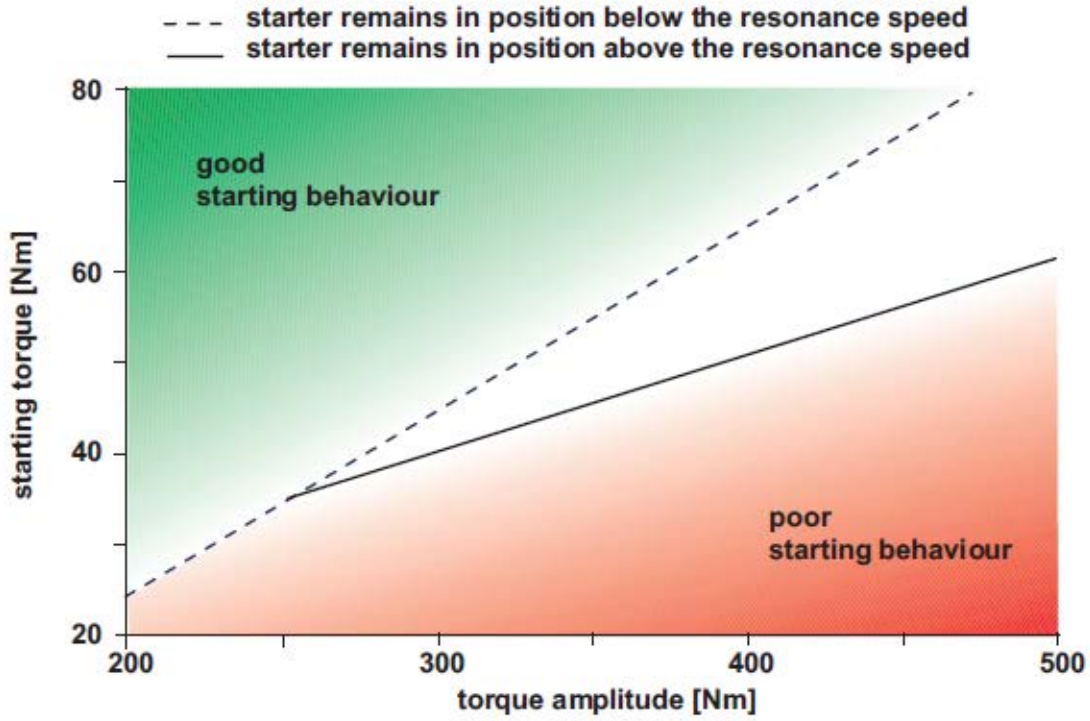


Figure 2.8b – Limit lines for good engine starting behavior and poor engine starting behavior, *Luk Kolloquium, 1998*

As it can be seen there is a limit line between good and poor engine starting behavior which is diagonal. The range which can be considered safe for the engine is above this diagonal line. The smaller the starting torque is, the more the line is shifted downwards. A large starter inertia is considered to reduce the engine irregularities, which is later on reduced on the crankshaft.

The starting engine behavior can also be improved by the following options;

- Higher engine starting torque
- Starter left in a position higher than the resonance speeds
- Higher starter speed
- Means of damping
- Higher primary mass for the dual-mass flywheel
- Smaller secondary mass for the dual-mass flywheel
- Flat spring rate for the rotation damper

### 2.1.3. Inertia Calculations for the Dual Mass Flywheel

Figure 2.9 – Example of the testing of rotational Amplitude for the Clutch Plate, *Juliska, 2016*

The inertia calculations for the chosen DMF was done using the testing equipment at the automotive lab facilities in Juliska, Prague.

The massed parts of the dual-mass fly wheel were connected to the string, with an already determined stiffness of “k”. Please see figures below for the basic testing scheme;

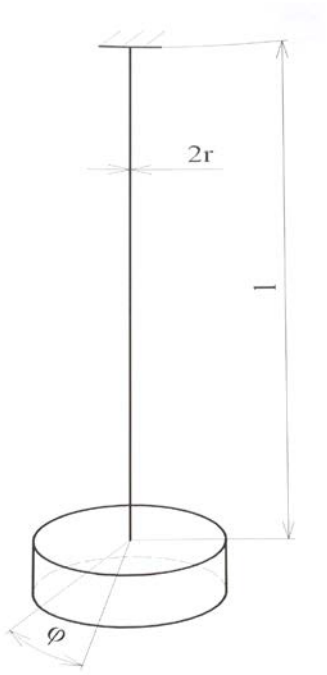


Figure 2.10 – Basic Scheme of the Testing Model

For figure 2.10 the variables will follow as;

$r \rightarrow radius\ of\ the\ string$

$\varphi \rightarrow Angular\ Rotation\ for\ the\ connected\ mass$

$l \rightarrow The\ length\ of\ the\ string$

$k \rightarrow torsional\ stiffness\ of\ the\ string$

After connecting the necessary massed parts to the testing equipment, the part is rotated with a small amplitude, where a part of the mass is set to trigger the optical laser sensor each time it rotates back and forth to the same position. Afterwards, using the LabView software, the time amplitude is viewed and used for further calculations to reach the inertia of the part.

$$I \cdot \varepsilon + k \cdot \varphi = 0$$

$$\ddot{\varphi} + \frac{k}{I}\varphi = 0$$

$$I = \frac{kt^2}{4\pi^2}$$

$$k = \frac{Gd^4\pi}{32l}$$

$$G = 8{,}05e10\ Nm^{-2}$$

$$k = \frac{4\pi^2 I}{t^2}$$

And for the circular plate;

$$I = \frac{1}{2}mr^2$$

To be able to reach the inertia of the connected parts through the measurement of time amplitude;

$$\omega^2 = \frac{k}{I} = \left(\frac{2\pi}{t}\right)^2$$

$$k = \frac{4\pi^2 I}{t^2}$$

And finally;

$I = \frac{kt^2}{4\pi^2}\ (kg * m^2) \rightarrow where\ t =$
$2\tau\ and\ \tau\ is\ the\ measured\ time\ amplitude\ through\ LabView$

| | Primary Mass | Secondary Mass |
|---|---|---|
| t=2τ | **2.742** | **1.744** |
| Inertia (kg*m^2) | **0.0743** | **0.0301** |

Table 2.1 - The Results of Inertia Calculation for the masses of the DMF

### 2.1.4. Torsional Stiffness of the Dual Mass Flywheel

The torsional stiffness between the masses of the DMF is needed both to be put in the simulation, and also to get to the limit dynamic torque. The limit dynamic torque will be dependent on both the torsional stiffness, and the maximum angular phase difference between the first and the secondary mass of the DMF.

The springs within the dual-mass flywheel are both circular springs. To be able to get to the torsional stiffness, first it is needed to calculate the longitudinal stiffness of each mass, and then transform these into actual torsional stiffness.

The basic longitudinal stiffness for wire springs will be used;

$$k = \frac{G * d^4}{8 * n * D^3}$$

Where;

$k \rightarrow Spring\ Constant\ \left(\frac{N}{mm}\right)$

$G = 81000\ Mpa\ for\ Steel \rightarrow\ Modulus\ of\ Elasticity\ in\ shear$

$d \rightarrow Wire\ diameter$

$D \rightarrow Mean\ Spring\ Diameter\ (mm)$

$n \rightarrow Number\ of\ active\ coils$

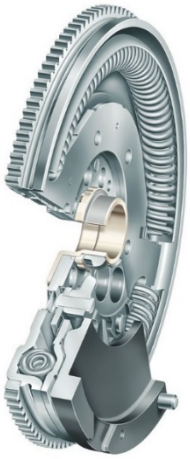

Figure 2.11 – Dual-Mass Flywheel Profile

| | Small Spring | Big Spring |
|---|---|---|
| d(mm) | 2,5 | 4 |
| D(mm) | 10,6 | 16,9 |
| n | 86 | 60 |

Table 2.2 - The Dimensions of the DMF Springs

Therefore, the longitudinal stiffness for the springs will be;

$$k_{small} = 3{,}861348674 \frac{N}{mm}$$

$$k_{big} = 8{,}950012317 \frac{N}{mm}$$

2.1.4.1. **Translation of Longitudinal Stiffness to Torsional Stiffness**

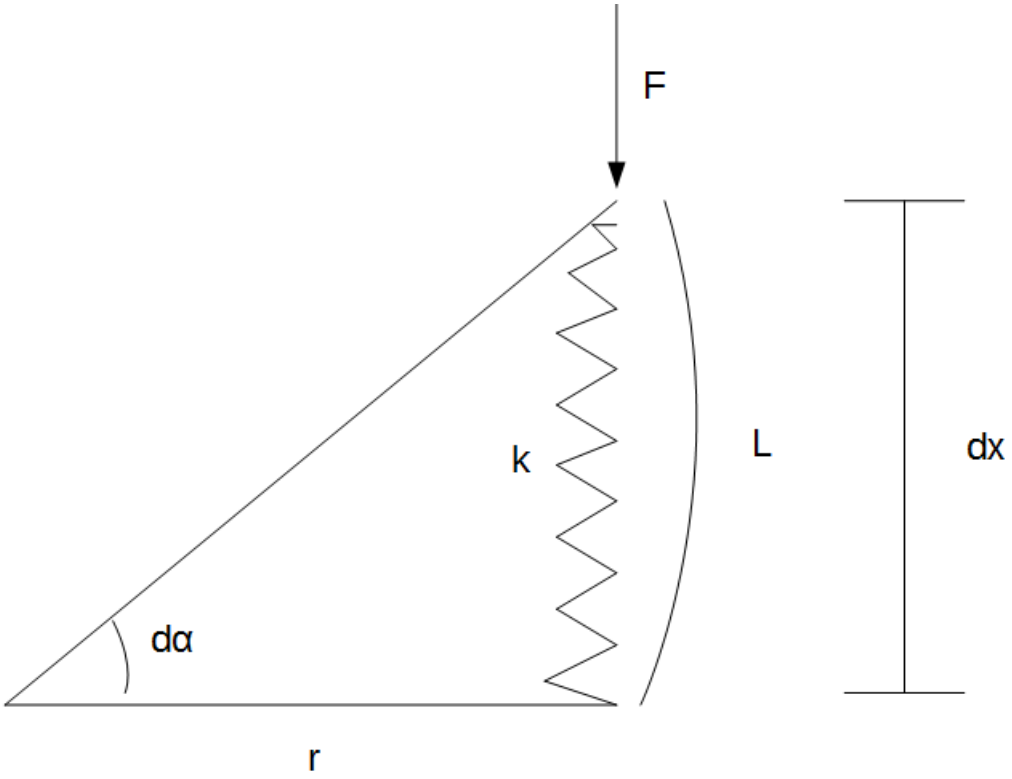


Figure 2.12 – Basic Scheme of the Translation

The springs in the DMF masses are placed within the primary mass and to circularly go around it. After the initial calculation of the longitudinal stiffness of the springs, the next step will be calculating the torsional stiffness through differential equations. Please see figure 2.12 where;

$d\alpha \rightarrow The\ angle\ between\ the\ 2\ beams$

$k \rightarrow Longitudinal\ stiffness\ of\ the\ spring$

$L \rightarrow Arc\ length\ between\ the\ beams$

$dx \rightarrow Vertical\ distance\ between\ the\ end\ points\ of\ the\ beams$

$F \rightarrow Force\ applied\ to\ the\ beam\ therefore\ the\ spring$

$r \rightarrow Spring\ distance\ to\ the\ rotational\ center$

Now to translate the stiffness;

$T = F * r \rightarrow Torque\ Applied\ on\ the\ beam\ in\ Nm$

$L = \alpha * r \rightarrow Arc\ length\ in\ mm$

For very small lengths the difference between dx and L can be neglected therefore;

$L = dx \rightarrow dx = d\alpha * r$

The definition of torsional stiffness follows as;

$$C_T = \frac{T}{d\alpha}$$

And if we apply the previous equations to this equation in differential form;

$$C_T = \frac{F * r}{d\alpha} = \frac{k * dx * r}{d\alpha} = \frac{k * d\alpha * r * r}{d\alpha} = k * r^2 \rightarrow Torsional\ Stiffness\ in \frac{Nm}{rad}$$

$r = 0.12\ m$

So now it can be concluded that;

$$C_{Tsmall} = k_{small} * r^2 = 55{,}60342091 \frac{Nm}{rad}$$

$$C_{Tbig} = k_{big} * r^2 = 128.8801774 \frac{Nm}{rad}$$

$$C_T = 2 * \left(C_{Tsmall} + C_{Tbig}\right) = 368.9671965 = 369 \frac{Nm}{rad}$$

### 2.1.5. Maximum Phase Difference and Critical Dynamic Torque of the Dual Mass Flywheel

The main assumption for the limit angular phase difference for the DMF will be the limit of the springs. This means that, when the distance between the active coils of any spring between the masses reach zero, the DMF will not be able to transfer torque with damping anymore. Therefore, for the simulation and analysis of the dynamic torque, the calculation for the limit angular phase is needed.

$x_1 = 2.5\ mm \rightarrow Distance\ between\ the\ coils\ for\ the\ big\ spring$

$x_2 = 1.8\ mm \rightarrow Distance\ between\ the\ coils\ for\ the\ small\ spring$

$n_1 = 60 \rightarrow Number\ of\ coils\ for\ the\ big\ spring$

$n_2 = 86 \rightarrow Number\ of\ coils\ for\ the\ small\ spring$

$X_1 = x_1 * (n_1 - 1) = 147.5\ mm \rightarrow Limit\ arc\ distance$ for the big spring

$X_2 = x_2 * (n_2 - 1) = 153\ mm \rightarrow Limit\ arc\ distance\ for\ the\ small\ spring$

$2 * \pi * r = 753.9822369\ mm \rightarrow Perimeter\ of\ the\ whole\ Circle\ for\ the\ springs$

The smaller limit arc distance will be the limit for the maximum angular phase difference.

$753{,}9822369 \rightarrow 360^0$

$$\alpha = \frac{360 * 147.5}{753.9822369} = 70.43^0 \rightarrow Maximum\ Angular\ Phase\ difference\ between\ the\ masses$$

It is important that taking the limits of the dual-mass flywheel into account to generate a critical dynamic torque result. This result will be used later on when the DMF is simulated through GT-

Suite, and using the results obtained through to software, it can be seen if the DMF in question is relatively safe to use, or there should be improvements made upon. Depending on the simulation results, the options will be discussed later on.

The DMF in question is a LUK dual-mass flywheel with an OEM number 028 105 264. The maximum angular phase difference between the first and the second mass of this flywheel model is limited at 70.43 degrees. So it is needed to be found how much of a dynamic torque will create this kind of angular phase difference to obtain a critical value.

$C_T = 369 \frac{Nm}{rad} \rightarrow Torsional\ stiffness\ between\ the\ first\ and\ the\ second\ mass\ of\ DMF$

$\pi\ (rad) = 180^0 degrees$

$1\ rad = \frac{180}{\pi} = 57.9^0$

$C_T = 369 \frac{Nm}{rad} \rightarrow 57.9^0$

$C_T = \frac{369}{57.9} = 6.37\ Nm\ per\ degree$

$T_{crit} = C_T(per\ degree) * 70.43 = 448.81\ Nm \rightarrow Critical\ Dynamic\ Torque\ Value$

## 2.2. Planetary Gear Set

### 2.2.1. Calculation of the Gear Ratio

The planetary gear set that will be used in the final system is taken from a Citroen ZF 4HP20 automatic transmission. While the transmission itself has 4 forward and 1 reverse gear settings, only one of the forward gear settings will be used in the final engine tilting stand system. Therefore, the special planetary set from this automatic transmission is being used to obtain the necessary gear ratio.

To be able to provide the 4 forward and 1 reverse gear settings, the automatic transmission ZF 4HP20 has a Simpson type epicyclic gear train. This consists of 2 simple epicyclic gear sets that are connected together. The elements of the system are;

- Two sun wheels P1 and P2,
- Two sets of planet wheels S1 and S2,
- Two planet wheel carriers PS1 and PS2,
- Two rings C1 and C2,

And the two gear trains in the system are connected by;

- The planet wheel carrier PS1 and the ring C2 are joined together
- The planet wheel carrier PS2 and the ring C1 are joined together

While the maximum rotational speed of the dynamometer is 12000 RPM and maximum rotational speed for the engine is 6000 RPM, the bounding condition for the system is the rotational speed of the hydro elements. The maximum continuous operating speed for the pump is listed as 4000 RPM, and maximum self-priming speed is listed as 2300 RPM. Therefore, an average value of 3000 RPM is set as a boundary condition for the hydro elements and a gear ratio of minimum 2 is to be set on the planetary set.

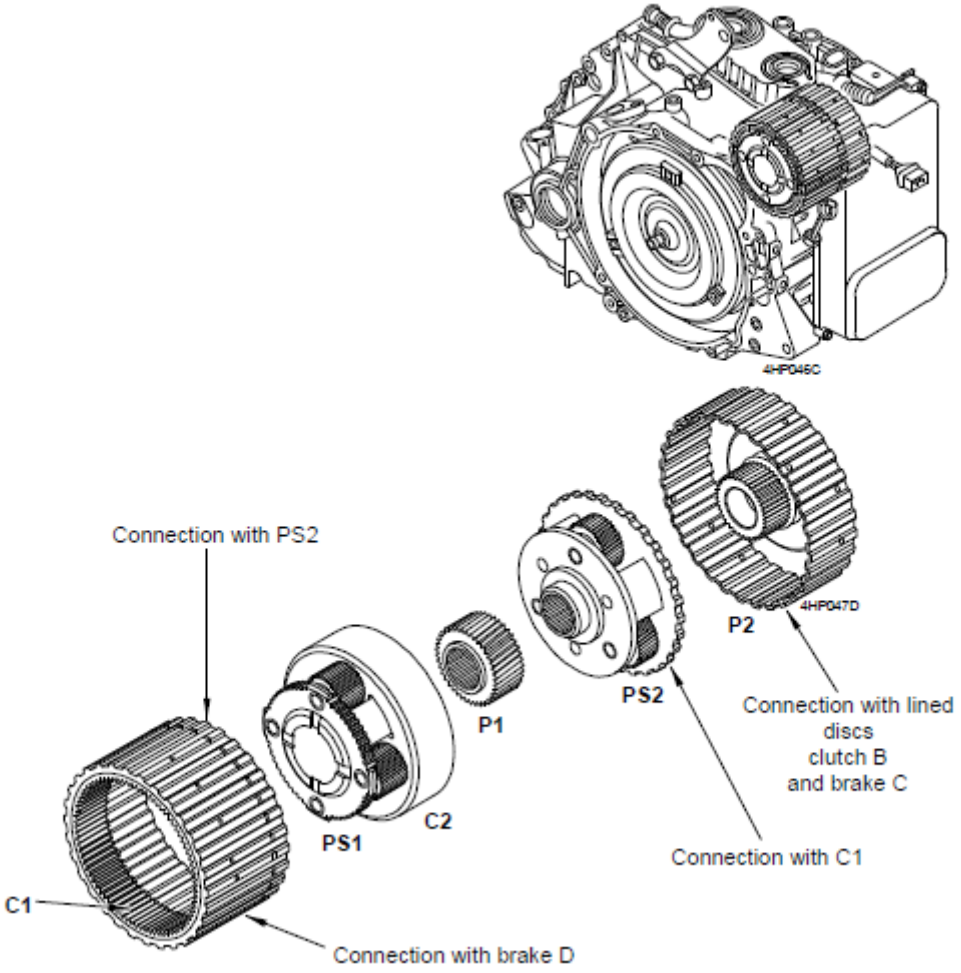


Figure 2.13 – A view of the disassembled planetary set, *Citroen ZF 4HP20 Technical Book*

| | |
|---|---|
| Sunwheel **P1** | 39 teeth |
| Sunwheel **P2** | 37 teeth |
| Planet wheel **S1** | 21 teeth |
| Planet wheel **S2** | 29 teeth |
| Ring **C1** | 81 teeth |
| Ring **C2** | 95 teeth |

Table 2.3 – Number of gear teeth for each planetary part, *Citroen ZF 4HP20 Technical Book*

For the system in use, the input will be sun wheel P1, and the output will be ring C1. Due to this, the ratio for the gear reduction will be;

$$i_{GR} = i_{P1C1}^{S1}(Sun\ to\ ring\ while\ planet\ is\ fixed) = -\frac{81}{39} = -2.077$$

A cross section picture of the planned assembly can be seen in figure 2.14.

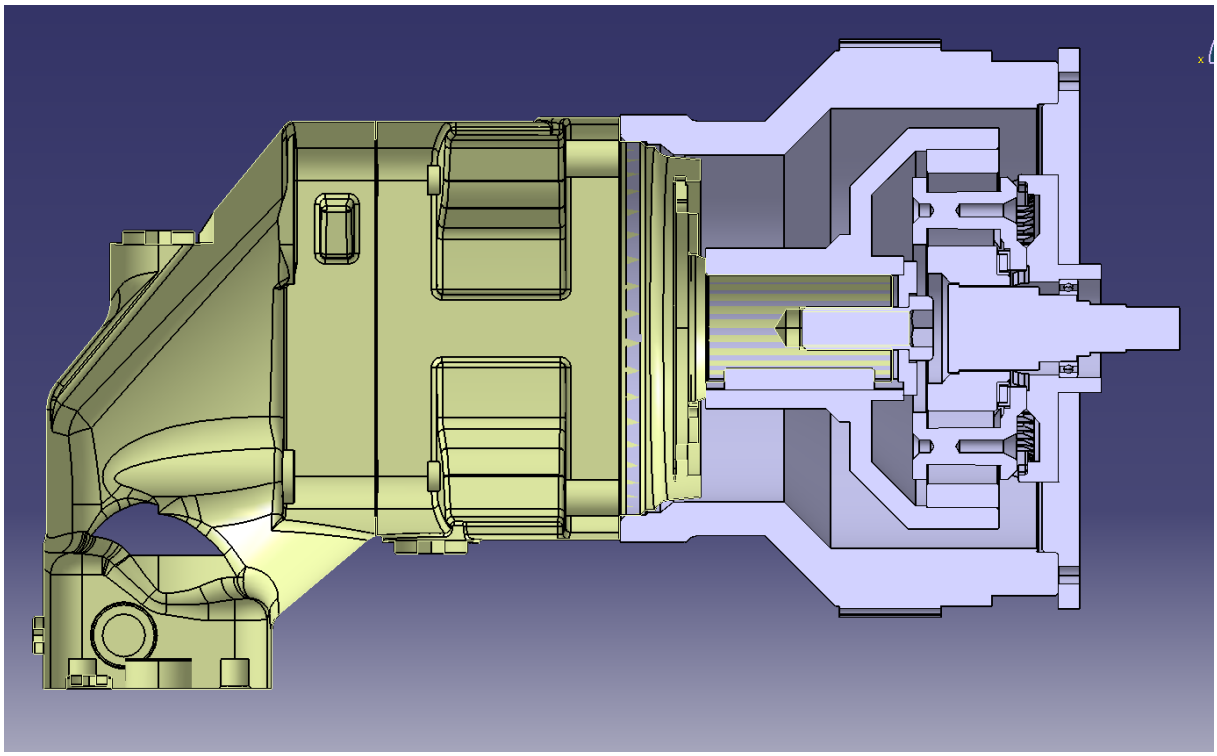

Figure 2.14 – A cross section view of the planned assembly, *David Svetlik, 2017*

### 2.2.2. Inertia and Torsional Stiffness Calculation for the Input Shaft

While the planetary set and all of its elements are a part of the system, the reduction system itself is still in the process of design and assembly. Due the possible changes that can be made to this assembly, and also possible new designs of special parts that can perfectly assemble the planetary set to the hydro generator, the inertia of the planetary elements will be neglected. During this section and afterwards during the build of the both analytical and dynamic model, the only part that will be taken into account from the assembly in figure 2.14 will be the input shaft. The torsional stiffness of the input shaft will take place between the secondary mass of the dual mass flywheel and hydro generator, while the inertia of the shaft will be added on the secondary mass inertia.

The input shaft that can be seen on the right side of the assembly in figure 2.14, which was specifically designed for the system by Mr. David Svetlik, can be assumed to consist of 6 cylinder parts with different diameters and lengths each, which will form the final state of the shaft. The inertia and the torsional stiffness of the input shaft will be obtained by analytical calculations using the dimensions of the shaft obtained through the design software.

The variables that will be used for the steel shaft will be;

$\rho = 7850\ (kgm^{-3}) \rightarrow Density\ of\ Steel$

$E = 2.05 * 10^{5} (Mpa) \rightarrow Young's\ Modulus$

$\mu = 0.3 \rightarrow Poisson's\ Ratio$

$G = 8.08 * 10^{4} (Mpa) \rightarrow Shear\ Modulus$

$J_p = \pi * \frac{D^4}{32}\ (m^4) \rightarrow Polar\ Moment\ of\ Inertia$

$I = Jp * \rho * L\ (kg * m^2) \rightarrow Inertia\ of\ a\ cylinder\ rotationg\ around\ its\ own\ axis$

$L \rightarrow lentgh\ of\ the\ shaft\ (m)$

$C = G * \frac{Jp}{L}\ (Nm * rad^{-1}) \rightarrow Torsional\ Stiffness\ Of\ the\ Shaft$

Therefore, using these formulas and the dimensions of the shaft;

| Element | D | L | Jp | I | C |
|---|---|---|---|---|---|
| | [mm] | [mm] | [m4] | [kg.m2] | [Nm.rad-1] |
| 1 | 16,00 | 20,00 | 6,43E-09 | 1,01E-06 | 2,60E+04 |
| 2 | 18,00 | 13,50 | 1,03E-08 | 1,09E-06 | 6,17E+04 |
| 3 | 20,46 | 5,00 | 1,72E-08 | 6,75E-07 | 2,78E+05 |
| 4 | 25,00 | 14,00 | 3,83E-08 | 4,21E-06 | 2,21E+05 |
| 5 | 31,00 | 30,00 | 9,07E-08 | 2,14E-05 | 2,44E+05 |
| 6 | 33,00 | 3,20 | 1,16E-07 | 2,92E-06 | 2,94E+06 |

Table 2.4 – The inertia and torsional stiffness calculation for the input shaft

Using these separate inertias and torsional stiffness, the final values of inertia and torsional stiffness will be calculated as;

$I_{IS} = I\_1 + I\_2 + I\_3 + I\_4 + I\_5 + I\_6 = \ 0{,}00003127\ kg * m^2$

$C_{IS} = \frac{1}{\frac{1}{C_1}+\frac{1}{C_2}+\frac{1}{C_3}+\frac{1}{C_4}+\frac{1}{C_5}+\frac{1}{C_6}} = 14868\ Nm * rad^{-1}$

### 2.3. Parker Hydraulic Pump F12-80

The hydraulic pump used on the system is a Parker F12-80 heavy duty motor pump. These pumps can be used in numerous applications, for both open and closed circuits. F12 series are produced within the standards of ISO and SAE, with proper mounting flange and shaft configurations, and due to their unique spherical piston designs, they can be used on very high shaft speeds, which also applies to our system. Without taking losses into account, this series motor pumps can take up to 480 bars of pressure.

The 40 degrees angle between the shaft and the cylinder barrel offers a light and compact design, and laminated piston rings offer low amount of thermal leakage and thermal shock resistance. Another advantage of these series is that they offer high torque both at start up and low speeds. Also the timing gear synchronizes the shaft and the barrel, offering optimal resistance against torsional vibrations. Thanks to the heavy duty roller bearings, the pump can also endure a significant amount of axial and radial loads on the shaft.

The pump F12-80 is to come after the planetary gear set on our system, which can be seen on the simulation model later on, and by in order the system will be set up as planetary gear set, hydro generator, hydro motor, and then the dyno, while the torsional stiffness values in between will be taken into account.

Please see figure 2.15 for an exemplary scheme of the pump being used on our system.

**F12 cross sections**

**F12-30, -40, -60 and -80**

(F12-60 shown)

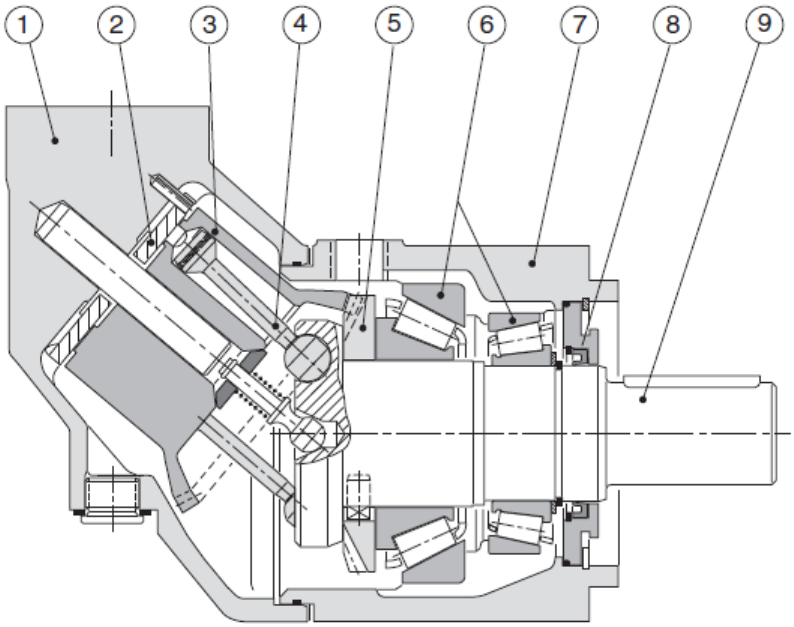


Legend:

1. Barrel housing
2. Valve plate
3. Cylinder barrel
4. Piston with piston ring
5. Timing gear
6. Tapered roller bearings
7. Bearing housing
8. Shaft seal
9. Output/input shaft
10. Port E (F12-110)
11. Needle bearings (F12-110)

Figure 2.15 – The F12 series cross section, *Parker Catalogue, March 2004*

While the for the system the F12-80 looks like an optimal fit, for the sake of the safety of the system and to properly be able to analyze the system on our simulation, the limits of the pump is needed to be known. The properties of the hydraulic motor/pump which are taken from the Parker catalogue follow as;

| | | |
|---|---|---|
| Displacement | **cm^3/rev** | **80.4** |
| Operating Pressure Max. Intermittent | **bar** | **480** |
| Operating Pressure Max. Continuous | **bar** | **420** |
| Motor Max. Intermittent Op. Speed | **rpm** | **5200** |
| Motor Max. Continuous Op. Speed | **rpm** | **4000** |
| Motor Min. Continuous Op. Speed | **rpm** | **50** |
| Motor Max. Intermittent Input Flow | **l/min** | **418** |
| Motor Max. Continuous Input Flow | **l/min** | **322** |
| Mass Moments of Inertia | **kg*m^2** | **0.0084** |
| Weight | **kg** | **26** |

Table 2.5 – The Properties of the F12-80, *Parker Catalogue, March 2004*

Since there is a reduction gearbox between the secondary mass of the dual-mass flywheel and the hydro generator the, the rotational speed of the pump/motor will always be the half of the dual-mass flywheel, therefore the engine. The engine is planned to go up to 6000 RPM, so the pump/motor rotational speed will be limited from 0 to 3000.

Using the formula above, the flow chart of the pump will be as below;

| RPM | Volumetric Ef. | Flow |
|---|---|---|
| 0 | 0,92 | 0 |
| 100 | 0,92 | 8,73913 |
| 200 | 0,92 | 17,47826 |
| 300 | 0,92 | 26,21739 |
| 400 | 0,92 | 34,95652 |
| 500 | 0,93 | 43,22581 |
| 600 | 0,93 | 51,87097 |
| 700 | 0,93 | 60,51613 |
| 800 | 0,93 | 69,16129 |
| 900 | 0,93 | 77,80645 |
| 1000 | 0,95 | 84,63158 |
| 1100 | 0,95 | 93,09474 |
| 1200 | 0,95 | 101,5579 |
| 1300 | 0,95 | 110,0211 |
| 1400 | 0,95 | 118,4842 |
| 1500 | 0,95 | 126,9474 |
| 1600 | 0,96 | 134 |
| 1700 | 0,96 | 142,375 |
| 1800 | 0,96 | 150,75 |
| 1900 | 0,96 | 159,125 |
| 2000 | 0,97 | 165,7732 |
| 2100 | 0,97 | 174,0619 |
| 2200 | 0,97 | 182,3505 |
| 2300 | 0,97 | 190,6392 |
| 2400 | 0,97 | 198,9278 |
| 2500 | 0,98 | 205,102 |
| 2600 | 0,98 | 213,3061 |
| 2700 | 0,98 | 221,5102 |
| 2800 | 0,98 | 229,7143 |
| 2900 | 0,98 | 237,9184 |
| 3000 | 0,98 | 246,1224 |

Table 2.6 – The Rotational Speed – Flow Chart of the F12-80

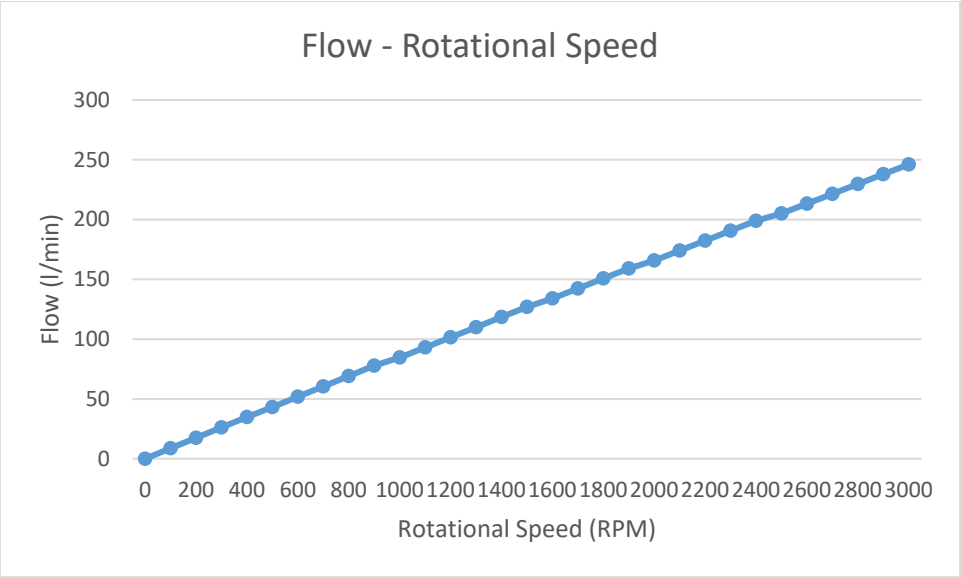


Figure 2.16 – The Graphical Display of the change of flow

All the values for the flow are within the given limit on the catalogue, including the rotational speed itself. Therefore, it can be said that the pump will not have any problems carrying the amount of flow through the system.

It is of dire importance to check the differential pressure, therefore the pressure the pump is projected to, but before running the system there is no way of properly getting this data. Due to this fact, the differential pressure, and the power data will be analyzed within the "dynamic model" section, where the whole system will be modeled and simulated on GT-suite.

### 2.3.1. Torsional Stiffness Between Hydro Motor and Hydro Generator

For the calculation of torsional stiffness between the hydro elements, a different approach has to be taken. The connection between the hydro elements are not of a conventional shaft/rotational system, therefore a combination of dynamics and fluid dynamics will be used to achieve the proper torsional stiffness value.

The first step will be to calculate the stiffness of oil that goes through the pipe between the hydro elements.

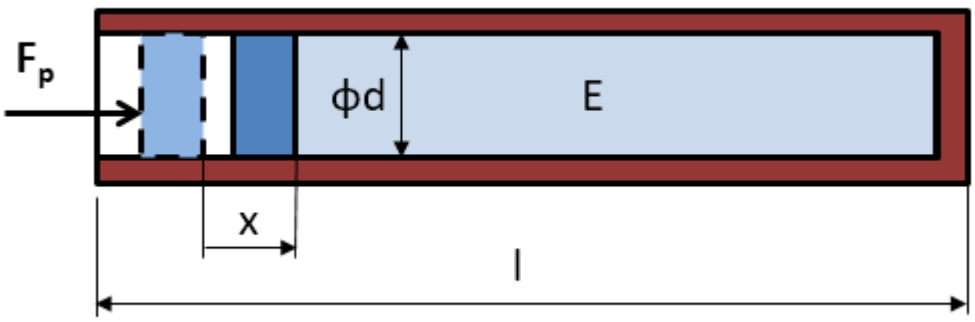


Figure 2.17 – Schematic of the pipe, *David Svetlik, 2016*

The necessary variables for the calculation of oil stiffness follow as;

$d \rightarrow piston\ diameter(m)$

$A \rightarrow Piston\ area\ (m^2)$

$E \rightarrow Elasticity\ module\ of\ the\ oil\ used(Pa)$

$F \rightarrow Force\ applied\ on\ the\ piston\ (N)$

$l \rightarrow length\ of\ the\ pipe\ (m)$

$x \rightarrow amount\ of\ piston\ movement\ in\ the\ pipe\ (m)$

$K \rightarrow stiffness\ of\ the\ oil\ in\ the\ pipe\ (Nm^{-1})$

$W \rightarrow Work\ required\ to\ deform\ the\ oil\ in\ the\ pipe\ (Nm)$

The calculation will require Hooke's law to get to the force required to move the piston in the pipe. The assumption of fully rigid pipe has been made to proceed with the calculation. Therefore;

$\sigma = \frac{Fp}{A} \rightarrow F_p = A.\sigma \rightarrow where\ \sigma\ is\ the\ pressure\ applied\ on\ the\ piston\ (Pa)$

$\varepsilon = \frac{x}{l} \rightarrow Ratio\ of\ the\ piston\ movement\ to\ the\ pipe\ length$

$\sigma = E * \varepsilon \rightarrow F_p = E * \varepsilon * A = \frac{E*x*A}{l}$

$K = \frac{F_p}{x} = \frac{E*x*A}{x*l} = \frac{E*A}{l}$

$K = \frac{1800*10^6*\pi*0.025^2}{3*4} = 294524.3113\ Nm^{-1}$

The next step will be proceeding to the connection between hydro generator and hydro motor.

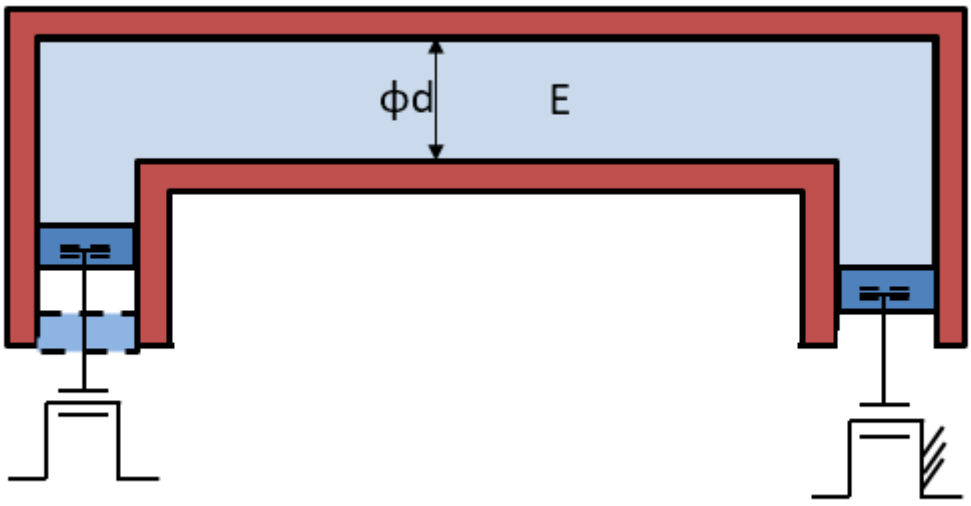


Figure 2.18 – The connection principle of the hydro elements, hydro generator on the left and hydro motor on the right, *David Svetlik, 2016*

The assumption of fully rigid pipe has been made, and the hydro motor shaft has been stopped as a boundary condition.

$M \rightarrow Torque\ moment\ applied\ on\ the\ pump$

$K \rightarrow Stiffness\ of\ the\ oil\ in\ the\ pipe$

$\delta \rightarrow Rotation\ angle\ of\ the\ shaft\ between\ the\ hydro\ elements$

The stiffness between the hydro elements will be calculated using the relationship between the torque moment and the rotation angle.

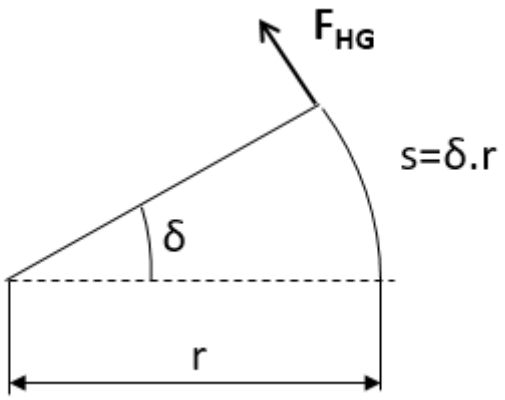


Figure 2.19 – Applying the torque moment on the shaft

The basic scheme of the force being applied on the shaft can be seen on the figure above, where;

$r \rightarrow radius\ of\ the\ shaft$

$s \rightarrow arc\ length\ where\ force\ is\ applied$

$F_{pump} = F_{HG} = Force\ being\ applied$

$W_{pump} = Work\ done\ by\ force\ F_{pump}$

$C \rightarrow Torsional\ Stiffness\ between\ the\ pump\ elements$

$M = F_{HG} * r$

$W_{pump} = \frac{1}{2} * F_{pump} * s = \frac{1}{2} * F_{pump} * \delta * r = \frac{1}{2} * M * \delta$

$C = \frac{M}{\delta} \rightarrow M = C * \delta$ therefore;

$W_{pump} = \frac{1}{2} * C * \delta^2$

Work done on the pump must equal to the work done by deforming the oil in the pipe to compress the piston.

$W = W_{pump}$

$\frac{1}{2} K * x^2 = \frac{1}{2} * C * \delta^2$

So $C = K * (\frac{x^2}{\delta^2})$

To get to the stiffness between hydro elements, a geometric relation between $x\ and\ \delta$ must be found. The geometric volume of the pump per revolution is listed as;

$V_g = 80.4\,\frac{cm^3}{rev}$

$The\ pump\ shaft\ is\ rotated\ by\ the\ angle\ \delta, and\ by\ each\ angular\ rotation$ ;

$The\ volume\ transmitted\ is \rightarrow\ \Delta V_g\ and\ r = 25\ mm$

$when\ \delta = 1^0 = \frac{\pi}{180}\ rad \rightarrow\ \Delta V_g = \frac{Vg}{360} * \delta = \frac{80.4}{360} * 1 = 223.3\ mm^3$

$x = \frac{\Delta V_g}{A} = \frac{223.3*4}{\pi*25^2} = 0.455\ mm = \ 4.55 * 10^{-4} m$

$\frac{x}{\delta} = \frac{4.55*10^{-4}*180}{\pi} = 0.02606\ m * rad^{-1}$

And finally;

$C = K * \left(\frac{x^2}{\delta^2}\right) = 294524.3113 * 0.02606^2 = 200\,\frac{Nm}{rad}$

### 2.4. Mayr Roba DS Couplings – Size 64

The coupling group that will be used on the system is a Mayr Roba DS type coupling on the hydro motor side, and a custom made Roba DS coupling that will be used on the dynamometer side. The size 64 resembles the bore diameter of the coupling. The Roba DS couplings are known for their fair advantages, and the types being used on the system are torsionally rigid shaft couplings, therefore for the connection between the hydro motor and the dynamometer the torsional stiffness value will be taken as a high number to express this rigid connection. The main advantages of using the Roba DS couplings are;

- For up to 100% of the nominal torque, the couplings are non-sensitive to alternating torques.
- High density and low mass inertia.
- Backlash free up to nominal torque.
- High torsional rigidity up to nominal torque.
- Wear and maintenance free.
- Optimum construction shape due to large variant shapes and custom product availability.
- High miss alignment compensation.

An example cross section view of the couplings can be seen in figure 2.21. and the coupling group itself on figure 2.22.

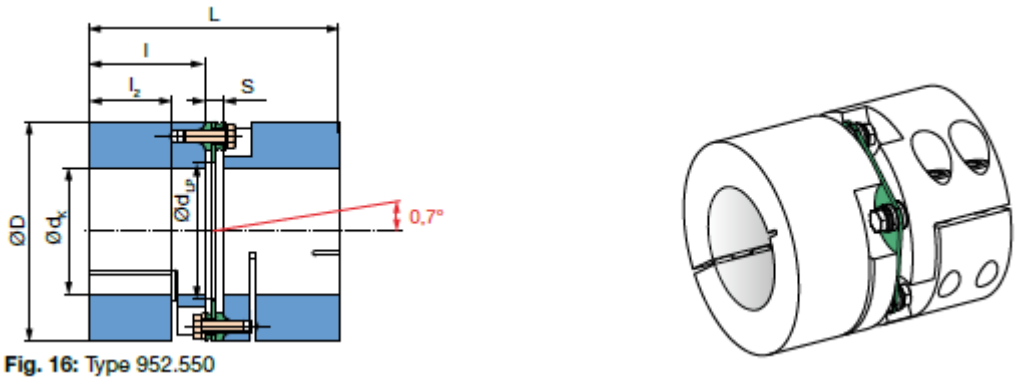

Fig. 16: Type 952.550

Figure 2.20 – Example cross section view of a Roba DS coupling group, *Mayr Catalogue*


Figure 2.21 – The Roba DS coupling group that will be used on the system

For the calculation of inertias and torsional stiffness, the same analytical method that was used for the input shaft of the planetary set will be used. Using the dimensions of the coupling group and the material properties of steel, a summed result of both inertia and torsional stiffness will be obtained.

| | D | d | l | ρ |
|---|---|---|---|---|
| | m | m | m | kg.m-3 |
| 1st Part | 0,123 | 0,04 | 0,034 | 7850 |
| 2nd Part | 0,155 | 0,06 | 0,065 | 7850 |

Table 2.7 – The Dimensions of the parts of coupling group

And the calculation for inertia will follow as;

$I = l * J_p * \rho \rightarrow Moment\ of\ inertia\ in\ kg\ m^2$

Where; $J_p = (D^4 - d^4) * \frac{\pi}{32} \rightarrow polar\ moment\ of\ inertia\ in\ m^4$

$m = \frac{\pi}{4} * (D^2 - d^2) * l * \rho \rightarrow Mass\ in\ kg\ where\ l = length\ of\ the\ part$

And finally for the torsional stiffness;

$C = \frac{G*Jp}{l} \rightarrow Nm\ rad^{-1}$

Therefore, the inertias will be calculated as;

| | D | d | l | ρ | I | m |
|---|---|---|---|---|---|---|
| | m | m | m | kg.m-3 | kg.m2 | kg |
| 1st Part | 0,123 | 0,04 | 0,034 | 7850 | 0,00593 | 2,84 |
| 2nd Part | 0,155 | 0,06 | 0,065 | 7850 | 0,02826 | 8,19 |

Table 2.8 – The inertia calculations of the coupling group

And for the torsional stiffness in between;

| D | d | l | ρ | Jp | I | m | C |
|---|---|---|---|---|---|---|---|
| m | m | m | kg.m-3 | m4 | kg.m2 | kg | Nm/rad |
| 0,04 | 0,035 | 0,3 | 7850 | 1,04004E-07 | 0,00024 | 0,69 | 28001 |

Table 2.9 – The torsional stiffness between the parts of coupling group

As stated before, the connection between the hydro motor and the dynamometer will be a rigid connection to the nature of the couplings. Therefore, the torsional stiffness between these elements will be taken as;

$C_{HD} = 650000(for\ rigid\ connection) + 28001\ (for\ the\ coupling\ connection) = 678001\ Nm * rad^{-1}$

### 2.5. AVL APA 202/12 PX Dynamometer

The dynamometer that will be used on the system is an AVL APA 202/12 PX top accuracy AC dynamometer. These dynamometers by AVL are produced specifically for engine and powertrain tests. The dynamometer will create proper conditions to perfectly perform high accuracy dynamic test cycles by combining extremely accurate speed and torque measurement.

This specific dynamometer was chosen for the system for its high torque and rotational speed capacity. A general use of a dynamometer like this can be explained as engine testing for passenger cars, light and heavy duty trucks, both with or without the vehicle drive train simulation. Testing of racing engines, friction rig tests, component and power pack tests, and

converter tests are also possible areas of use. The advantages of the dynamometer can be listed as;

- High measurement accuracy.
- Reasonable cost and benefit ratio.
- Short amount of time for installation due to pre commissioned components.
- High suitability for transient testing conditions, as well as high dynamic testing conditions.
- Compact design, and low maintenance.

Apart from these advantages, the APA 202/12 PX dynamometer also offers optional zero torque simulation, optional simulation of gear shifting oscillations in the drivetrain, a torque response time better than 3 ms, and good capability of lubrication. The technical data for the dynamometer can be seen on figure 2.23.

| Type (with roller bearings on cradled stator) | Type (with hydrostatic bearings on cradled stator) | Nominal power generator | Nominal torque generator | Max speed | Mass inertia motor (incl. coupling flange) |
|---|---|---|---|---|---|
| - | APA 102/22 Gx | 100 kW | 80 Nm | 22,000 rpm | 0.04 kgm² |
| APA 102/20 Px | - | 120 kW | 100 Nm | 20,000 rpm | 0.05 kgm² |
| APA 102/12 Px | APA 102/12 Gx | 120 kW | 255 Nm | 12,000 rpm | 0.13 kgm² |
| APA 104/8 Px | APA 104/8 Gx | 120 kW | 509 Nm | 8,000 rpm | 0.35 kgm² |
| APA 202/12 Px | APA 202/12 Gx | 220 kW | 525 Nm | 12,000 rpm | 0.32 kgm² |
| APA 204/8 Px | APA 204/8 Gx | 220 kW | 934 Nm | 8,000 rpm | 0.94 kgm² |
| APA100 208/3.5 | - | 220 kW | 1,867 Nm | 3,500 rpm | 4.6 kgm² |
| APA 302/10 Px | APA 302/10 Gx | 330 kW | 700 Nm | 10,000 rpm | 0.53 kgm² |
| APA 304/8 Px | APA 304/8 Gx | 330 kW | 1,400 Nm | 8,000 rpm | 1.9 kgm² |
| APA 308/4 Px | - | 330 kW | 2,801 Nm | 3,500 rpm | 6.5 kgm² |
| APA 402/10 Px | APA 402/10 Gx | 440 kW | 934 Nm | 10,000 rpm | 0.69 kgm² |
| APA 404/8 Px | APA 404/8 Gx | 440 kW | 1,867 Nm | 8,000 rpm | 2.5 kgm² |
| APA 404/6 Px | APA 404/6 Gx | 440 kW | 2,334 Nm | 6,000 rpm | 3.5 kgm² |
| APA 404/4.2 Px | APA 404/4,2 Gx | 440 kW | 2,801 Nm | 4,200pm | 4.5 kgm² |
| APA 408/4 Px | - | 440 kW | 3,735 Nm | 3,500 rpm | 11.1 kgm² |
| APA 504/5 Px | - | 500 kW | 3,000 Nm | 5,000 rpm | 4.5 kgm² |
| APA 602/10 Px | - | 600 kW | 818 Nm | 10,000 rpm | 0.67 kgm² |
| APA 604/5.5 Px | APA 604/5.5 Gx | 660 kW | 3,500 Nm | 5,500 rpm | 7.2 kgm² |
| APA100 604/3.5 | - | 660 kW | 4,400 Nm | 3,500 rpm | 10.7 kgm² |
| APA 704/5 Px | - | 750 kW | 3,500 Nm | 5,000 rpm | 4.5 kgm² |
| APA 802/12 Px | APA 802/12 Gx | 800 kW | 764 Nm | 12,000 rpm | 0.53 kgm² |
| APA100 802/10 | APA 802/10 Gx | 800 kW | 1,060 Nm | 10,000 rpm | 1.3 kgm² |
| APA100 804/8 | - | 800 kW | 3,396 Nm | 8,000 rpm | 6.4 kgm² |
| APA100 804/4 | - | 800 kW | 5,500 Nm | 4,000 rpm | 16.8 kgm² |
| APA 1004/4 Px | APA 1004/4 Gx | 1000 kW | 4,500 Nm | 4,000 rpm | 10.8 kgm² |

Figure 2.22 – Technical data sheet of the dynamometer, *AVL Dyno exact data sheet, 2004*

As can be seen on the data sheet, the features of the dynamometer can be listed as;

- 220 kW nominal power.
- 525 Nm nominal torque.
- 12000 RPM maximum rotational speed.
- 0.32 kg*m^2 moment of inertia.

For the analytical model and dynamic model, the inertia information of 0.32 kg*m^2 will be used. The maximum rotational speed is already above the necessary range (which is 6000 RPM for the engine and 3000 RPM for the hydro elements), as well as the nominal power and torque.

# 3. Evaluating the Natural Frequencies of the System Using the Analytical Model

## 3.1. Building the Analytical Model

For building the analytical model, the scheme of the system that can be seen on figure 1.2 will be used. The analytical model will be built by using a total of 5 inertias, and 4 torsional stiffness. These 5 inertias will be serially linked, while having a torsional stiffness in between each, and the inertia of connection elements apart from the main elements will be added on the main element inertias to create a more proper model. On table 3.1, the inertias of the whole system and how they were changed by the gear ratio can be seen. All of the data were previously calculated on section 2, while the only data that were assumed during this process were the crankshaft inertia, and the torsional stiffness between hydro motor and the dynamometer.

| Name of the Part | I=[kg.m2] | | i(gear ratio) | Ired=[kg.m2] |
|---|---|---|---|---|
| Crankshaft | $I_{CS}$ | 0,01000 | 1 | 0,01000 |
| Primary mass of DMF | $I_{PM}$ | 0,08000 | 1 | 0,08000 |
| Secondary mass of DMF | $I_{SM}$ | 0,07000 | 1 | 0,07000 |
| Input shaft | $I_{IS}$ | 0,00007 | 1 | 0,00007 |
| Hydraulic Pump | $I_{HP}$ | 0,00840 | 2,077 | 0,03623700 |
| Hydraulic Motor | $I_{HM}$ | 0,00840 | 2,077 | 0,03623700 |
| 1st half Roba DS Coupling | $I_{1DS}$ | 0,00593 | 2,077 | 0,02558333 |
| 2nd half Roba DS Coupling | $I_{2DS}$ | 0,02826 | 2,077 | 0,12193272 |
| Dynamometer | $I_{dyno}$ | 0,32000 | 2,077 | 1,38045728 |

Table 3.1 – Inertias of the elements of the system

The first 4 elements that will be taken into account are directly connected to the engine powertrain, therefore the gear ratio for these elements is 1, and the inertia values are not to be changed. However, for the elements that come after the gear reduction on the system, the reduction of inertia with gear reduction principle will be applied therefore;

$I_{red} = I_{nominal} * i_{gearratio}^2$ where;

$I_{red} \rightarrow reduced\ inertia$

$I_{nominal} \rightarrow nominal\ inertia\ before\ the\ gear\ reducion$

$i_{gearratio} \rightarrow precalculated\ gear\ ratio$

As expressed before, the crankshaft inertia is an estimation to be around 0.01 kg*m^2, which will be placed by the actual value in the future development of the engine tilting stand project.

By adding each of 2 inertias on table 3.1, except hydraulic pump, the final inertia values that will be used on both models will be obtained.

| | [kg.m2] |
|---|---|
| **$I_1$** | 0,09000 |
| **$I_2$** | 0,07007 |
| **$I_3$** | 0,03624 |
| **$I_4$** | 0,06182 |
| **Idyno** | 1,50239 |

Table 3.2 – The final inertia values that will be used on the models

The same principle will be applied to obtain the torsional stiffness, all of which were previously calculated on section 2.

| C=[Nm.rad-1] | | i | Cred=[Nm.rad-1] | |
|---|---|---|---|---|
| $C_{DMS}$ | 369 | 1 | 369 | $C_1$ |
| $C_{IS}$ | 14868 | 1 | 14868 | $C_2$ |
| $C_{HsD}$ | 200 | 2,077 | 46 | $C_3$ |
| $C_{DS}$ | 678001 | 2,077 | 157166 | $C_4$ |

Table 3.3. – The final torsional stiffness values that will be used on the models

An important difference between reducing the inertias and torsional stiffness is the way used to obtain a torsional stiffness after a certain gear ratio.

$C_{red} = \frac{C_{nominal}}{i^2_{gearratio}}$ where;

$C_{red} \rightarrow Reduced\ torsional\ stiffness$

$C_{nominal} \rightarrow Nominal\ torsional\ stiffness\ before\ the\ gear\ reduction$

$i_{gearratio} \rightarrow precalculated\ gear\ ratio$

The next step will be calculating the natural frequencies of the system by using the matrix method.

### 3.2. Setting Up the Matrixes and Explanation of Method

For the use of matrix method, the first step will be creating the mass and stiffness matrixes. The mass matrix will consist of inertias, and the stiffness matrix will consist of torsional stiffness of the system serially linked through matrix method.

$$M = \begin{bmatrix} I_1 & 0 & 0 & 0 & 0 \\ 0 & I_2 & 0 & 0 & 0 \\ 0 & 0 & I_3 & 0 & 0 \\ 0 & 0 & 0 & I_4 & 0 \\ 0 & 0 & 0 & 0 & I_5 \end{bmatrix} = \begin{bmatrix} 0.09 & 0 & 0 & 0 & 0 \\ 0 & 0.07003 & 0 & 0 & 0 \\ 0 & 0 & 0.03624 & 0 & 0 \\ 0 & 0 & 0 & 0.06182 & 0 \\ 0 & 0 & 0 & 0 & 1.50239 \end{bmatrix}$$

$$K = \begin{bmatrix} C\_1 & -C_1 & 0 & 0 & 0 \\ -C\_1 & C_1 + C_2 & -C_2 & 0 & 0 \\ 0 & -C_2 & C_2 + C\_3 & -C_3 & 0 \\ 0 & 0 & -C_3 & C_3 + C_4 & -C_4 \\ 0 & 0 & 0 & -C_4 & C_4 \end{bmatrix}$$

The eigenvector of the system can be calculated through the following equation;

$$E = eig(M^{-1} * K) \rightarrow eigen\ vectors\ of\ the\ system$$

$$E = 1000000 * \begin{bmatrix} 0 \\ 0.0003 \\ 0.0078 \\ 0.6252 \\ 2.6476 \end{bmatrix}$$

And finally for the natural frequency values in hertz;

$$N = \frac{E^{0.5}}{2*\pi} \rightarrow Natural\ frequencies\ of\ the\ system\ in\ Hertz$$

$$N = \begin{bmatrix} 258.97 \\ 125.85 \\ 14.02 \\ 2.55 \\ 0 \end{bmatrix}$$

The next step will be evaluating these natural frequencies using a Campbell diagram to estimate where the resonant frequencies will appear during the use of the system.

### 3.3. Evaluating the Results and Campbell Diagram of Natural Frequencies

The natural frequencies by order and their values in rotation per minute can be seen on table 3.4.

| Natural | Frequencies | |
|---|---|---|
| **Nr.** | **Hz.** | **RPM** |
| 1 | 0 | 0 |
| 2 | 2,550 | 153 |
| 3 | 14,02 | 841,2 |
| 4 | 125,85 | 7551 |
| 5 | 258,97 | 15538,2 |

Table 3.4 – The Natural frequencies obtained by analytical model

By converting the natural frequencies to RPM, and then multiplying engine RPM by 4 orders, the following Campbell diagram is obtained to evaluate the critical resonance areas for the system.

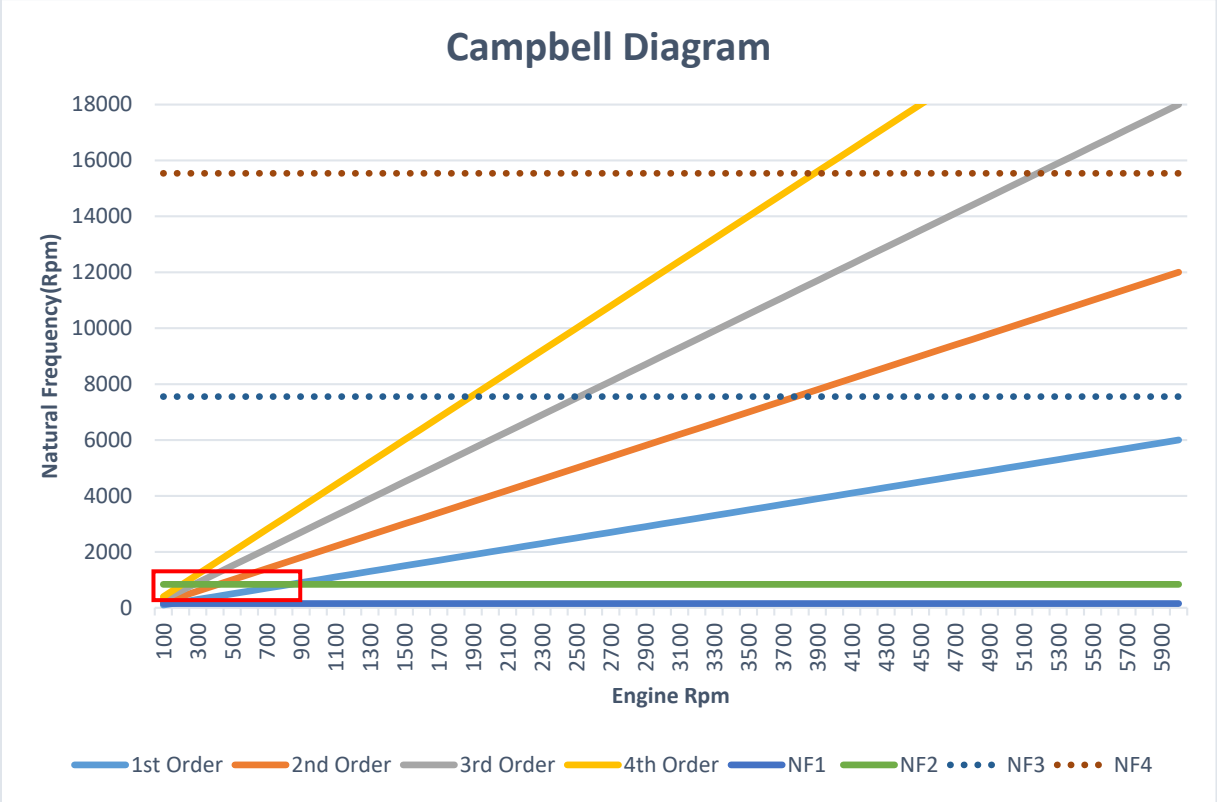


Figure 3.1 – The Campbell Diagram for engine RPM vs. natural frequencies (RPM)

By eliminating the 0 hertz natural frequency, the rest of the 4 natural frequencies can be seen as a straight line that goes through the diagram horizontally. The natural frequencies above 6000 RPM is described as dash lines due to the fact that of them being above the maximum rotational speed of the engine, which will have the highest rotational speed in the system as well as the dual mass flywheel. The rest of the elements in the system will rotate at rotational speed a little less than half of the rotational speed of the engine.

If you take a look at the red rectangle which states the where the RPM of the engine go through the natural frequencies, we can determine where the system will go into resonance during It's run.

The natural frequencies 150 and 841,2 RPM cross with each order, while most importantly on the $1^{st}$ order of the engine (which can also be referred to as natural or $0^{th}$ order) the system goes into resonance 2 times, 1 being in between 0-100 RPM and the other being in 900-1000 RPM.

For $2^{nd}$ engine order the critical rotational speed can be determined as between 0-500 RPM, while for $3^{rd}$ and $4^{th}$ engine order this range gets smaller, and finally for $4^{th}$ engine order the critical area goes down in between 0-100 RPM.

All of these natural frequencies will be evaluated once again during the dynamic simulation of the system, including full load, transient engine starting and stopping conditions. The use of the software GT-Suite and its justification of use and accuracy can be justified if the analytical method results match with the GT-Suite dynamic simulation results.

# 4. Assessment of Natural Frequencies and Dynamic Variables Using the Dynamic Model

### 4.1. Characteristics of the Engine

The engine in question's characteristics are important to be able to analyze many aspects of the torsional system, which will be connected to the engine through a dual-mass flywheel. In this report, the ways of analyzing the dynamic moment between the first and the second mass of the flywheel will be in consideration using the GT-Suite software. Through the phase of the project, the torsional system which will act as a mechanical transmission, will be modeled in 1-D and then simulated through this software. Please keep in mind that the engine in question is a 1.6 Cl Diesel engine.

To be able to even start simulating, first it is needed to get all the necessary input information for the software. The second part of the input data will be the torque characteristics of the engine, and to get this information it is essential to know the characteristics of the engine.

The characteristics of the engine will follow as;

$D = 76.5\,mm \rightarrow Bore\ diameter$

$Z = 86.9\,mm \rightarrow Stroke$

$l = 140\,mm \rightarrow Connecting\ rod\ length$

$\varepsilon = 10.5 \rightarrow Compression\ Ratio$

$m_p = 0.2653\,kg \rightarrow Piston\ mass$

$m_o = 0.3695\,kg \rightarrow Connecting\ Rod\ mass$

$m_S = 0.4501\,kg \rightarrow pos.Mass$

$i_v = 4 \rightarrow Number\ of\ cylinders$

$Fo = 1 - 3 - 4 - 2 \rightarrow Firing\ order$

$S_p = 4596\,mm^2 \rightarrow Piston\ Area$

$V_z = 1597690\,mm^3 \rightarrow Stroke\ Volume$

$\omega \rightarrow Crank\ rotational\ Speed\ in\ \frac{rad}{sec}$

$\lambda = 0.31$

$r = 43.45\,mm$

$x_k = 9.147$

Using these characteristics, first the torque profile of each cylinder will found, and then using the angular phase difference between them, torque characteristic of the engine for each of the given RPMs starting from 1000 RPM to 6000 RPM will be reached.

To start the calculations, first the pre-given data has to be evaluated. Apart from the engine characteristics, the pressure profile for each of the engine RPMs are given. Please take a note

that the pressure characteristics are given in *bars*, and has to be converted to *MPa* to continue with the calculations.

The pressure profile for the engine can be seen at table 4.1. It has to be acknowledged that these profiles are a function of the crank angle between -360 and +360 degrees. This will affect the results that are taken from GT-Suite, which will be generated also as a function of the crank angle, but to achieve the proper dynamic torque results for each of the RPMs, the results will be re-evaluated for each of the RPM case.

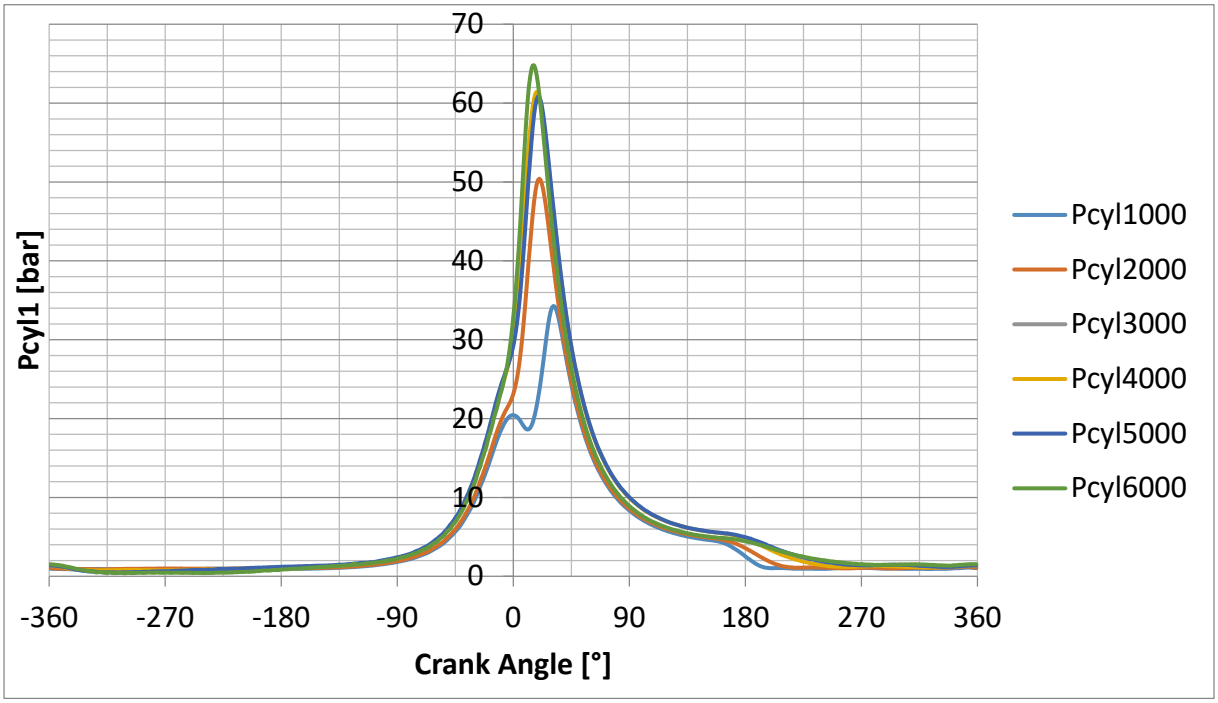


Figure 4.1 – Cylinder Pressure-Crank Angle Comparison

### 4.2. Calculation of the Torque Profile for Full Load

The next step of the calculations will be converting the pressure that is pre-given from bars to MPa, as mentioned earlier.

$$P(MPa) = P(bar) * 0.1$$

And then the alfa angle will be defined, which is the crank angle in radians.

$$\alpha = 0.0174532925 * (Crank\ Angle\ in\ degrees)$$

And then the rest of the variables that need to be used will follow as;

$\beta = Arcsin\frac{(Z*Sin\,\alpha)}{2l} \rightarrow$
$The\ angle\ between\ the\ connecting\ rod\ and\ the\ piston\ normal\ line\ in\ radians$

$x = \left(\frac{Z}{2}\right) + l - \left(\frac{Z}{2}\right) * \cos\alpha - l * cos\beta \rightarrow$
$Distance\ between\ the\ piston\ and\ top\ dead\ end\ in\ mm$

$x_k = \frac{Z}{\varepsilon - 1} \rightarrow Distance\ between\ Top\ dead\ Center\ and\ cylinder\ head\ in\ mm$

$\mathrm{S_p} = \frac{\pi * \mathrm{D}^4}{4} \rightarrow Piston\ Area\ in\ mm^2$

$V = (x + x_k) * S_p \rightarrow Piston\ Swept\ Volume\ in\ dm^3$

$\mathrm{c} = \left(\frac{\mathrm{Z}}{2}\right) * \omega * \sin\alpha + \left(\frac{\lambda}{2}\right) * sin2\alpha \rightarrow Piston\ speed\ in\ ms^{-1}$

$a_p = \left(\left(\frac{Z}{2}\right) * \omega^2 * cos\alpha + \lambda * cos2\alpha\right) * 0.001 \rightarrow Piston\ Acceleration\ in\ ms^{-2}$

$F_p = p * S_p \rightarrow in\ N$

$F_S = -m_s * \left(\frac{Z}{2}\right) * \omega^2 * (cos\alpha + \lambda * cos2\alpha) \rightarrow in\ N$

$F_o = \frac{F_p + F_S}{cos\beta} \rightarrow in\ N$

$F_T = F_o * \sin(\alpha + \beta) \rightarrow in\ N$

$F_R = F_o * \cos(\alpha + \beta) \rightarrow in\ N$

$M_{T1} = F_R * \left(\frac{Z}{2}\right) * 0.001 \rightarrow Torque\ Moment\ of\ the\ first\ cylinder\ in\ Nm$

$M_{T3} \rightarrow Torque\ Moment\ of\ the\ third\ cylinder\ in\ Nm\ with\ 180^o phase\ difference\ to\ M_{T1}$

$M_{T4} \rightarrow Torque\ Moment\ of\ the\ fourth\ cylinder\ in\ Nm\ with\ 180^0 phase\ difference\ to\ M_{T3}$

$M_{T2} \rightarrow Torque\ Moment\ of\ the\ second\ cylinder\ in\ Nm\ with\ 180^0 phase\ difference\ to\ M_{T4}$

After achieving the calculation of the torque moment of the first cylinder, the rest of the cylinder torque moments will be calculated by delaying the results 180 degrees towards the crank center. Which is to say, torque moment of the 3rd cylinder will be the same as the 1st, but the starting point will be at -180 degrees instead of -360 degrees. So the results can be copied to the start from -180th result of the 1st cylinder until +360 degrees, and then the results between -360 and -180 can be copied to the bottom of the table to replace the missing values after the first step. This is caused by the angular phase difference between the cylinders, and the firing order in between the cylinders.

The last step to achieve the torque profile of the given RPM will be adding all these torque values per cylinder together and achieving the engine torque profile of the engine on that RPM.

$\boldsymbol{M_T} = \boldsymbol{M_{T1}} + \boldsymbol{M_{T2}} + \boldsymbol{M_{T3}} + \boldsymbol{M_{T4}} \rightarrow Engine\ Torque\ profile\ on\ the\ given\ RPM\ in\ Nm$

After calculating each of these variables, the results for the cases of RPMs will follow as;

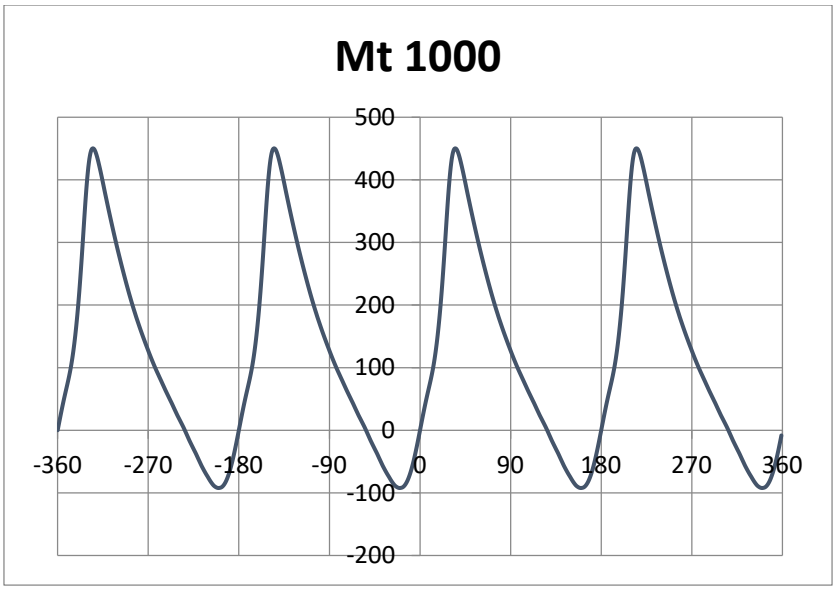


Figure 4.2 – Torque Profile for 1000 RPM

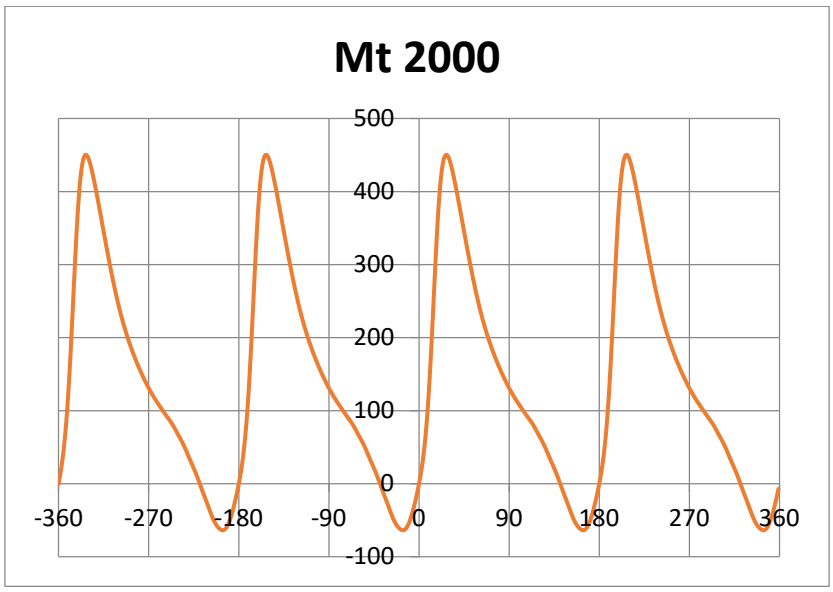


Figure 4.3 – Torque Profile for 2000 RPM

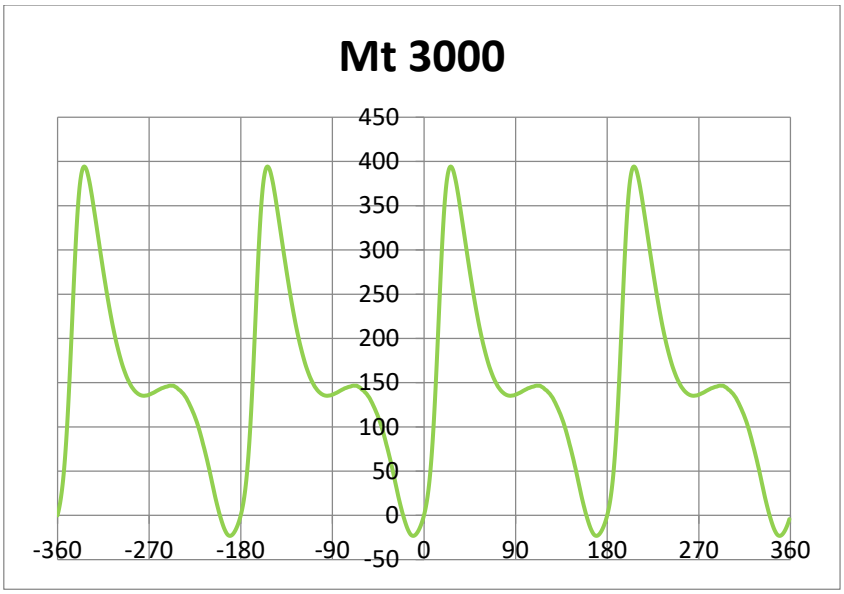


Figure 4.4 – Torque Profile for 3000 RPM

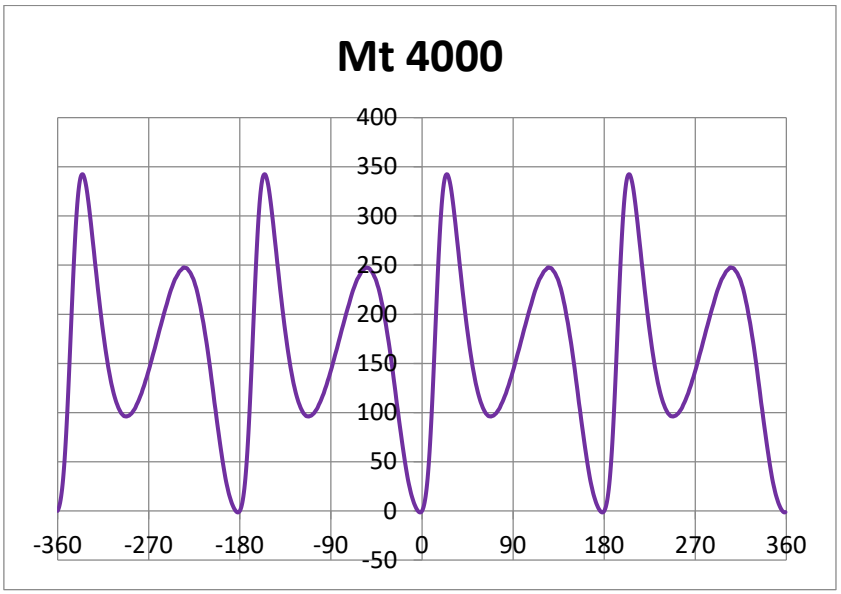


Figure 4.5 – Torque Profile for 4000 RPM

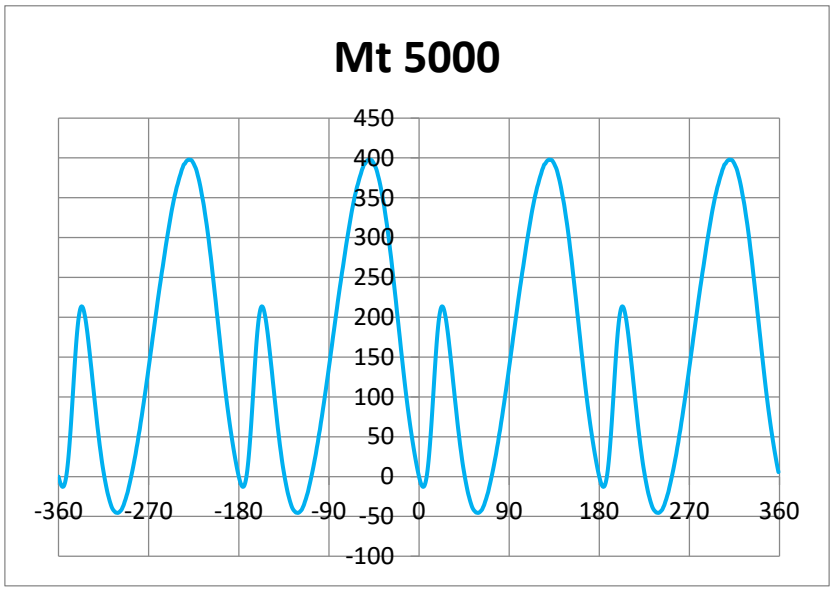


Figure 4.6 – Torque Profile for 5000 RPM

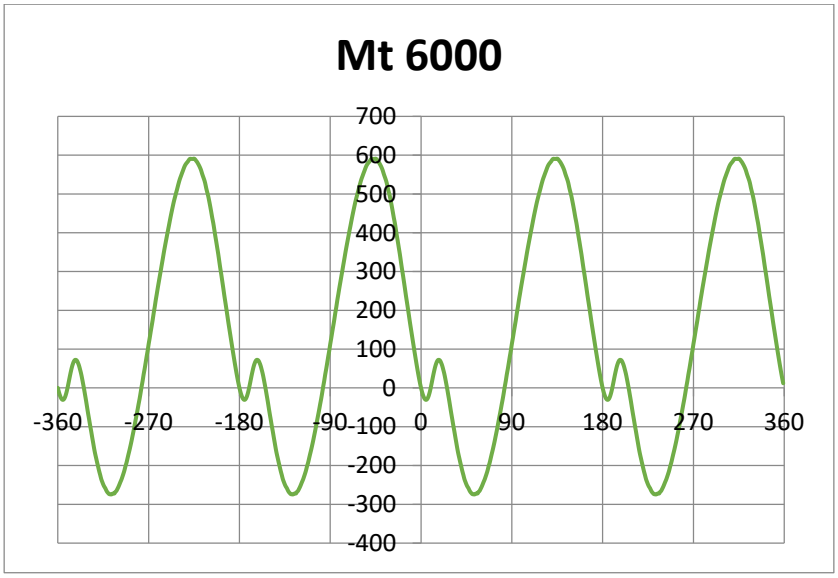


Figure 4.7 – Torque Profile for 6000 RPM

### 4.3. Calculating the Engine Motor and Idle Torque Profiles

The same method for calculating the full load torque profiles will be used to calculate the engine motor and torque profiles. The cylinder pressure data is a given, and using the formulas 4.1 - 4.29, the torque values for the engine will be obtained.

For the idle state, the pre given data is different than the full load and motor conditions. Instead of receiving single cylinder pressure data for different set of RPM, pressure values of the 4 cylinders are given separately for only 1 value of RPM.

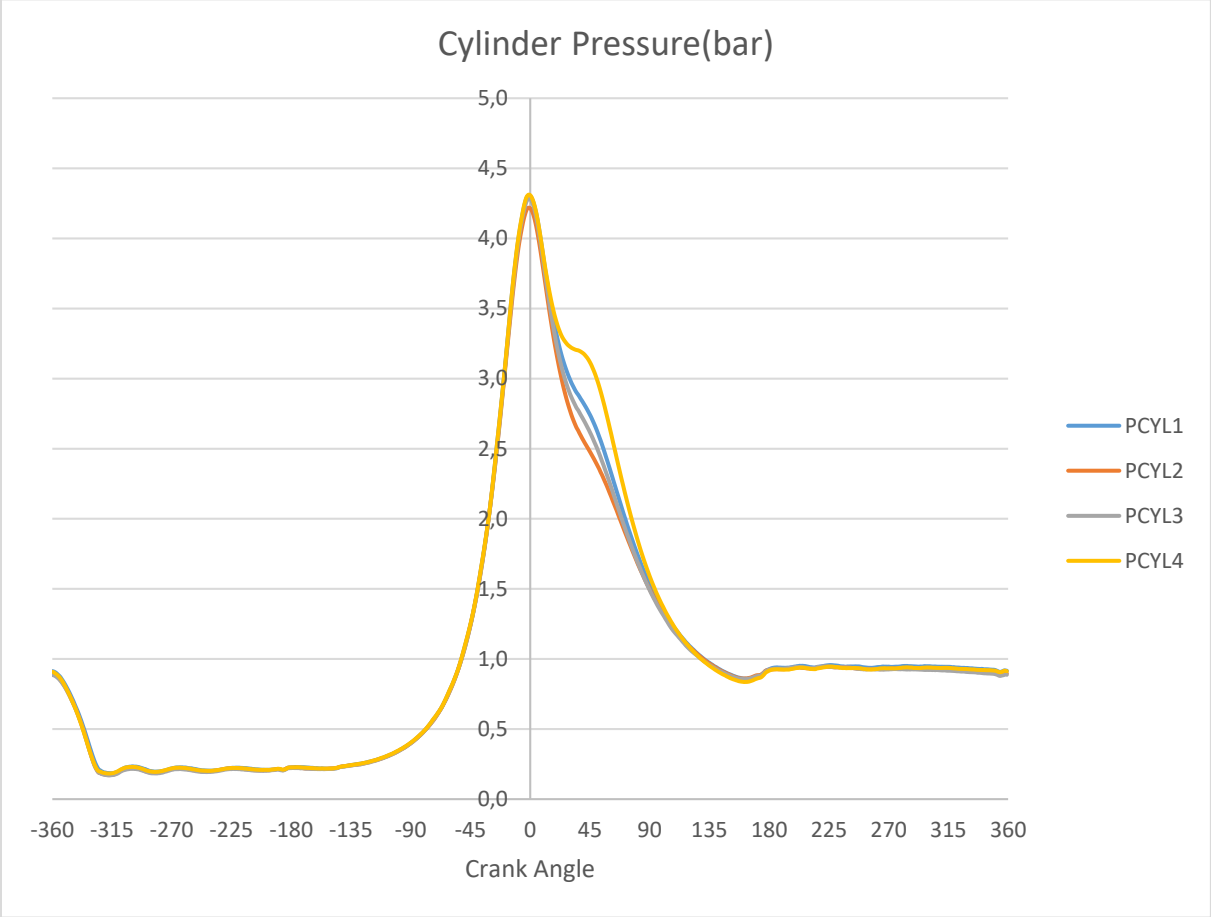


Figure 4.8 – Cylinder Pressure data for idle state at 1000 RPM

So instead of calculating the torque values for 1 cylinder and then applying a 180 degree of phase difference to it, the torque values will be calculated for each of the cylinder. And then the phase difference will be taken into account for each cylinder depending on the firing order. To be exact, after the 1st cylinder, the 3rd cylinder values will be added to the profile with 180 degree of a difference, 4th cylinder with be added with 360, and finally 2nd cylinder with 540 degrees.

Example torque profile of the 1st cylinder can be seen on figure 4.9. The torque profile of idle state for 1000 RPM for the whole engine can be seen on figure 4.10.

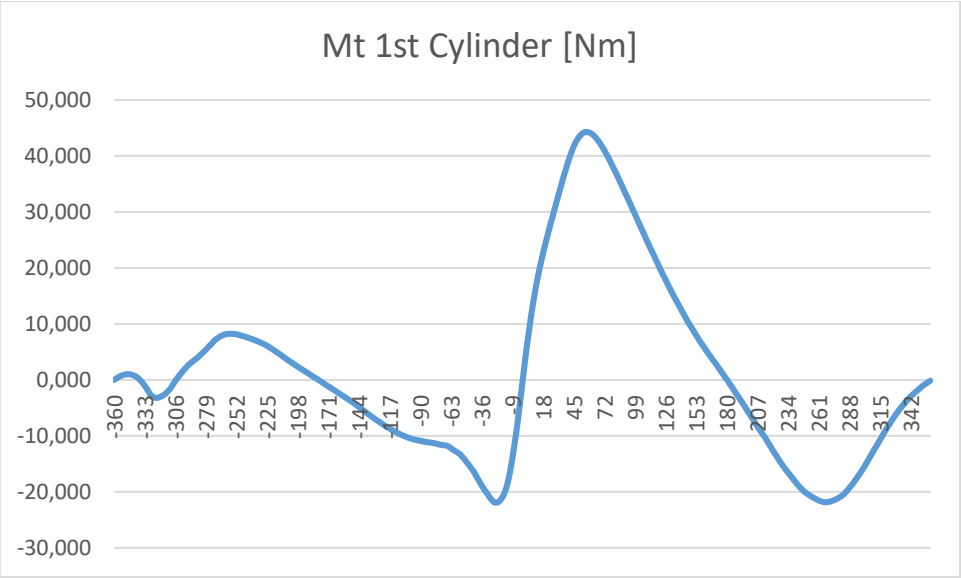


Figure 4.9 – Torque profile of the 1st cylinder in idle state, 1000 RPM

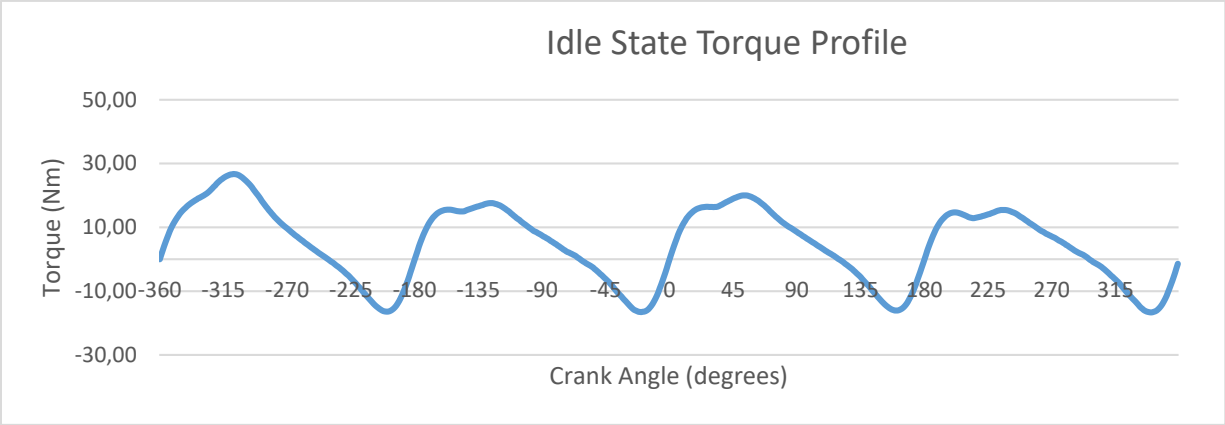


Figure 4.10 – Torque profile of the whole engine, 1000 RPM

The idle state torque profile will be used for the dynamic simulation of engine starting and stopping behavior as a limit condition.

For the motoring conditions of the engine, the pressure data is given for only 1 cylinder, therefore the method used for full load torque profiles will be used exactly once again. After calculating the values for the 1st cylinder, in firing order, 3rd, 4th and 2nd cylinder torque profiles will be obtained by applying a 180 degree of a difference one after the other. The torque profiles for the RPM values 1000, 1700, 2500, 3500, 4000 and 4500 can be seen on figures through 4.11 – 4.16.

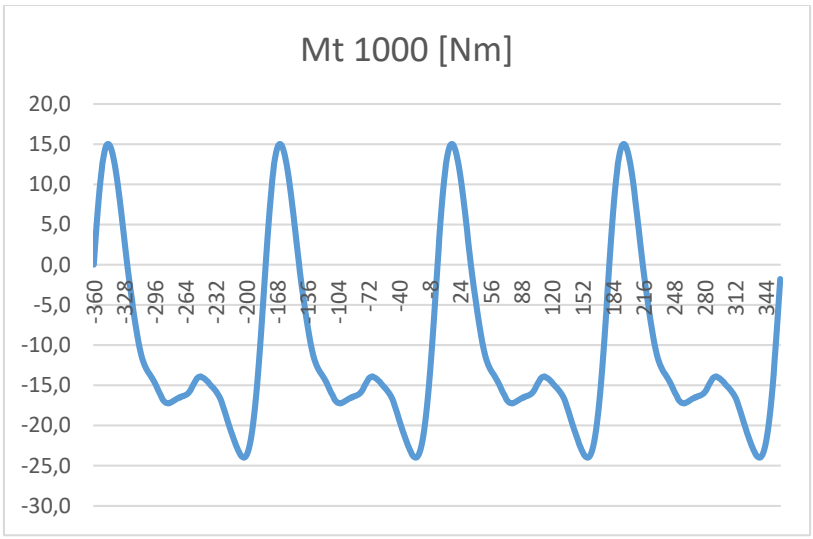


Figure 4.11 – Motoring torque profile, 1000 RPM

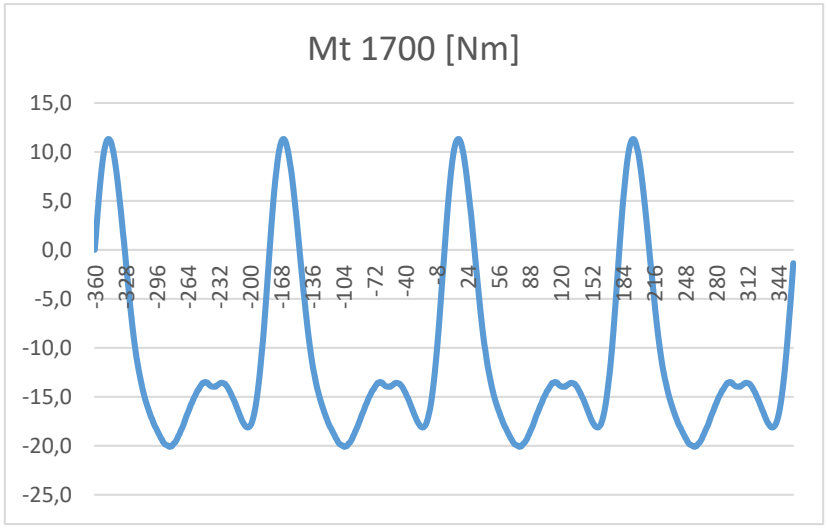


Figure 4.12 – Motoring Torque Profile, 1700 RPM

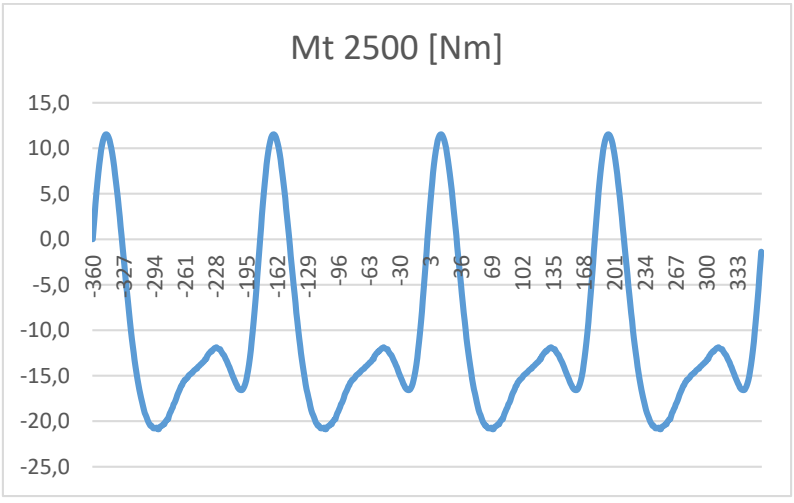


Figure 4.13 – Motoring torque profile, 2500 RPM

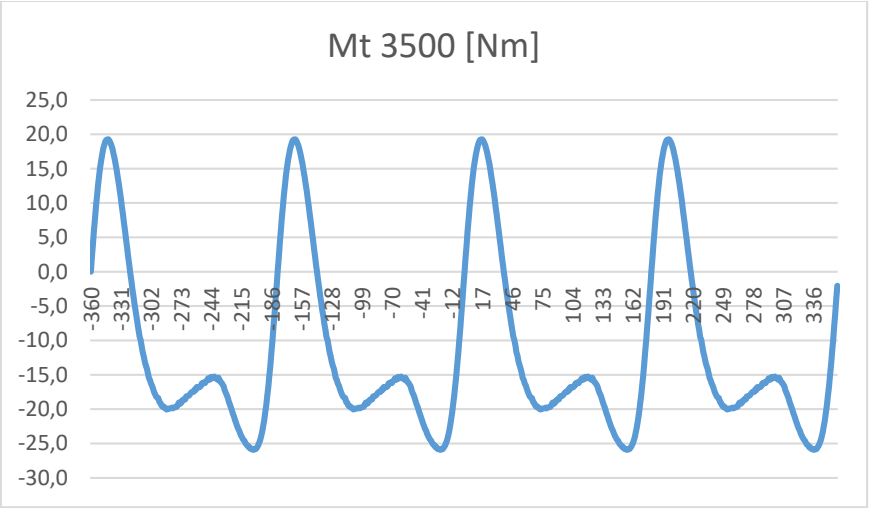


Figure 4.14 – Motoring torque profile, 3500 RPM

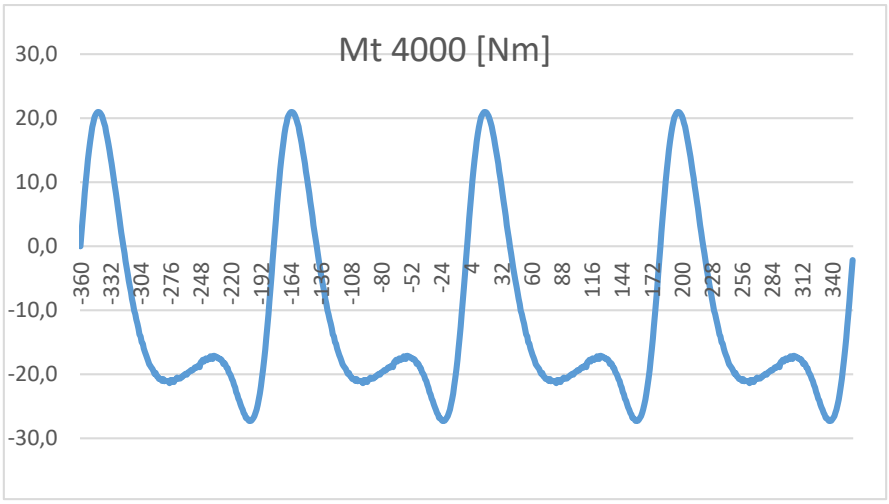


Figure 4.15 – Motoring Torque Profile, 4000 RPM

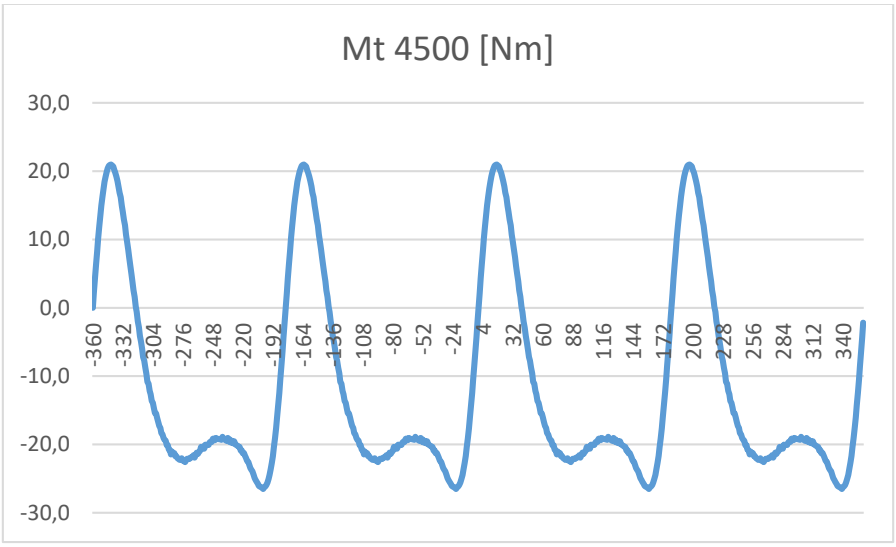


Figure 4.16 – Motoring Torque Profile, 4500 RPM

### 4.4. Setting Up the Dynamic Model Using GT-Suite

To be able to simulate the conditions of the built system properly, it is essential that both the DMF and the hydraulic pump are modeled properly and all the input data is put in properly. Please see the figure 4.17 to examine the model built on the software before the input data is discussed.

- As it can be seen, the DMF is modeled as 2 separate rotational parts, with a torsional stiffness element in between. The torque that comes from the engine will be modeled with a torque element. This input will travel through the first mass, torsional stiffness, second mass, torsional stiffness between the planetary gear set and the second mass, hydro generator, torsional stiffness of the pump, hydro motor, torsional stiffness between the hydro motor and the dynamometer in order. Finally, the simplistic model will be finished with a boundary condition, which is a rotational boundary element that is connected to the dyno.

- The goal here is, as discussed before, simulating the torque profile of the engine on the system and generating results of the dynamic torque between first and secondary masses of the dual-mass flywheel, the torque between the hydro generator and the hydro motor, and the frequency analysis of the whole system to monitor the critical resonance areas.

- An important matter to be discussed here is the damping values for each of the torsional stiffness elements that are put on the dynamic model. The dynamic model will work properly without any damping coefficient, however, removing any sort of damping from the system can result in unbalanced results where none of the cycles reach to steady state. To explain this with an example, with a high damping coefficient the system will start reaching steady state after only about 50 cycles, while the rest of the vibrations will be damped completely, hence an overdamped situation. Setting a really low damping value will, naturally, end up with an underdamped condition. Therefore, the damping values are set as a default value of 5 Nms/rad which has been obtained by trial-failure method. This value of damping will help the system reach to steady state after about 250 cycles for each case.

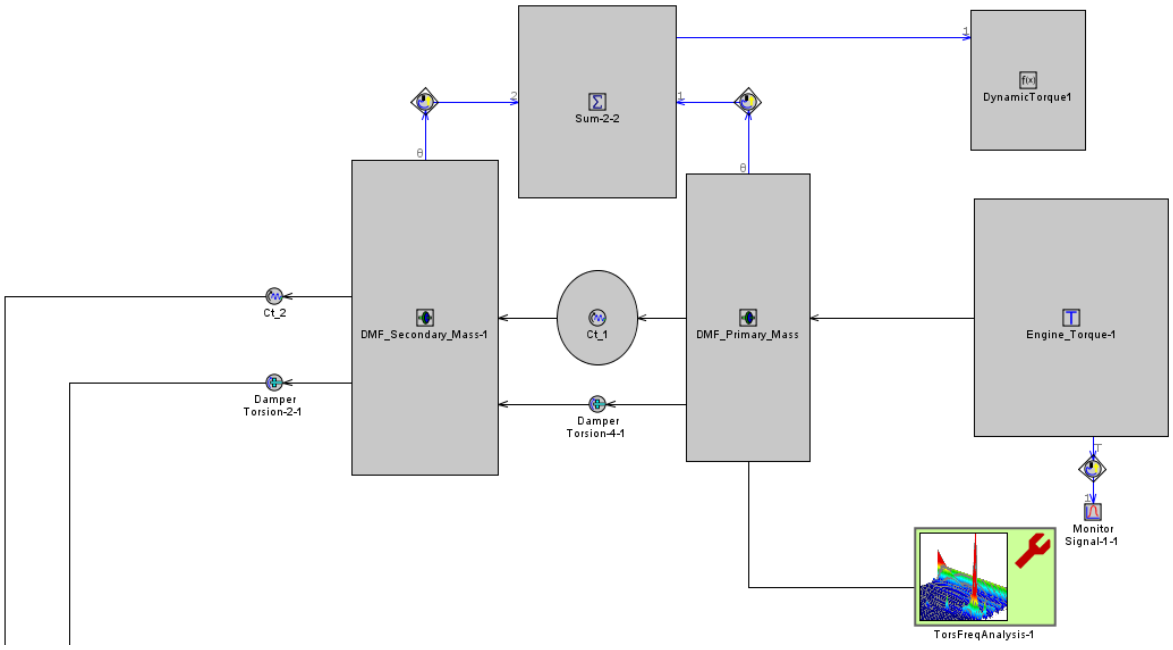


Figure 4.17a – The upper part of the dynamic model

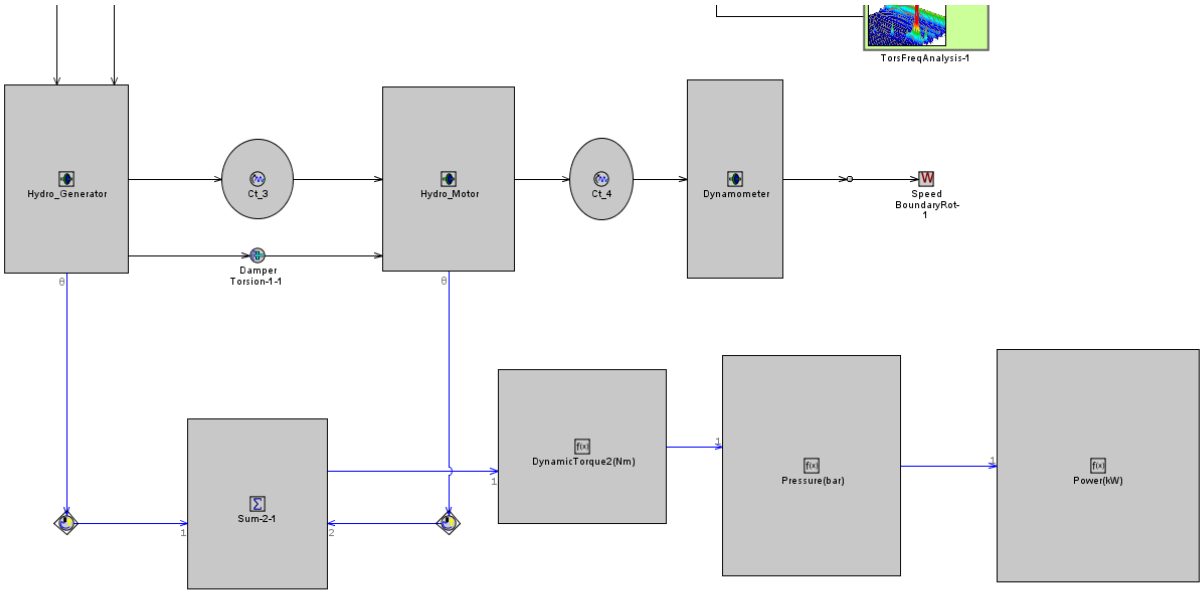


Figure 4.17b – The lower part of the dynamic model

- **Putting in the engine torque profile;**

The torque profile data that was calculated will be put in the software using the “Profile Angle” branch. Through the previously done calculations, we have received 6 different torque profiles from the engine, starting at 1000 RPMs and finishing at 6000 RPMs. By choosing the “Profile Angle” branch, a new profile angle can be defined within an XY coordinate system. To be able to proceed with a proper simulation, all 6 of the torque profiles were defined.

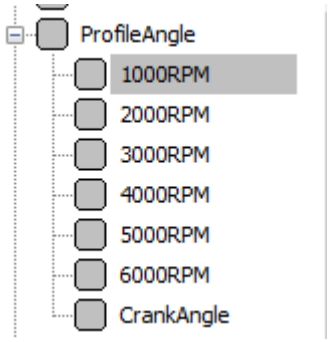


Figure 4.18 – Profile Angle Branch

This is a simple step that requires the data calculated previously from Microsoft Excel copied, and then pasted by choosing the “Profile Angle” branch to be put in. In our case these profiles are named after the amount of RPMs.

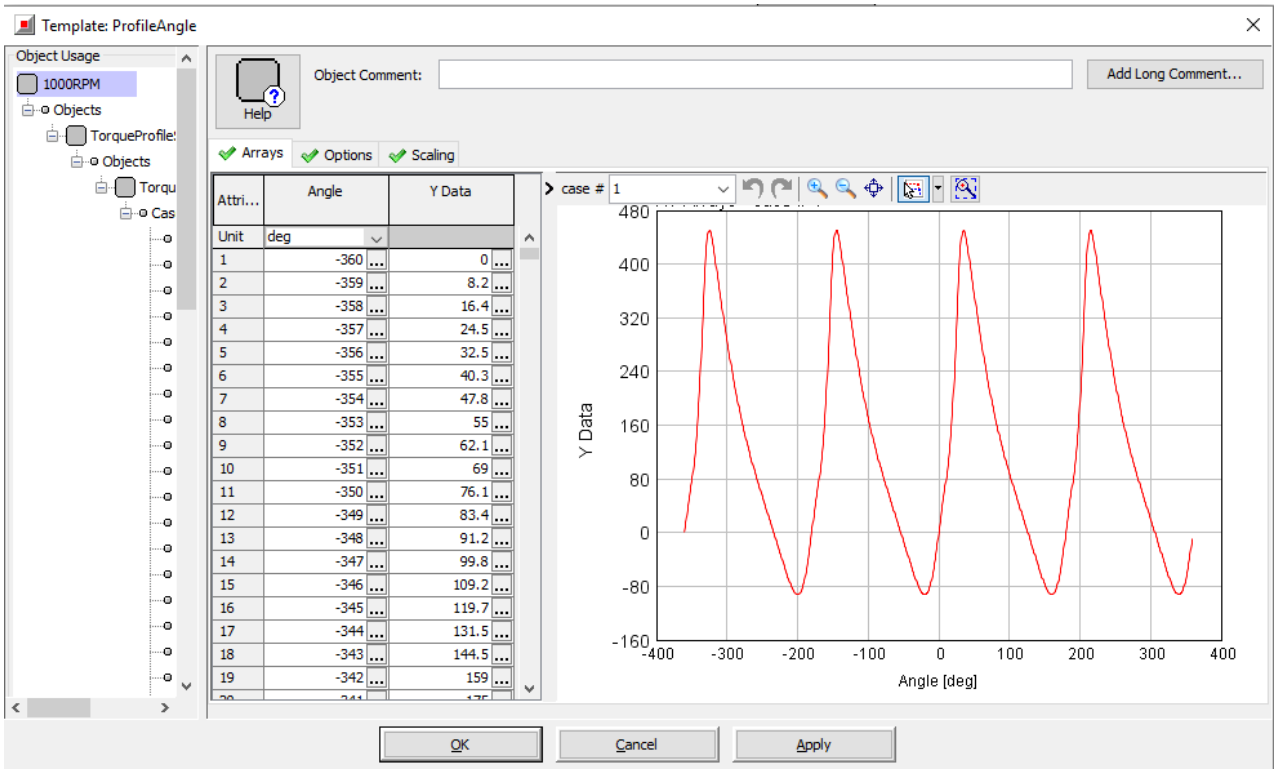


Figure 4.19 – Example of the Profile Angle Branch for 1000 RPM

- **Creating torque profile speed;**

As mentioned, we have 6 different torque profile speeds for 6 different RPM setups. But unfortunately this will not be enough to create a proper simulation. It may be that these profiles could be used as sole input data, but then the software would simulate and generate only 6 different set of results for each of these profiles. So to be able to create proper results, we will command the software to use these torque profiles as base information, and then using linear interpolation, the software will be able to create torque profiles for any given RPM, then generate results for these recreated torque profiles.

The start of this linear interpolation process is to define a torque speed, for which the software will use 2 of the RPM data close to each other to define a speed for torque profile, we need to use the “XY Table Dependency” branch. As can be seen on figure 4.4, each of the torque profiles calculated are put in as a Y coordinate variable, while for X coordinates, the amount of RPMs that are being used as variables.

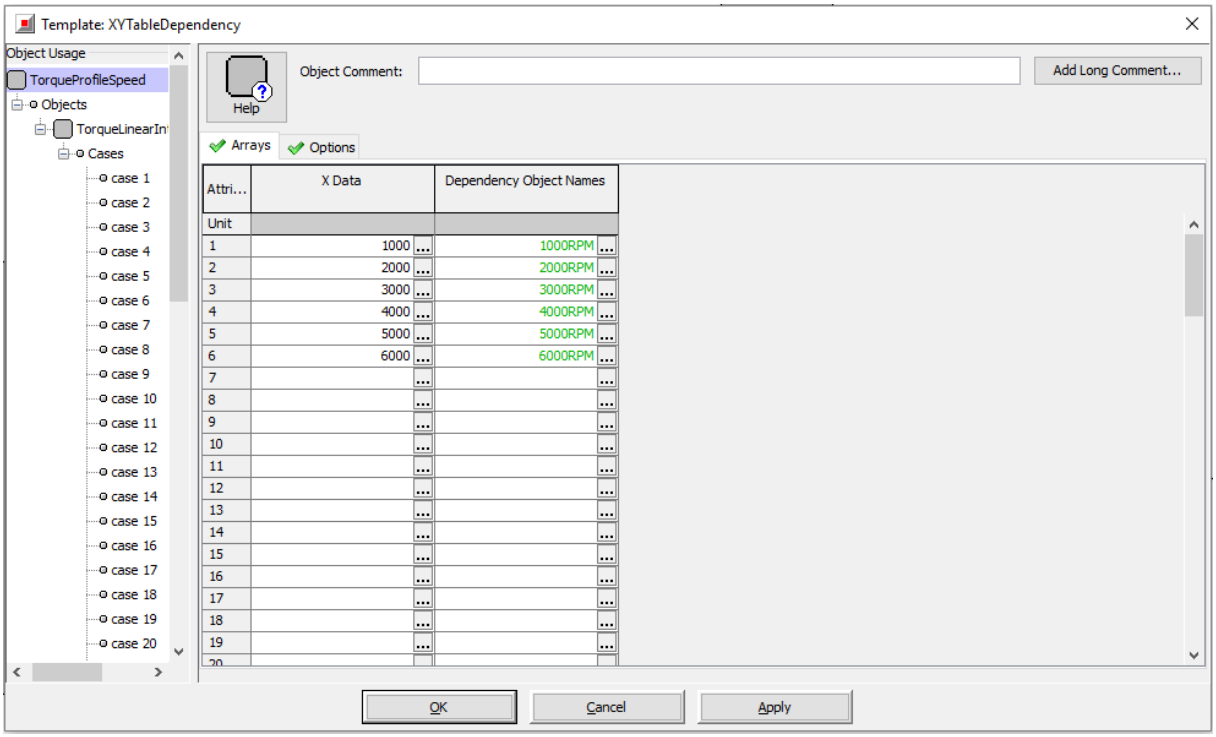


Figure 4.20 – Defining Torque Profile Speed

This table dependency will help us create the proper linear interpolation for the whole simulation process. It is also essential to choose “interpolate-linear” option to give the command to the software to interpolate the remaining areas for the torque profile, while although we have the data for each of the 1000 Rpms, the rest needs to be logically filled by the software.

- **Defining a linearly interpolated torque profile for the whole simulation;**

The next step before we simulate the system and examine the results will be defining the linear interpolation of the engine torque profile. To be able to do this, it is needed to use “RLT Dependence XY” branch. This step will finally create a proper interpolation that takes the given torque profile data as base, and then matching it with the RPM variables we input. To be exact, this step is needed for the software to fill up the necessary input data for the RPMs we don’t have the torque profile of. In our case, we will start the simulation from 500 RPM, and then gradually raise to 6000 RPM. Please note that to be able to do this, all the needed RPMs has to be defined in the case setup by creating different cases for each of them.

On the “RLT Dependence XY” branch, the “initial X input” option will be chosen, and then defined as “RPM” which was created in the case setup as mentioned. For “Input RLT Variable”, the predefined input unit “rpm+” will be chosen, and finally to give the software base information, “Torque Profile Speed” which was created in the previous step will be chosen. This dependence will be saved and referred as “Torque Linear Interpolation” from now on.

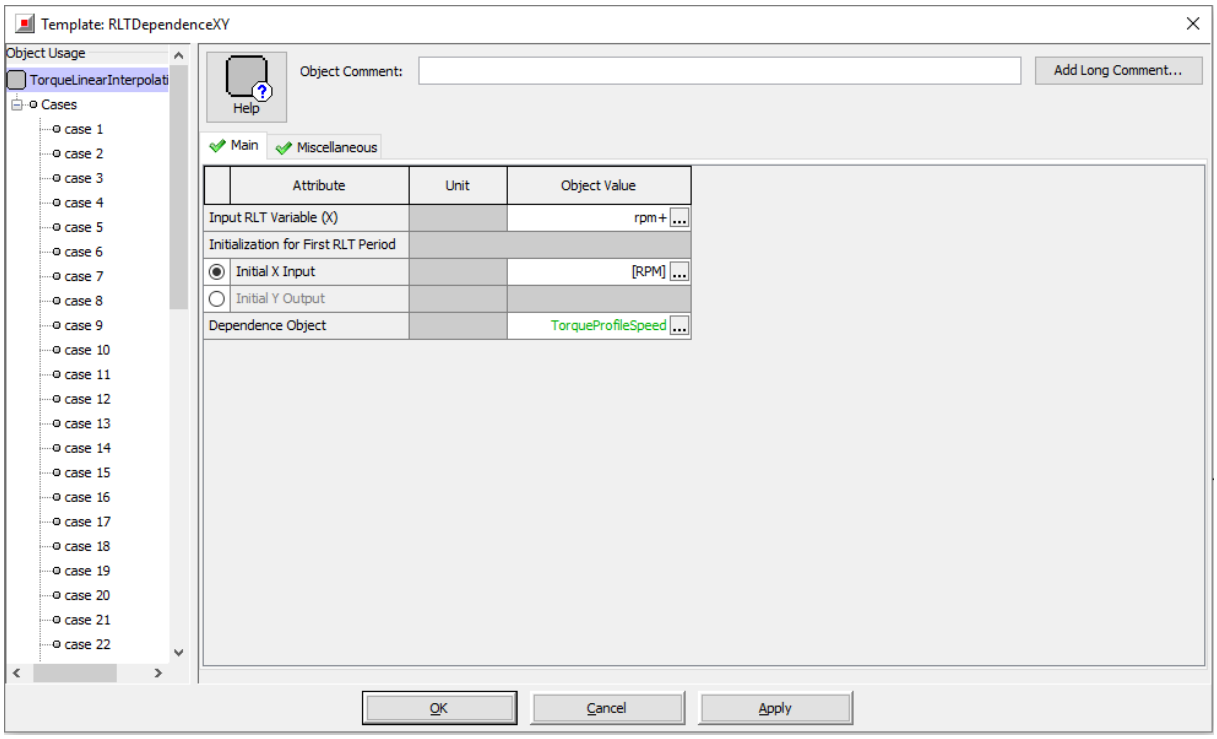


Figure 4.21 – Torque Profile Linear Interpolation Setup

- **Case setup and putting in variables;**

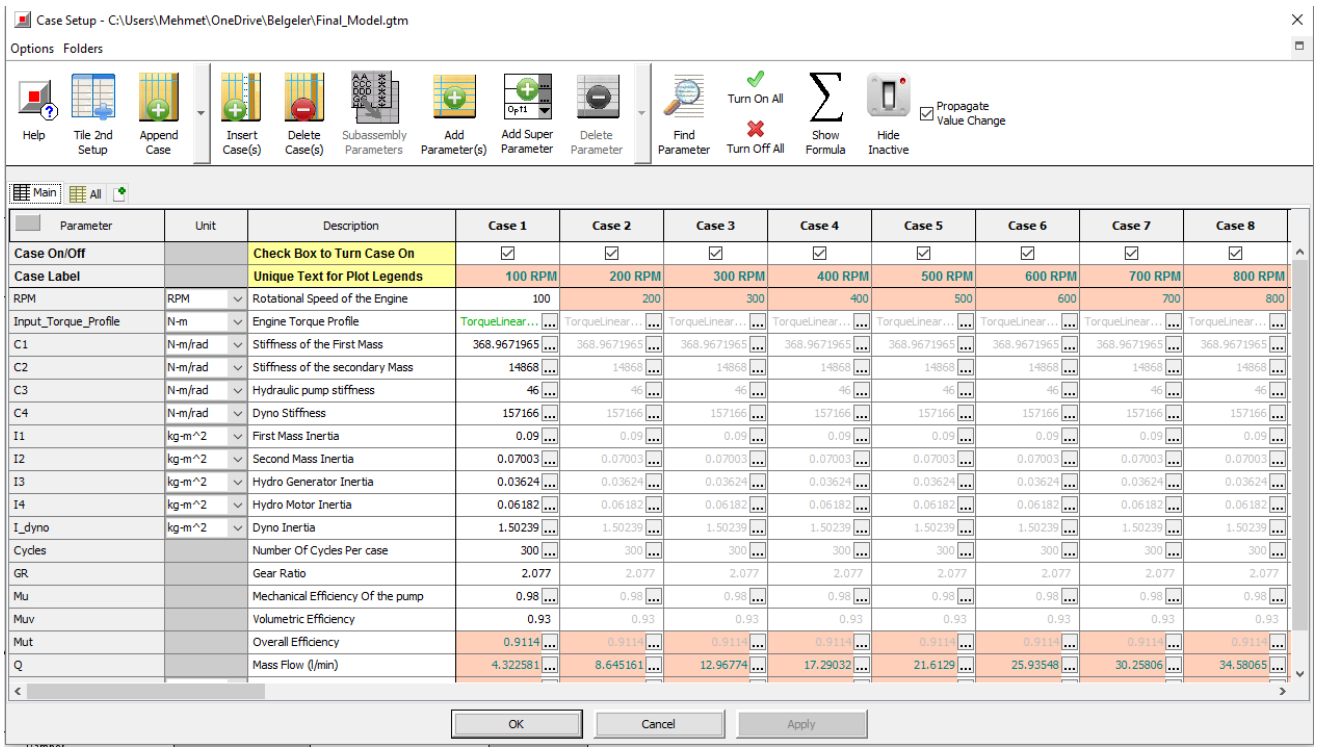


Figure 4.22 – Case setup view

Please check the case setup window above. A unique case for the each of the demanded RPM is created, which will result in 56 different cases for our simulation. After this, all of the input data is defined in the case setup, which include the demanded RPMs, input torque profile which will use the “Torque Linear Interpolation”, inertias of the masses that are modeled on the software, and finally the torsional stiffness data to be put in between the masses.

Finally, 300 cycles are chosen and defined for each of the cases. This means that the software will complete each of the RPM cases in 300 cycles. More cycles mean that the software will try to generate and create more detailed results, but since out input data about the torque profile is limited, 300 cases are enough to give us an idea about the dynamic torque between the masses of the DMF, the torque between the pump elements, and the frequency analysis.

- **Function elements and final setup;**

For each of the inertia elements on the system, the degrees per cycle is chosen as 720. This is due to the input data coming from the crankshaft. Also note that the output data from the masses of the DMF will be set as “angular position” only for the moment.

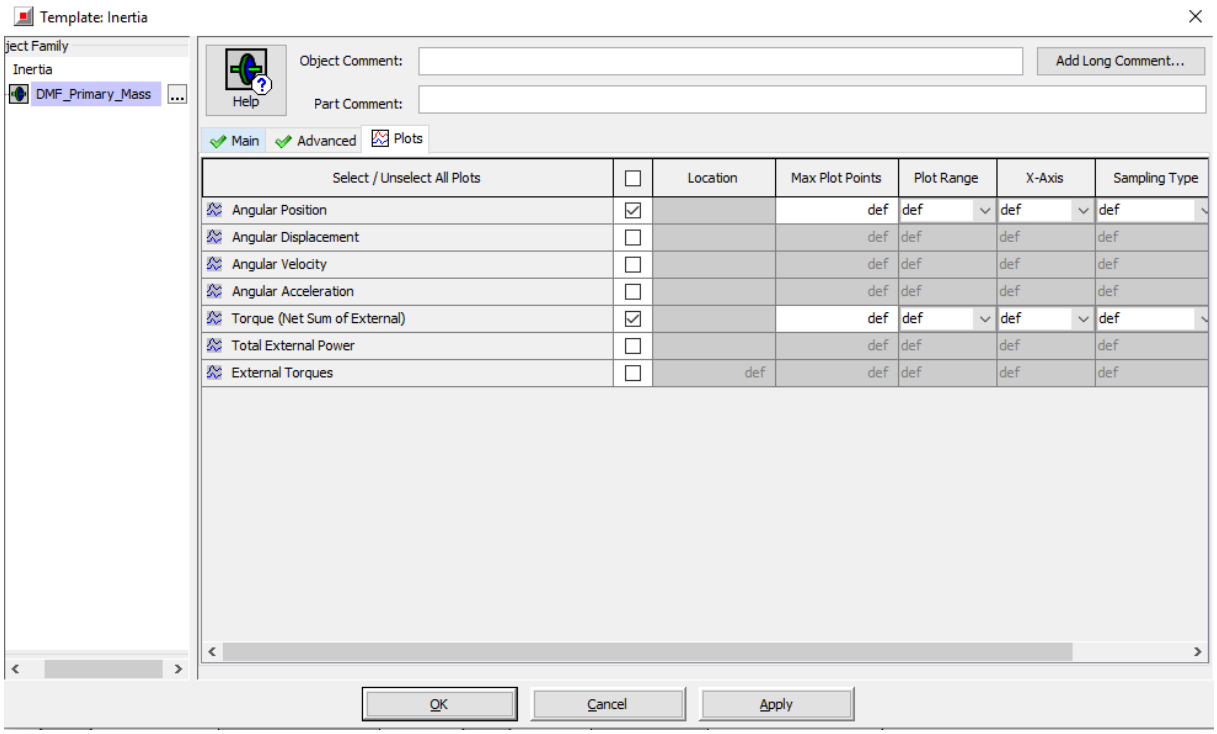


Figure 4.23 – Choosing the Output Plots of the Inertia Elements

This is needed to generate results in angular position for each of the masses of the DMF. Afterwards by adding first a “Sum” element, and then a “Mathematical Equation” element into the system, we will define a function that uses the angular difference between the masses to calculate the dynamic torque results for the dual-mass flywheel. The placing of these elements can be seen on Figure 5.1. On figure 5.8, the function that is used to calculate the dynamic torque between the masses can be seen.

The same will be done for the pump, but this time the torque values will be translated to pressure. The necessity of this was discussed during the section where the elements of the system were being introduced. There is a pressure limit between the hydro generator and hydro motor, which must be followed both for critical conditions and bypass areas. The limit pressure

for the pump elements is 360 bars, and after this value the pump will start bypassing to reduce the pressure created in between.

Another way to measure the torque between the pump elements is to monitor the torsional stiffness in between directly. By monitoring the torque, and then translating it into pressure in bars, the pressure analysis can also be completed. The difference here is simply the matter of choice, and to make sure that if any parameters on the system is changed, the mathematical functions can stay intact without any changes made on them.

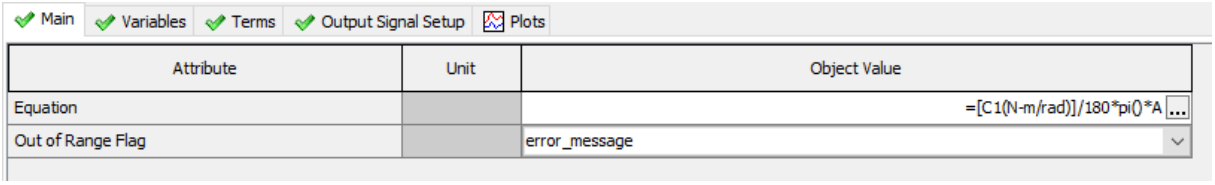


Figure 4.24 – Setting up the Math Equation for Dynamic Torque

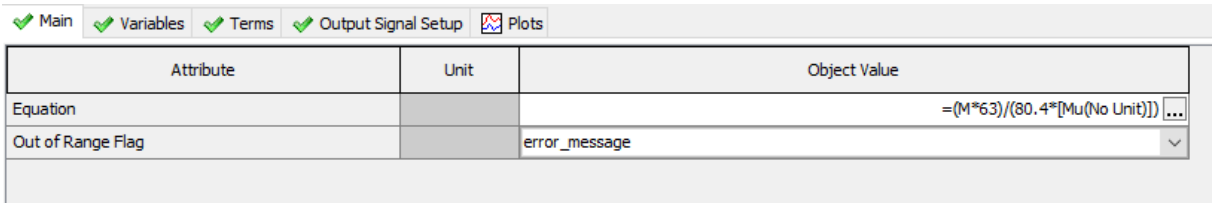


Figure 4.24 - Setting up the Math Equation for the Pressure

$C_1 \rightarrow Torsional\ Stiffness\ between\ the\ masses\ in\ \frac{Nm}{rad}$

$A \rightarrow$
$Output\ data\ from\ the\ Sum\ element, the\ angular\ phase\ difference\ between\ the\ masses$

$M \rightarrow Output\ data\ from\ the\ first\ math\ function\ element, the\ torque\ value$

Finally, before starting the simulation, run setup will be defined. One important note here is to set the reference object as a driver, which will tell the software to run the torque profile through the whole system instead of just 1 element. The time control flag will be set as periodic, and the maximum simulation duration will be set as “Cycles” which was already defined in the case setup. Flow control should be defined as the default explicit, and the ODE control should be defined as the default implicit options before starting the simulation. The run setup can be seen on figure 4.25.

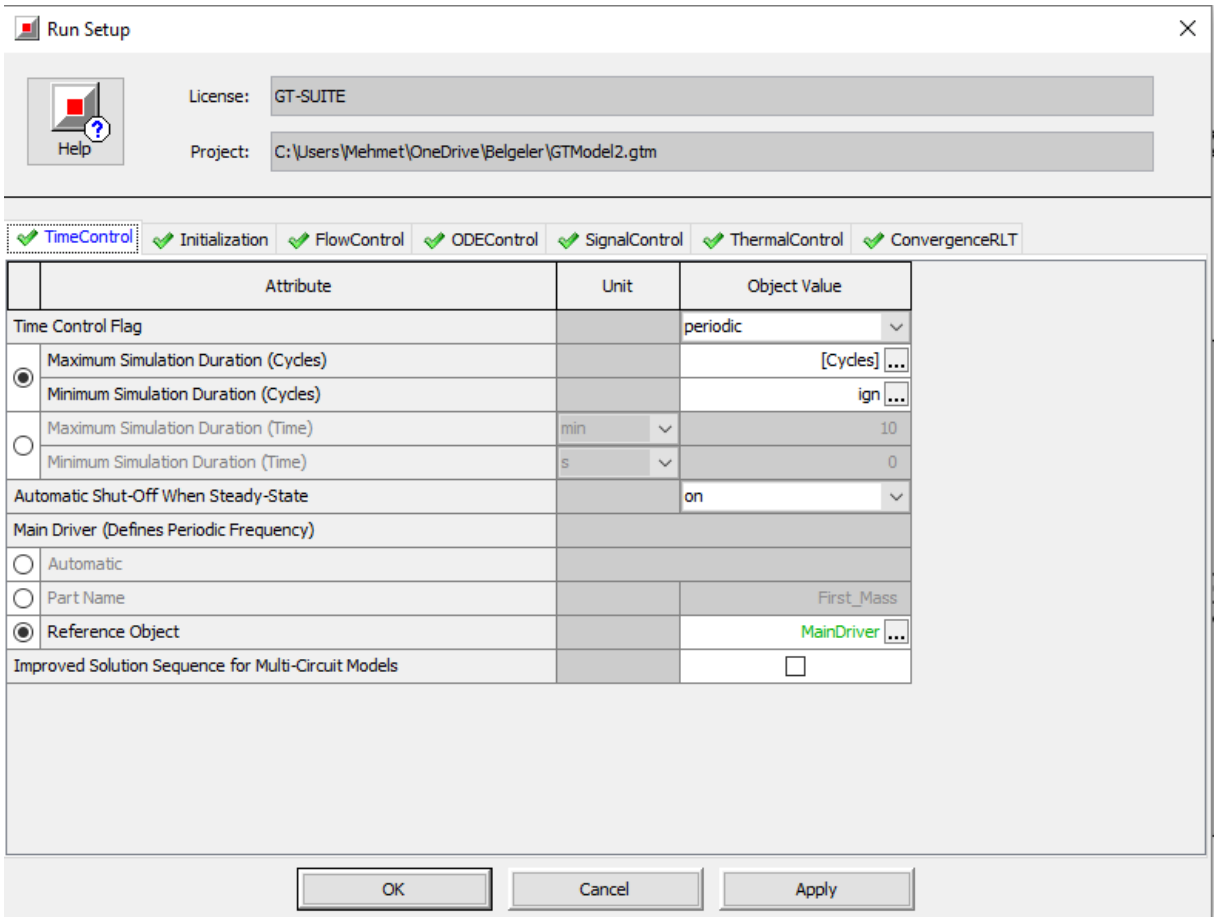


Figure 4.25 – Run Setup of the System

# 5. Evaluating the Results

## 5.1. Dual Mass Flywheel

As it was stated before, there is a limit dynamic torque that can only pass through the both masses of the dual mass flywheel without breaking the part, or deforming the arc springs within. The necessary calculations were done in part 2 to obtain the critical torque value which was;

$$T_{crit} = C_T(per\ degree) * 70.43 = 448.81\ Nm \rightarrow Critical\ Dynamic\ Torque\ Value$$

To be able to get this value from the software, a math equation module needs to be used. By inserting a math equation on the dynamic model between the primary and the secondary mass of the dual mass flywheel, we first obtain the angular position difference with a sum module, and then by using the math equation itself we obtain the results for the dynamic torque values. The equation being used;

$$Tcrit = \frac{C_1}{180 * \pi * \alpha} \rightarrow where\ \alpha\ is\ the\ angular\ difference\ between\ the\ masses$$

The results can be seen on figure 5.1 and 5.2.

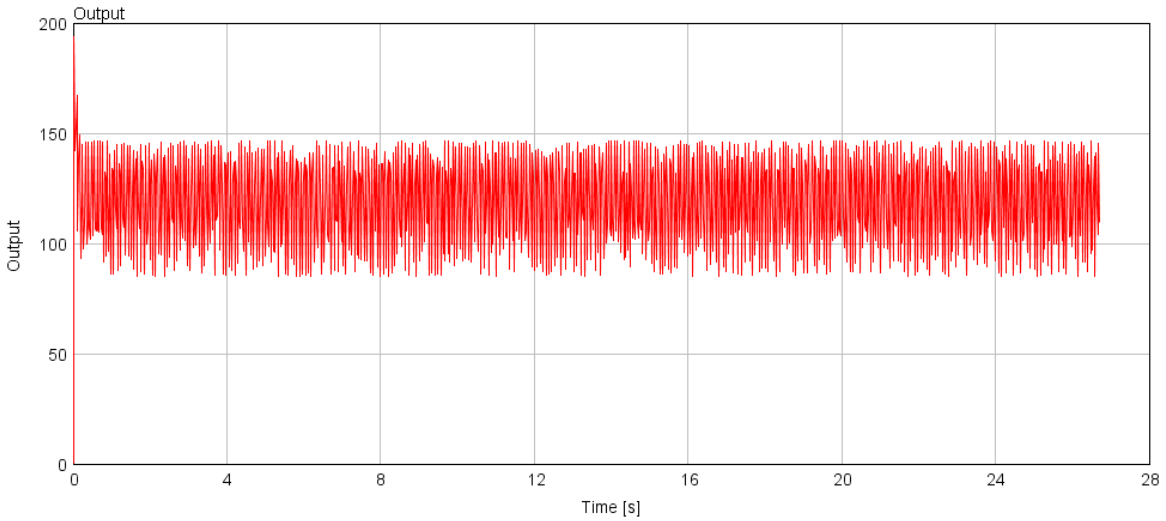


Figure 5.1 – An example view of the case 800 RPM for dynamic torque

While the critical torque is not exceeded in this case of RPM, it can be seen that the system doesn't quite reach the steady state. One of the natural frequencies of the system is 841 RPM and as the system gets close to this rotational speed, peak torques and underdamped conditions can be observed.

Another underdamped condition where the peak torque is relatively high can be observed in 200 RPM, where once again the system goes through the resonance frequency of 153 RPM.

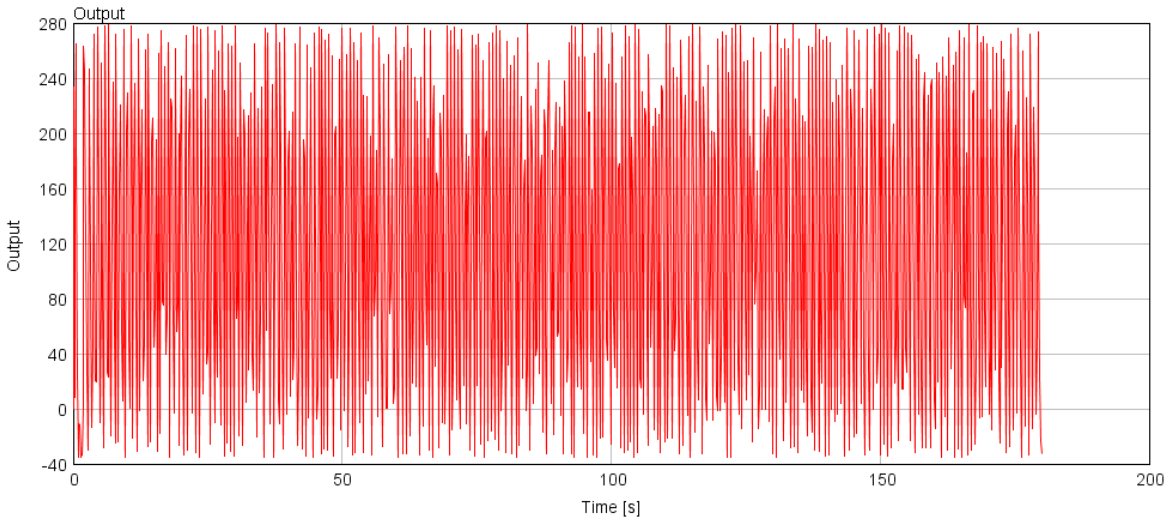


Figure 5.2 – Dynamic Torque Results for 200 RPM

On the other hand, on figure 5.3, the average torque value for each set of RPM can be seen.

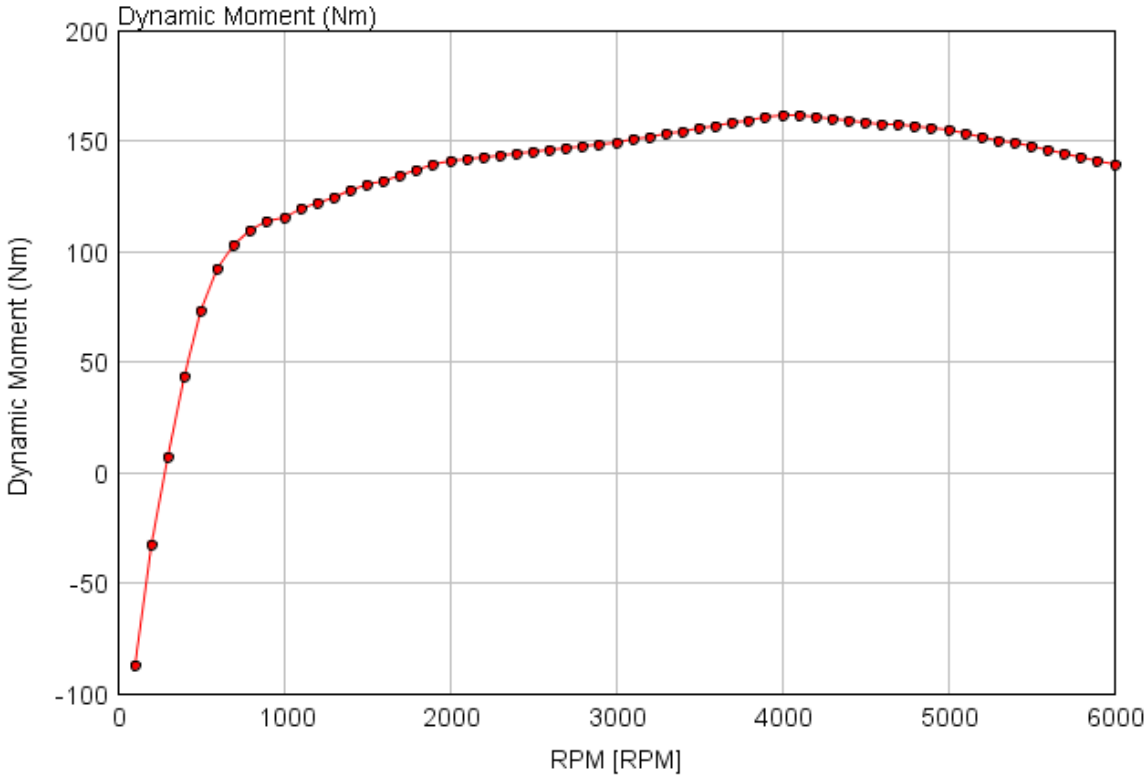


Figure 5.3 – Dynamic moment vs. engine rotational speed

Both by looking at this figure, and figures 5.1 and 5.2 where the resonant frequencies are either close or have been passed, it is relatively safe to say that the dynamic torque will never exceed the critical value under full load torque characteristics. So the dual mass flywheel is safe to be used, and a good match for the system.

### 5.2. Hydro Motor and Hydro Generator

It was stated in section 2 that both by catalogue, and for safety reasons, the differential pressure between hydro generator and hydro motor can't exceed 360 bars. The calculation for this variable is done with the same method used for calculating the differential torque for the dual mass flywheel.

A sum module, and a math function have been used to get to the torque value between the hydro elements, and afterwards the following formula was used to obtain the differential pressure in bars;

$M = \frac{D*\Delta p*\mu}{63} \rightarrow Torque\ generated\ by\ the\ hydro\ elements$ where;

$D \rightarrow Displacement\ in\ \frac{cm^3}{rev}$

$\Delta p \rightarrow differential\ pressure\ in\ bars$

$\mu \rightarrow Mechanical\ efficiency$

All of these values have already been stated on section 2, taken by the Parker catalogue. For the mechanical efficiency a new parameter has been defined in GT- Suite which changes depending on the RPM being used. The results can be seen on figures 5.4 and 5.5.

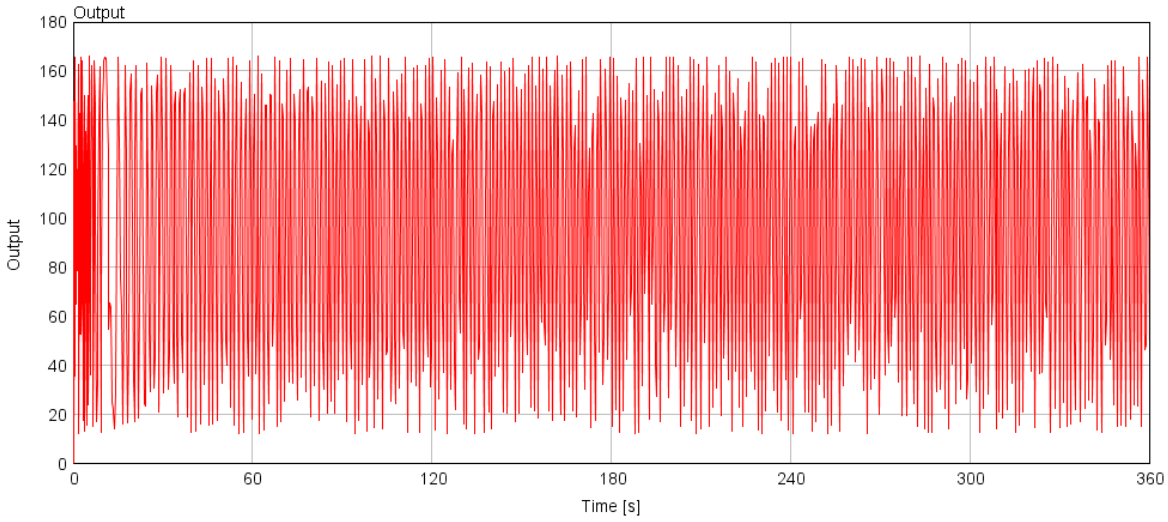


Figure 5.4 – The differential pressure results for 100 RPM

Just like for the case of the dynamic torque, since the torque amplitudes increase close to resonant frequencies, the 100 RPM results are underdamped and with a high maximum value of differential pressure. Once again, the resonant frequency 153 RPM creates a high amplitude of torque in between hydro elements, therefore a high differential pressure, but even then the values are below 360 bars.

On figure 5.5 the results are laid versus rotational speed, where once again the average differential pressure values are below the critical pressure value. It is once again relatively safe to say that the hydro elements are safe to be used on the system under full load conditions, and bypass on the pipe is not necessary.

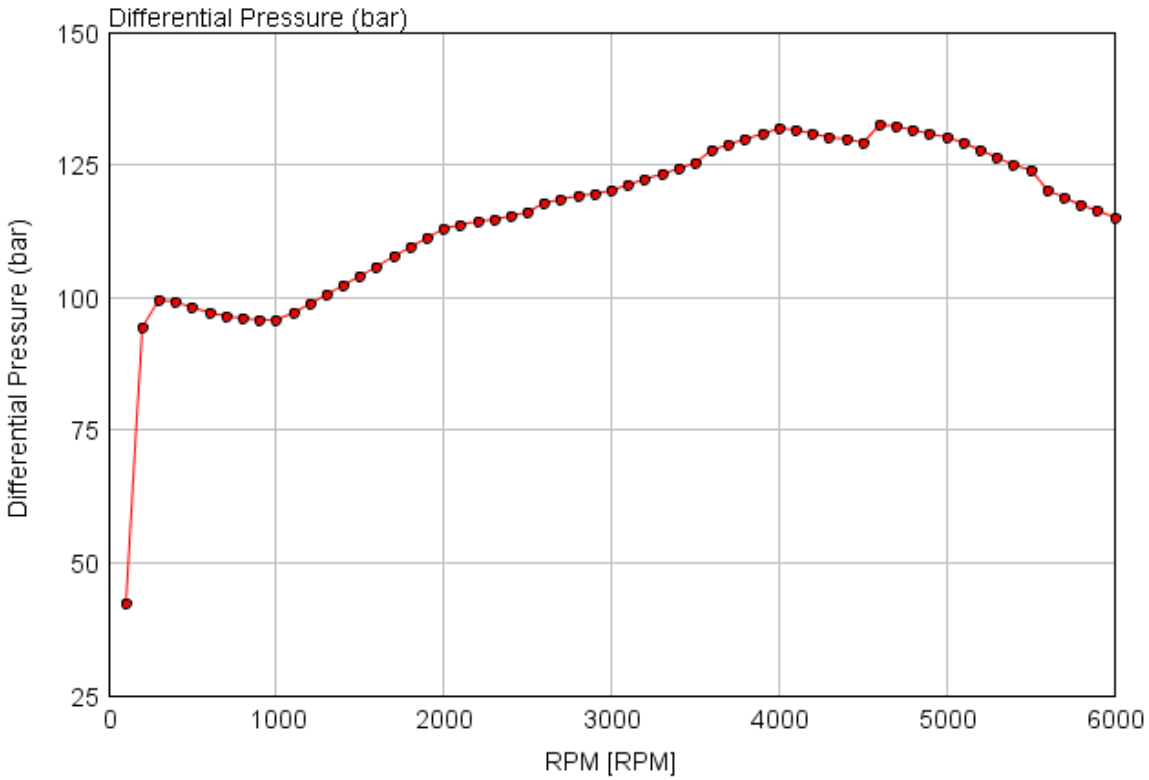


Figure 5.5 – Differential pressure v. rotational speed

### 5.3. Resonant Frequencies

The frequency analysis on the system is done by adding a forced frequency analysis module on the system. After setting up the RPM range that is desired to be analyzed, number of orders, and the requested plots are put into the module. The first thing that needs to be checked is if the natural frequency results for the GT-Suite dynamic match the analytical method results.

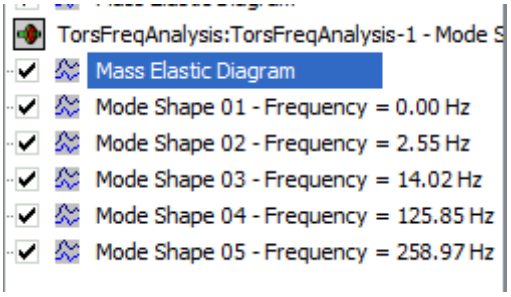


Figure 5.6 – The natural frequency results

As it can be seen the natural frequencies match the results from the analytical method. This can justify that at least the setup of the system was done properly on the software. By using the frequency analysis, we can not only obtain the natural frequencies of the system, but also the contour plots for torque amplitudes, angular acceleration amplitudes, angular velocity amplitudes, and also Campbell diagrams that show all of these amplitudes versus engine speed and engine order.

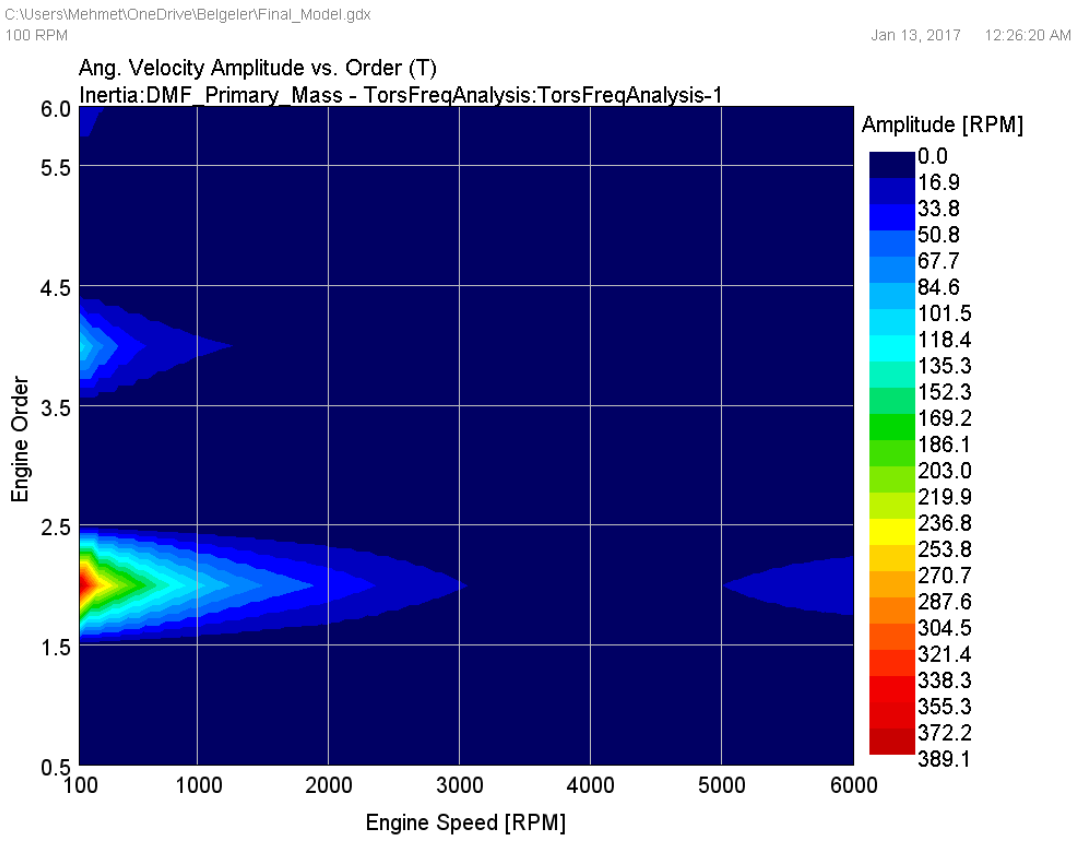


Figure 5.7 – Angular velocity amplitude vs. order frequency analysis

On section 3, the Campbell diagram of natural frequencies showed that the system had critical areas between 0 and 1000 RPM. As it can also be seen on figure 5.7, the second engine order is under high angular velocity amplitudes, while for 4$^{th}$ order even though there can be still the observation of amplitudes around 100 RPM, the condition is not as critical as the second order. These results were taken as an example for dual mass flywheel primary mass. Because of the RPM reduction in the system, the amplitudes are significantly less for the elements that come after the gear reduction.

The torque amplitudes can also be monitored by choosing the torsional stiffness elements on the frequency analysis results. Once again, the amplitudes appear between 100-1000 RPM for the second order, and close to 100 RPM for the 4$^{th}$ order.

Both the angular velocity amplitude and torque amplitude results can be seen on figures 5.8 and 5.9.

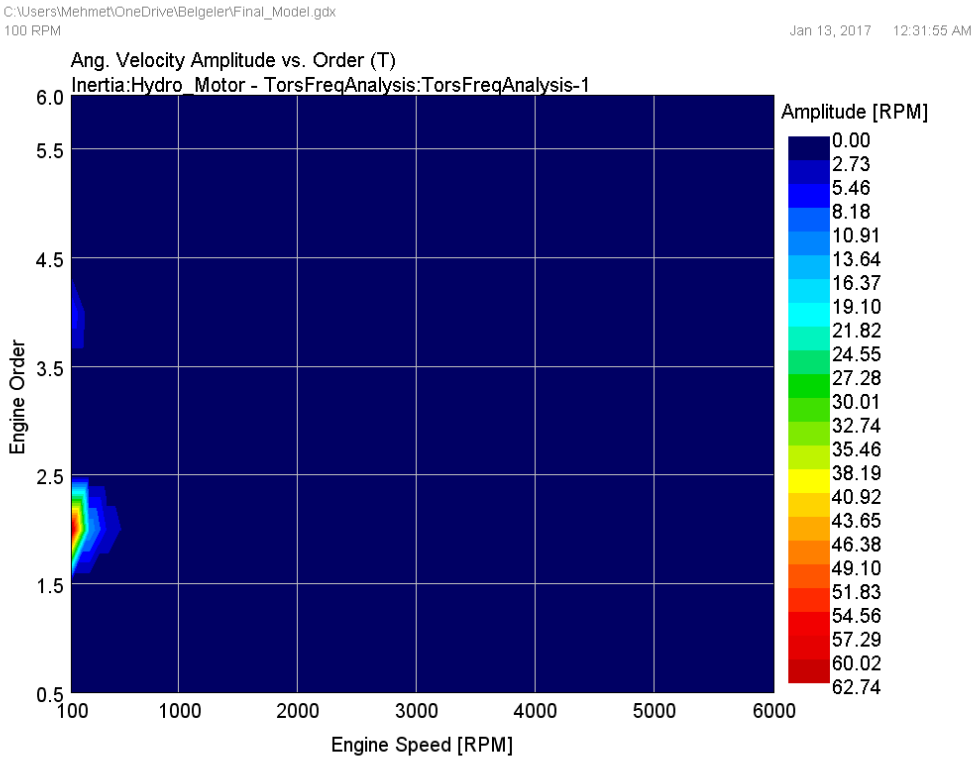


Figure 5.8 – Angular velocity amplitude vs. order for hydro motor

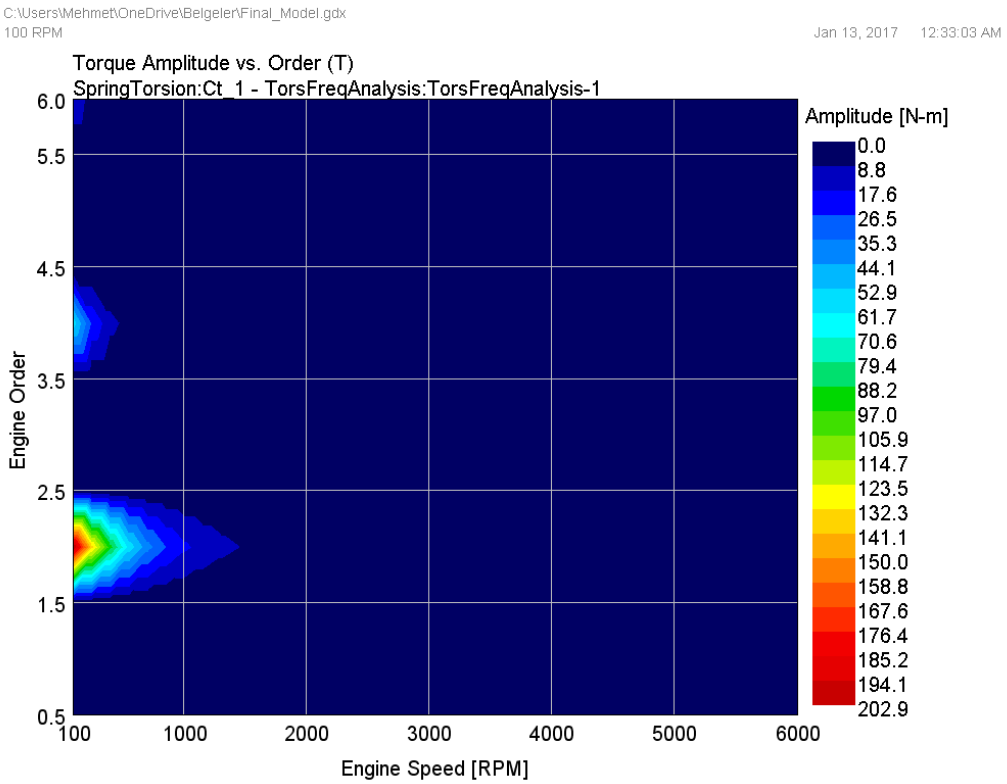


Figure 5.9 – Torque amplitude vs. order for the dual mass flywheel torsional stiffness

All of these results show that there will be significant torque amplitudes in the system between 0 and 1000 RPM due to natural frequencies 153 and 841 RPM, and both of these conditions has to be gone through as fast as possible to avoid any damage to the parts or the system itself. Figure 5.10 shows the torque amplitudes for the torsional stiffness between the dynamometer and the hydro motor, which can help us conclude that the maximum torque amplitudes in the system are about 200 Nm.

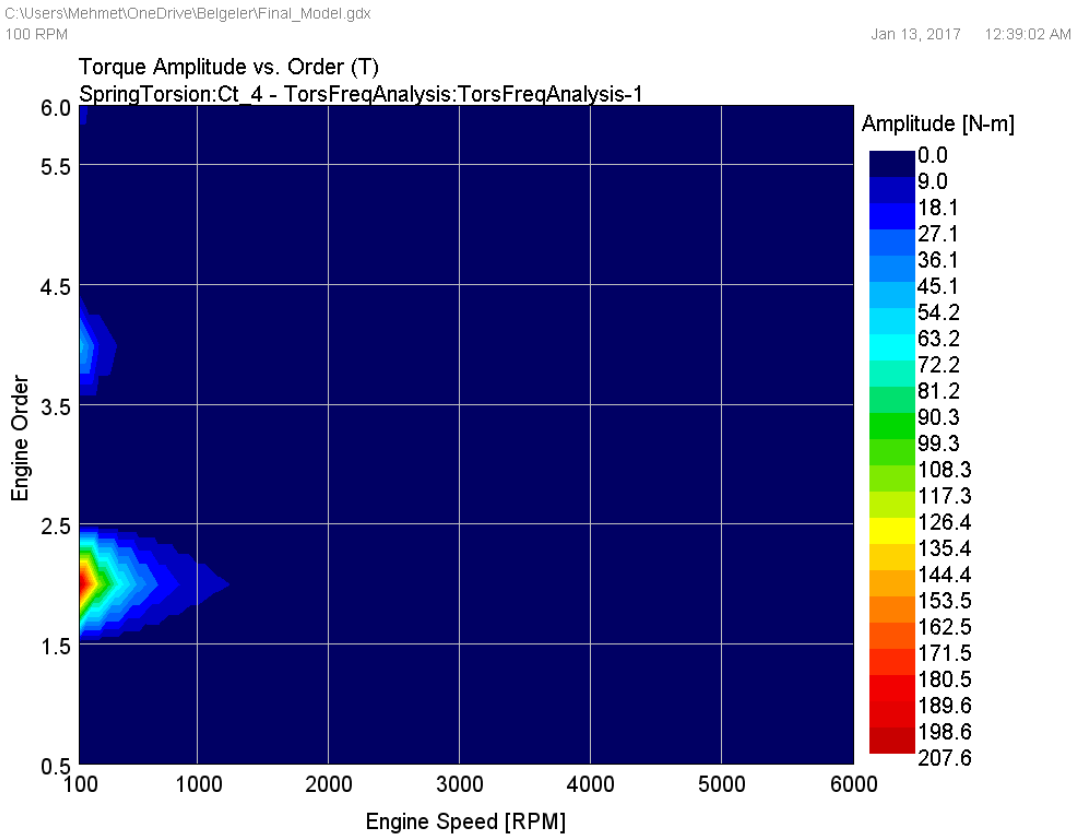


Figure 5.10 – Torque amplitude vs. the order for the dyno-hydro motor stiffness

### 5.4. Transient Behavior for Engine Start

For the engine starting transient behavior, the dynamic model that was built for the full load condition was used in a different way. During engine start, the dynamometer will be rotating the system with a steady torque value, while the engine will be resisting to this torque value with its motoring torque condition. The motor torque values were calculated and shared on section 4.

For the starting condition, once again a torque profile with linear interpolation was introduced to the software where the system will start from 0 condition (where there will be a torque profile of constant 0 value) and then keep resisting to the steady torque coming from the dynamometer. Instead of running the system periodically, the continuous setup was used and the system was run for 0.4 seconds for a total of 13 cases.

The RPM settings for engine starting behavior was used as 10 RPM (stop condition) and 1000 RPM (final condition). The steady torque that was used from the dynamometer side was 50 Nm.

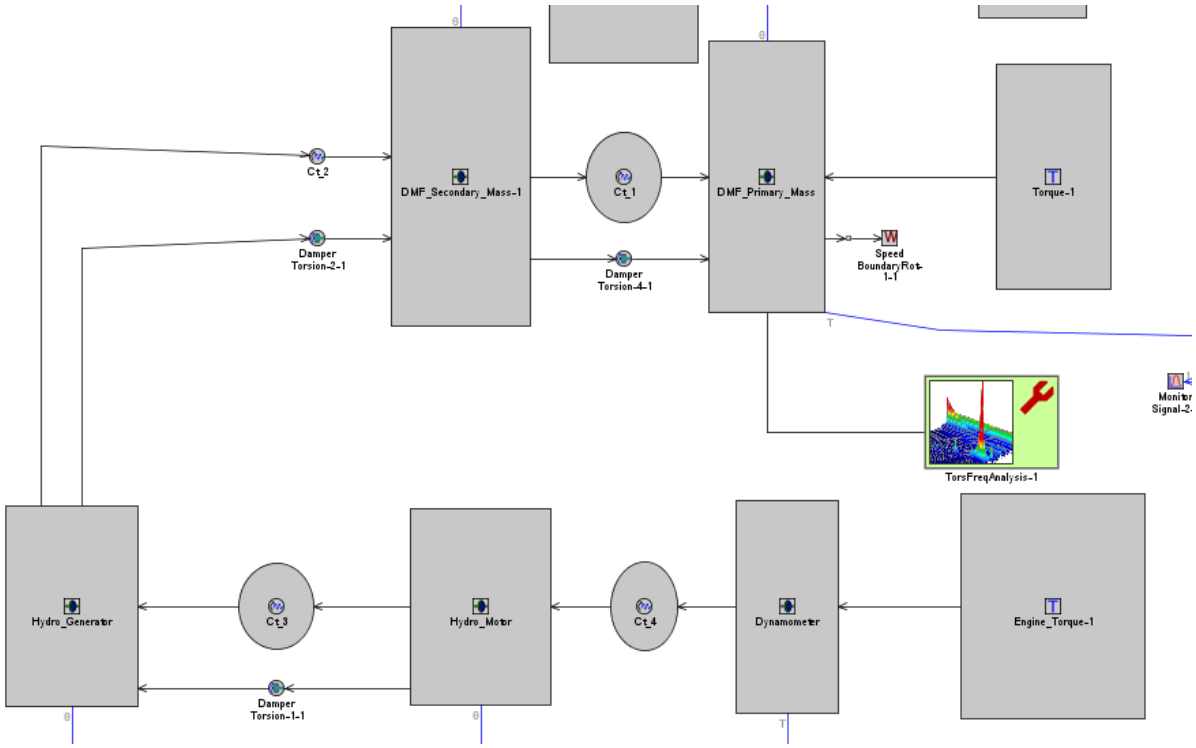


Figure 5.11 – A view of the engine starting model

Unfortunately, for transient behavior a whole other model has to be built for more accurate results that can be seen directly by using GT-Post. For this condition, example results were obtained by post processing the data obtained by running the simulation with a continuous time condition. The excel files that were used to post process can be seen in the appendices.

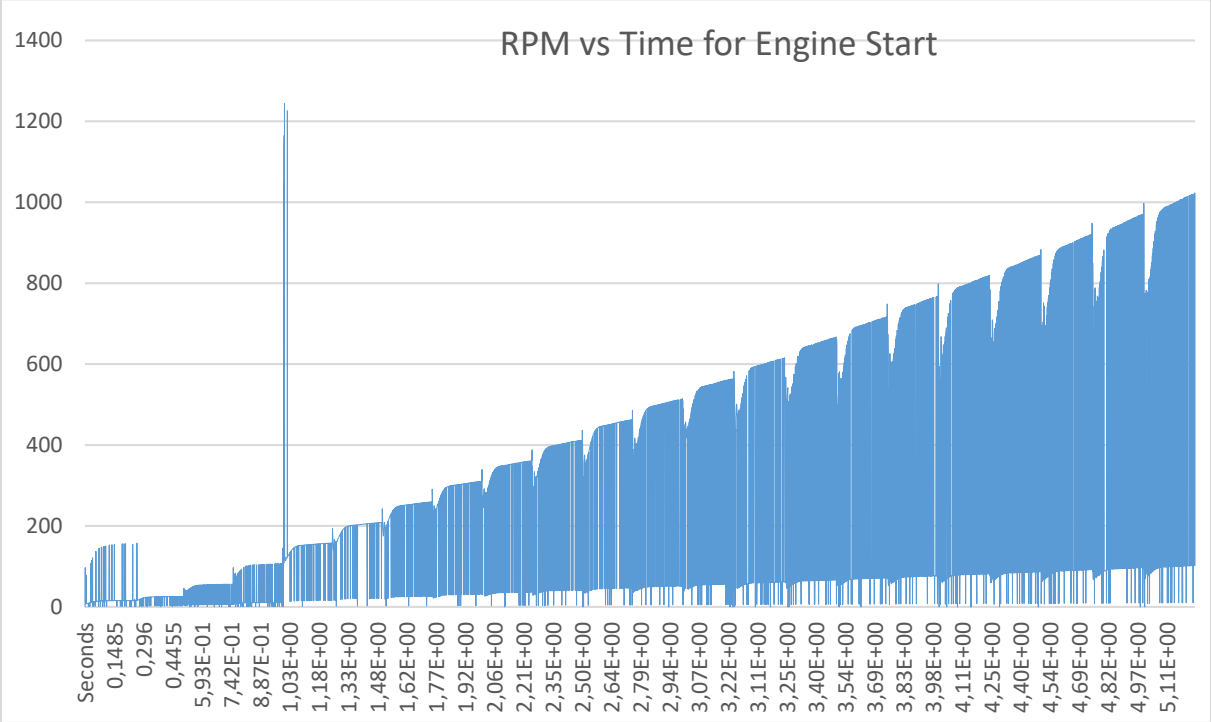


Figure 5.12 – Rotational speed vs. time diagram for the secondary mass of the DMF

Figure 5.12 shows that during the engine start, the rotational speed is almost always consistent except going through 0-200 RPM at the beginning of the simulation. The second peek seen around 1 second through the simulation can be a result of false computation and can be neglected.

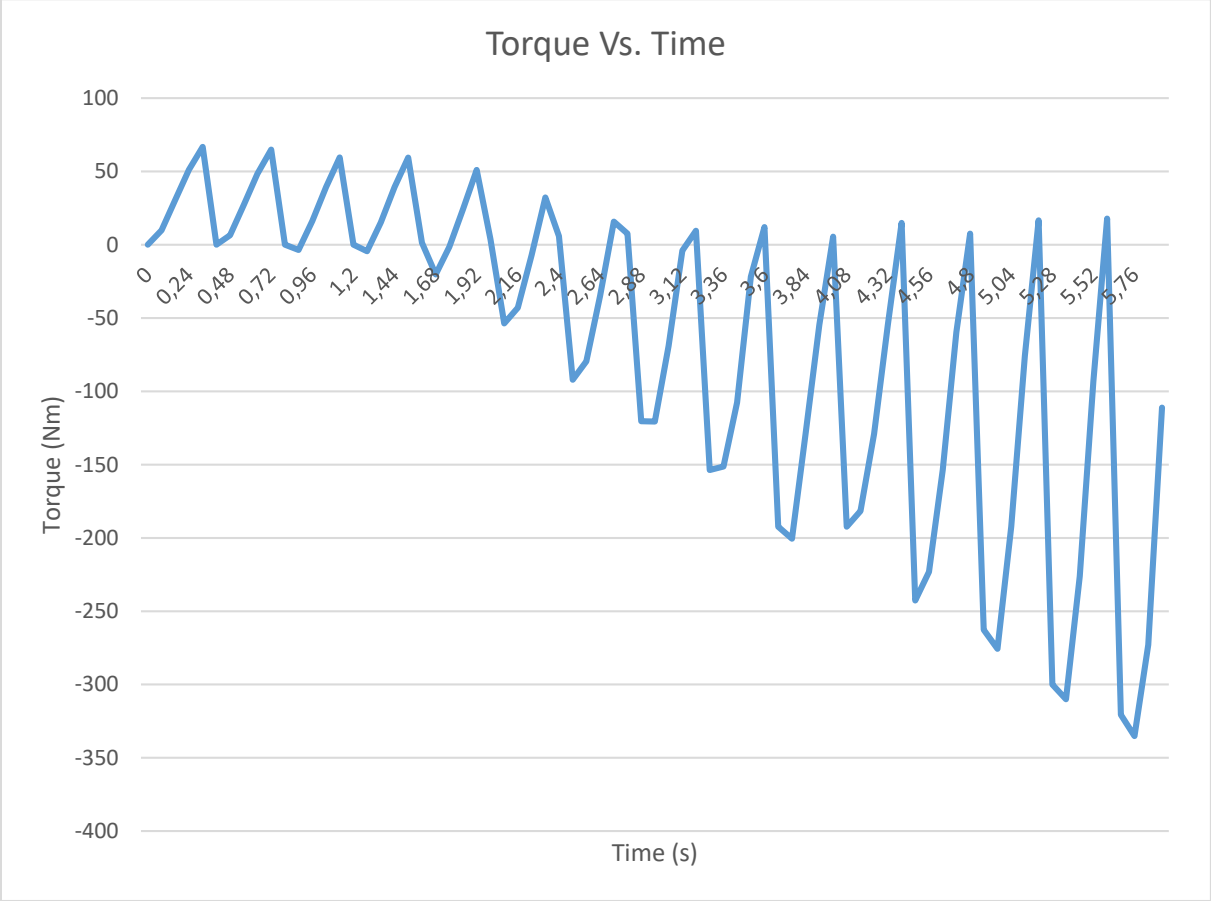


Figure 5.13 – Torque Vs. time for the dual mass flywheel torsional stiffness

Figure 5.13 shows an example of torque change through the simulation against time. The steady torque coming from the dyno side is defined as a negative value, therefore under these conditions we can say that the steady torque starts defying the motoring torque profile around 3.5 seconds and after this period of time, under these conditions, the engine is safe to start fueling.

### 5.5. Transient Behavior for Engine Stop

A similar method was used to build the engine stopping model for transient behavior. In this case, it was assumed that there will be no torque coming from the dynamometer side, the engine will be running under motoring conditions with no fuel, so the engine will stop by dissipation of energy.

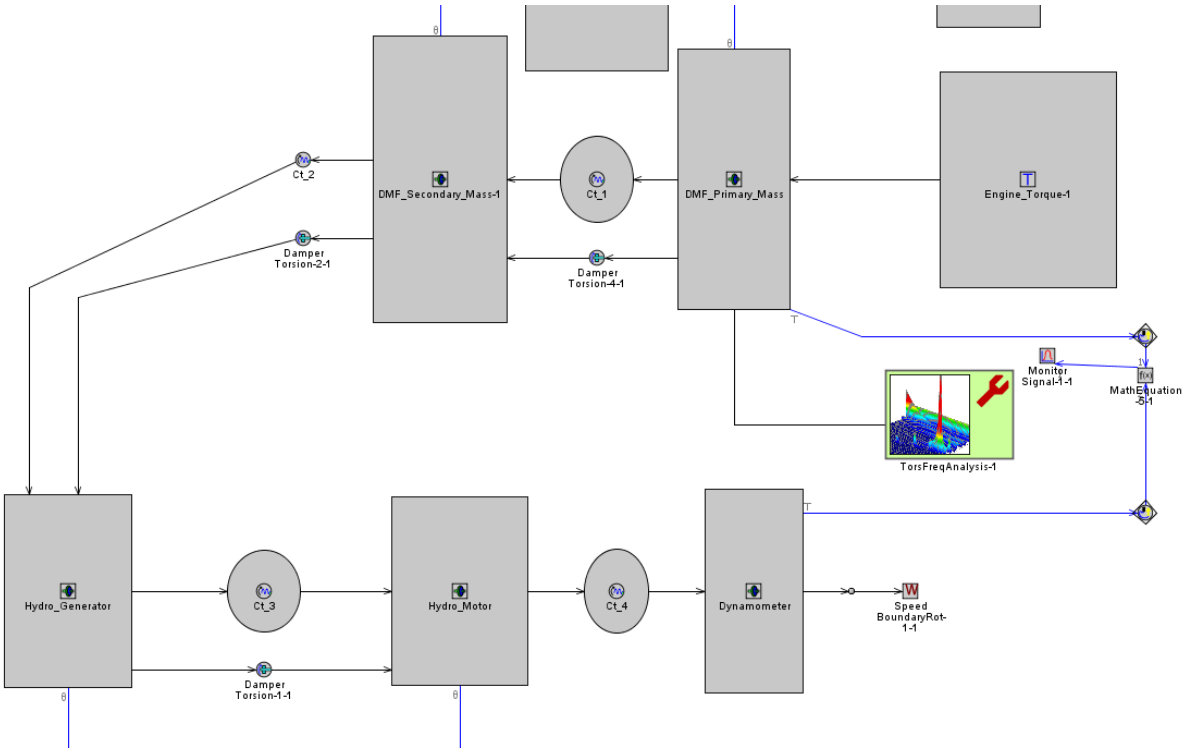


Figure 5.14 – A view of the engine stopping model

A total of 13 cases for introduced to the software once again, starting from 1000 RPM and ending at 10 RPM. Once again the motoring torque profiles were used, with an addition of 1 RPM torque profile, which is a constant 0 value. The simulation was run with a 0.4 second time step.

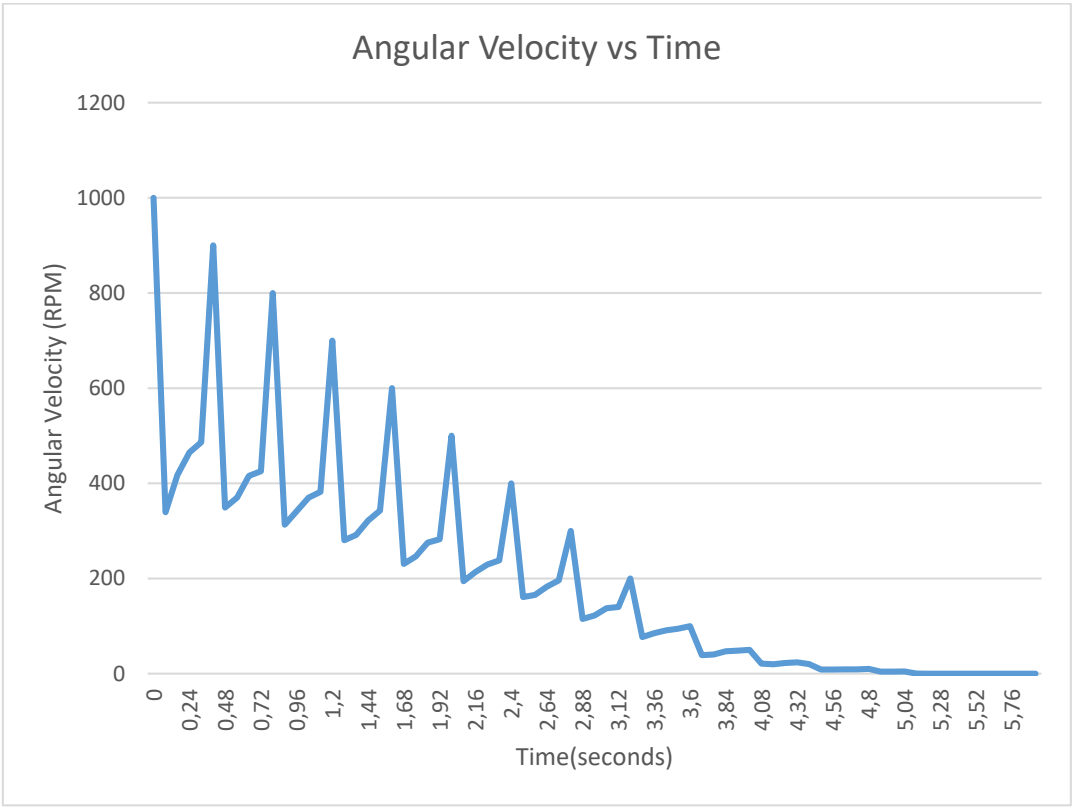


Figure 5.15 – Angular velocity vs. time for primary mass of the DMF

Figure 5.15 shows an example result for the change of angular velocity against time for the primary mass of the dual mass flywheel. The rotational speed as can be seen reduces over time and reaches zero by the end of the simulation, while no speed amplitudes are seen close to the natural frequency values. This is caused by the speed used to pass through each of the RPM of the system. Since the natural frequencies are passed through in a very short amount of time, no speed amplitudes in these results can be observed.

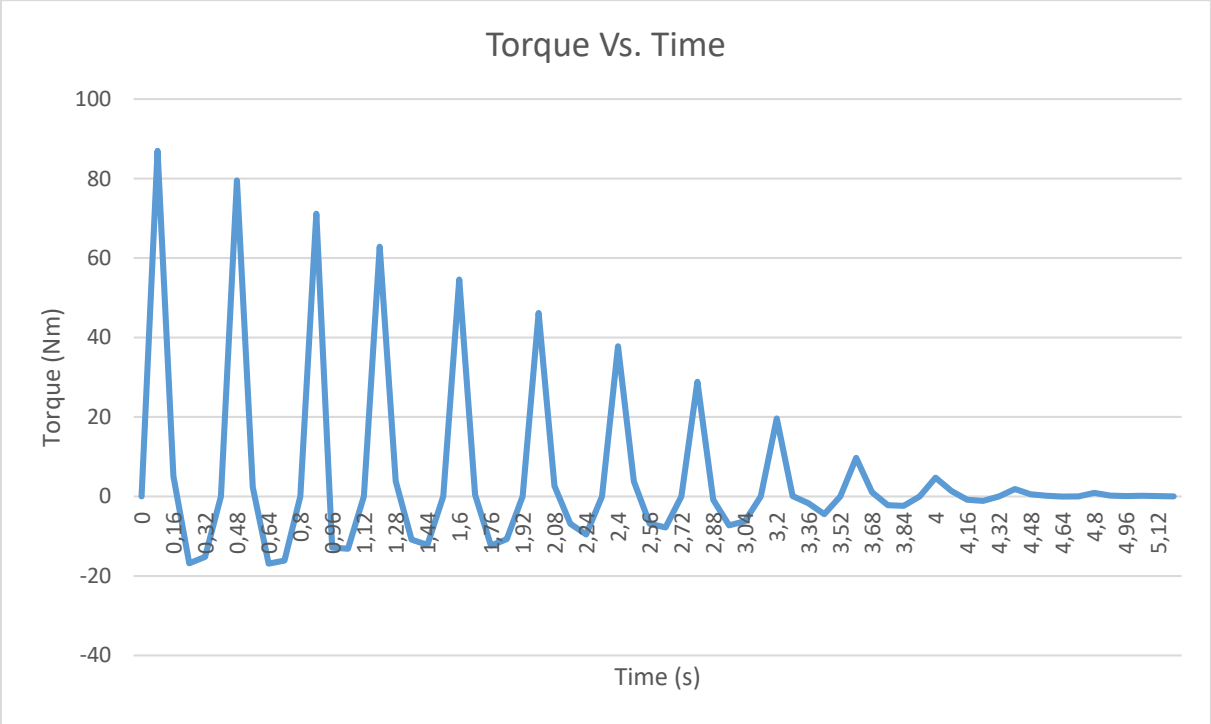


Figure 5.16 – Torque vs time for the dual mass flywheel torsional stiffness

Once again the torque change over time can be seen as steady on figure 5.16. The amplitudes can't be observed due to short amount of time used to pass through natural frequencies.

Both for engine starting and engine stopping transient conditions, a whole other more detailed transient model can be built using the GT-Suite software, where the engine is modeled not only as a torque module, but as a 4 cylinder in-line engine with proper crankshaft, cylinder, piston, and pressure values for motor conditions. This can generate much more detailed results by putting in the amount time for transient acceleration or deceleration of the engine being planned to use during the actual testing.

# 6. Conclusion

While improvements both on the analytical and dynamic model are possible, and even reasonable, it is safe to say that this study provides a thorough evaluation on the natural frequencies and dynamic variables of the engine tilting stand that will be built.

For the parts dual mass flywheel and the hydro elements, the results seem to always stay below the critical values even when the system goes through resonant frequencies. For engine start and stop transient behavior the simulation gives steady results, although through the research it can be concluded that by using a 1-D model with torque modules, a detailed time simulation where the change of torque and speed amplitudes can be observed is not possible.

The natural frequencies from the analytical model, and the study of them, matching the results from the software can justify that the dynamic model built on GT-Suite can provide detailed results on a theoretical level, while there is a possibility of moving further with the dynamic model. This will be discussed in the next sub section.

## 6.1. Possible Next Steps

- The first necessary step that should be taken to move the project further is to build a more detailed model of the system. While during this research most of the inertias and the stiffness were taken into account, a more detailed study on the planetary gear set, the shaft inertias, and the couplings, can provide results that are much more accurate and close to the practical values. Due to the fact that planetary gear set was only recently added to the system instead of a reduction gear box, the assembly and the input shaft is still in the design process. Therefore, it should be definitely taken into account that each element of the planetary gear set will have an inertia of its own that will affect the system.

- Introducing the planetary gear set to the system can make things more complicated. But this can be overcome by adding another mass into the model. Adding an extra mass that will rotate with the total mass moment of inertia of the planetary elements while adding another torsional stiffness for the connection between the planetary set and the hydro generator, will introduce another natural frequency into the system. This will also change the other natural frequencies of the system.

- Another way of adding the planetary set to the system can be with 2 masses added into the analytic model. By adding a mass before gear reduction with a total inertia of non-reduced elements, and adding a second mass with the total inertia of reduced elements, can show yet another natural frequency that can cause critical conditions in the system. Please take a note that there should be another torsional stiffness defined in between, which will be a sum of the torsional stiffness of planetary elements in contact during gear reduction.

- As it was stated before, setting up a case for each RPM and running the simulation does not provide proper results for engine transient behavior, both for starting and stopping. It is highly suggested that for engine transient behavior, a more detailed model is built. This model should include all 4 cylinders of the engine, crankshaft and pistons. While throughout this study we have used the cylinder pressure values to obtain the torque values, in a model built like this cylinder pressures can be used directly. The biggest advantage of building a separate model for engine transient behavior is to be able to introduce a transient acceleration or deceleration to the system in a single case, where starting and stopping behavior can be properly observed and evaluated. A detailed example of this kind of model can be found in GT-Suite, where engine transient behavior between 1000-5000 RPM both for accelerating and decelerating is modeled.

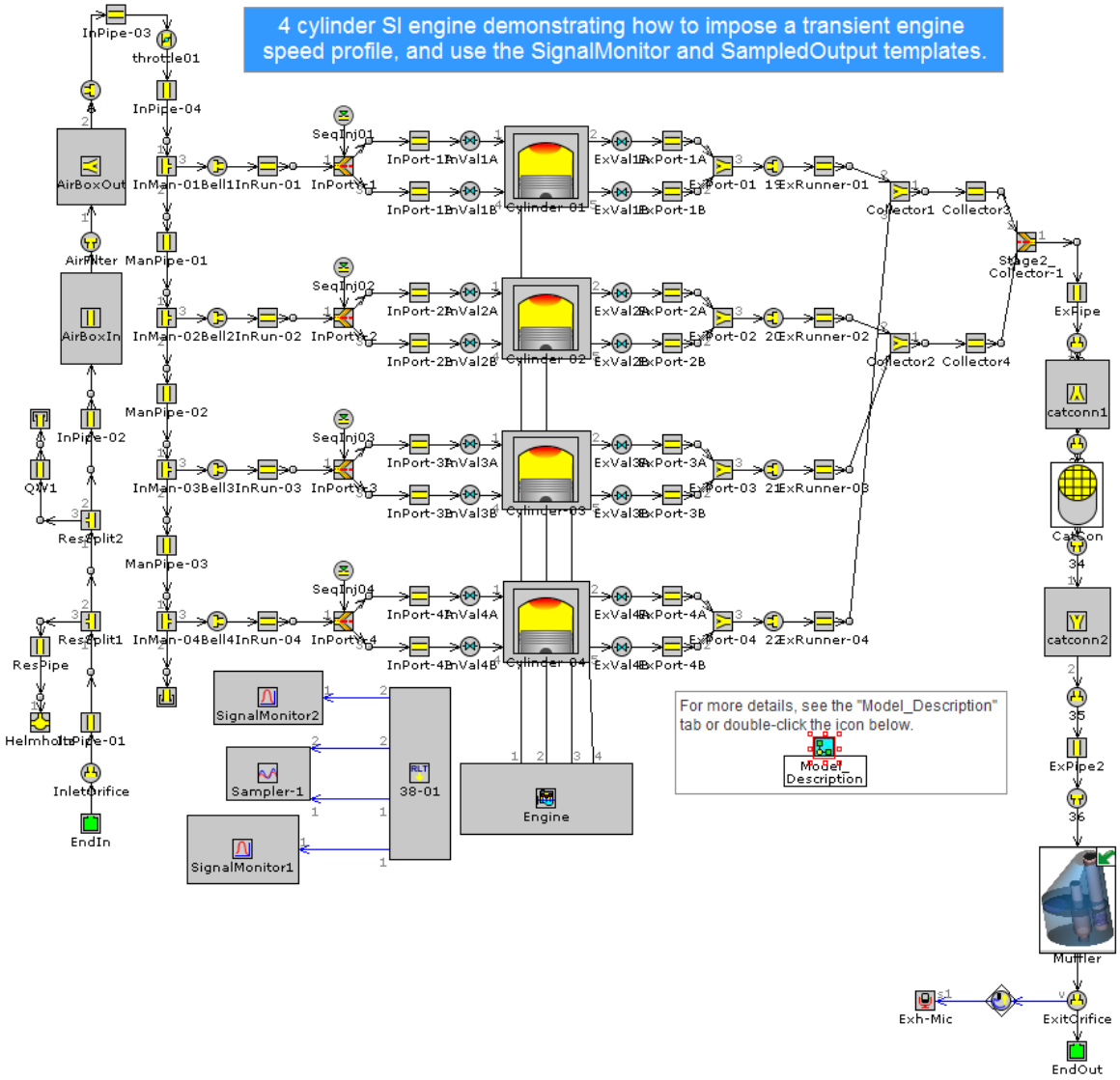


Figure 6.1 – Example transient behavior build on GT-Suite

The example transient build is not for a testing case with a dynamometer present. But once the engine layout is done properly, and the transient behavior profiles are set, the elements for the tilting test stand can be added into the system. For steady torque coming in or going out from the dynamometer side can be defined with a torque module, and a crankshaft can be added to the system of transient behavior for frequency analysis. An example of this can be seen on figure 6.2. Both of these examples can be found in the software with references “SI_4Cyl_Imposed_Speed_Transient.gtm” and “Dyno-frequency-dynoassy.gtm”.

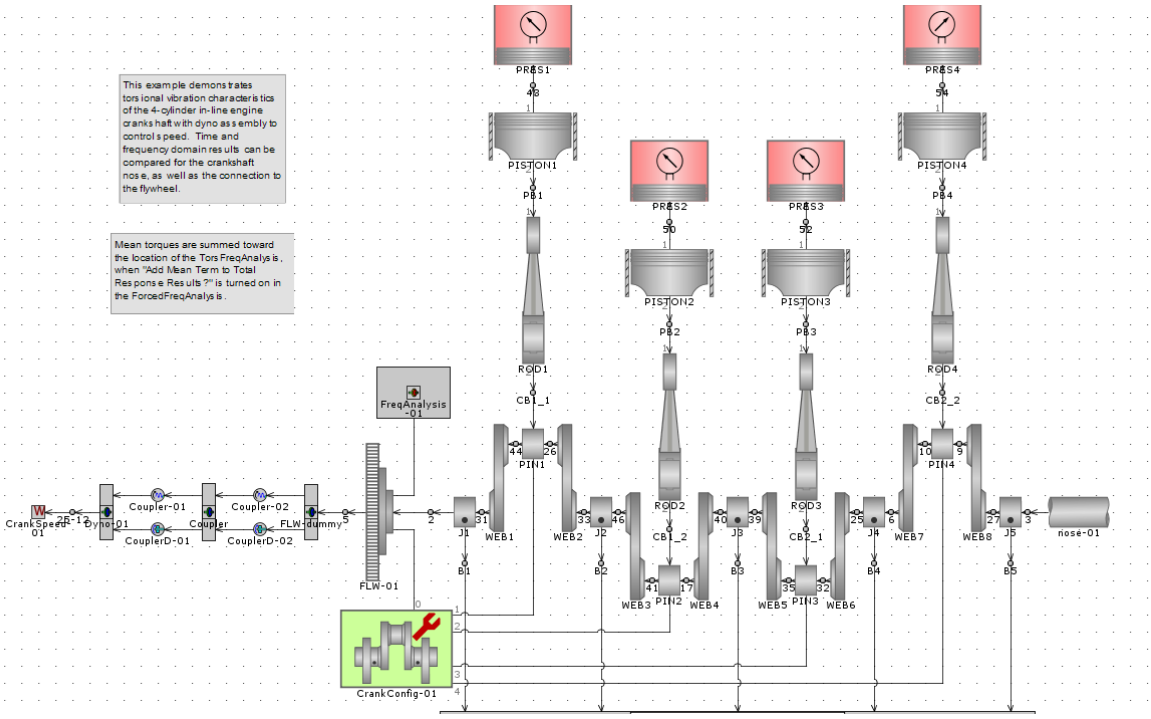


Figure 6.2 – A crankshaft assembly with a dynamometer present

# References


1. Schrand, David, The Basics of Torque Measurement, Technical Notes and Articles, Sensor Developments Inc. *1050 W. Silver Bell Rd . Orion, MI 48359-1327 . USA, 2016*
2. Reik, Wolfgang; Seebacher, Roland; Kooy, Ad, 6th Luk Symposium, *p. 69-93, 1998*
3. Reik, W., Albers A.; Schnurr M. u.a. Torsionsschwingungen im Antriebsstrang, Luk Symposium, *1990*
4. Harihara, Parasuram; Childs, Dara W., Solving Problems in Dynamics and Vibrations Using Matlab, *Department of Mechanical Engineering Texas A & M University College Station, p.11-21*
5. Tiwari P.; Guwahari T., Torsional Vibration of Rotors I: The Direct and Transfer Matrix Methods, *p.271-340, 2010*
6. ZF 4 HP20, Citroen Automatic Transmission Handbook
7. Parker Hydraulic Motor/Pump Series F11/12, Catalogue HY17-8249/US, 2004
8. Kooy, Ad; Gillmann, Achim; Jackel, Johan; Bosse, Michael, DMFW, Nothing New? 7th Luk Symposium, *p.5-15, 2002*

# Appendices

**Appendix A** **Photographs**

**Appendix B** **Supplementary Files/CD**

# Appendix A

## Photographs

Photo 1 – Planetary gear set elements

Photo 2 – Planetary Ring

Photo 3 – Roba DS coupling top view